CNRS
Centre National de la Recherche Scientifique

INFN
Instituto Nazionale di Fisica Nucleare

Mirror and marionette actuation calibration for VSR1

F. Marion, B. Mours, L. Rolland

VIR-015B-08

June 23, 2008

VIRGO * A joint CNRS-INFN Project
Project office: Traversa H di via Macerata - I-56021 S. Stefano a Macerata, Cascina (PI)
Secretariat: Telephone (39) 50 752 521 – Fax (39) 50 752 550 – e-mail virgo@pisa.infn.it

Abstract

This document summarizes the results of the mirror and marionette actuator calibration during the Virgo first scientific run (VSR1) which lasted from May 18th 2007 21h UTC (GPS 863557213) to October 1st 2007 6h UTC (GPS 875253614). Precise measurements of the actuators are necessary in order to estimate the sensitivity of the Virgo interferometer and to reconstruct the gravitationnal wave strain h(t).

The mirror actuator transfer functions have been modeled for the arm mirrors (WE, NE, NI) and for the BS mirror with a statistical precision of the order of 1% in modulus and within 0.05 rad in phase below 1 kHz. Systematic errors of $^{+2\%}_{-4\%}$ have been estimated. The frequency dependence of the actuation response is similar for the arm mirrors but flatter for the BS mirror. The frequency dependence is assumed to be due to Eddy currents induced by the coil currents into the reference masses.

The PR mirror actuator has been measured below 100 Hz only with low precision. The measurements indicate a trend similar to the arm mirror actuations.

The marionette actuator transfer functions of WE and NE have been modeled below 100 Hz with a statistical precision of 2% on the modulus and within 0.03 rad on the phase. Systematic errors have been estimated to less than 3% and 0.03 rad on the modulus and the phase respectively.

Contents

Introduction

This document summarizes the results of the mirror and marionette actuator calibration during the Virgo first scientific run (VSR1) which lasted from May 18th 2007 21h UTC (GPS 863557213) to October 1st 2007 6h UTC (GPS 875253614).

During VSR1, the Virgo interferometer longitudinal movement was controlled through the WE, NE, BS and PR mirrors for frequency up to a few 100 Hz. Movement at lower frequencies, up to a few 10 Hz, were controlled through the WE and NE marionettes. The NI mirror was used for the hardware injections to simulate gravitationnal signals in the interferometer. None of the injections had features above 1 kHz. The WI mirror was not used for contols nor injection.

Precise measurements of the actuators (within a few Hz) from 10 Hz to $\sim$ 1 kHz are necessary in order to estimate the sensitivity of the Virgo interferometer and to reconstruct the gravitationnal wave strain h(t). We aim at reducing the error of the reconstructed signal at the 10% level for the VSR1 data. The calibration of the actuator should thus be better than 10%. At higher frequency, the mirrors are free. Thus the knowledge of the actuation at higher frequency is not usefull for the sensitivity estimation and the h-reconstruction[1].

Calibration data were taken in May 2007 before the run, during VSR1 for monitoring and after the run, up to December 2007 in order to improve the measurements before the mirror actuators are changed for the Virgo+ upgrade.

A detailed description of the methods used to extract the calibration coefficients is the subject of another note in preparation.

The definitions of the mirror and marionnette actuation transfer functions are given in the first chapter after a brief overview of the actuation electronics.

The second chapter is dedicated to the measurements of the mirror actuation TFs. The results from the main calibration stream are given for every mirror. They are then compared to independent measurements in order to estimate the systematic errors of the calibration.

The third chapter deals with the WE and NE marionette actuation TFs. The results are also compared to other measurements in order to estimate the systematic errors.

[1] The knowledge of the mirror actuation up to higher frequencies could be usefull for high frequency hardware injection and estimation of the errors of the reconstructed h(t) signal at high frequencies.

Chapter 1

Actuation transfer function definition

1.1 Mirror actuation transfer function

The mirror movements are controlled through magnets glued on the mirror and coils generating a magnetic field set on the reference mass. The current flowing in the coil is controlled through the so-called coil actuation composed of

- a DSP. It relays the correction and calibration signals to the DAC. Some gain and shaping filters can be applied.
- a DAC. It relays the DSP output to the analog electronics.
- a coil driver. The analog electronics convert the DAC voltage output into a current flowing in the coil.

The mirror suspensions have two modes. The High Power (HP) mode has a large dynamic but is too noisy to take science data. It is used during the lock acquisition of VIrgo. The Low Noise (LN) mode has a reduced dynamic but a noise level suitable for the science data. It is used for data taking. The gain and shaping filters of the DSPs and coil drivers are different between the HP and the LN mode. Note that the PR actuation was used in HP mode during VSR1 data taking.

During VSR1, the arm and PR mirrors were controlled through two coil drivers only: the up (U) and down (D) coils. The BS mirror was controlled through four coils: up-left (UL), up-right (UR), down-left (DL) and down-right (DR). The hardware injections were also sent to the U and D coils of the NI mirror actuation. A detailed description of the gain and filters used in the coil actuation during VSR1 can be found in the note [1].

Concerning the sensitivity estimation and the h-reconstruction, the actuation transfer function (TF) that must be calibrated is the the TF from the the signal at the input of the DSP (in V) to the mirror movement (in m) in LN mode (or HP mode for PR).

The dynamic of the coil drivers in LN mode is too low for a direct measurements of the mirror actuation in LN mode. The mirror actuation calibration is thus done in different steps. **The main mirror calibration stream is the following:**

- **the actuators are calibrated in HP mode from free swinging Michelson data ;**
- **the LN/HP actuator transfer function ratio is computed from electronics measurements ;**
- **the actuator TFs in LN mode are then computed.**

All the measurements are based on the actuator calibration in HP mode using free swinging Michelson data. The data and their analysis are described in section 2.1.1: a noise is injected at the level of the mirror actuation in the $zCorr$ channel (in V) and the mirror motion ΔL is reconstructed (in m) from the laser power measured on the detection bench before the output mode cleaner (the Pr_B1p channels, in W). The transfer function $\Delta L/zCorr$ is computed.

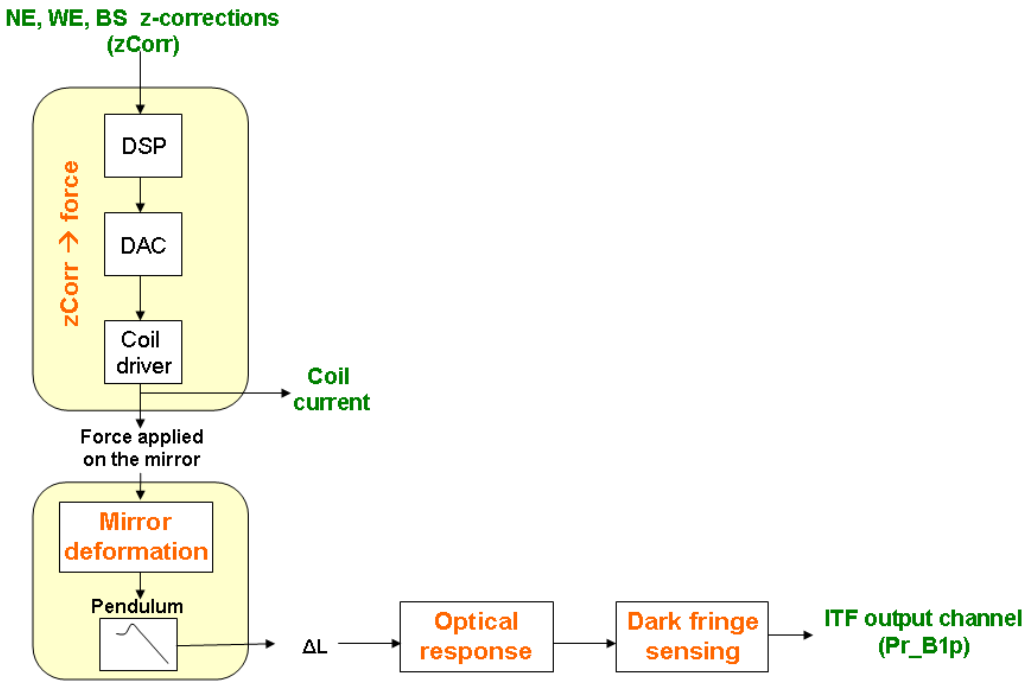

Figure 1.1: ***Calibration signal processing*** *from the noise stored in the channel zCorr to the detected power stored in the chanel* Pr_B1p.

The processing of the signal from $zCorr$ to ΔL is summarized on the figure 1.1. It goes through different parts:

- the actuation itself, which converts the $zCorr$ signal to a force on the mirror,

- the mirror deformation then propagates from the magnet position to the mirror center where is the ITF laser beam,
- the mirror motion is filtered by the pendulum mechanical response,
- optical response: the mirror motion is 'seen' by the laser beam which then propagates to the detection bench,
- power sensing: the power inpinging on the detection photodiodes is readout and stored in the DAQ.

The ΔL reconstructed from the ITF output channel is not corrected for the optical response and the dark fringe sensing. The actuation TF from $zCorr$ to ΔL given in this note thus includes these different conversions.

The delays induced in the measured TF are described in details in the note [3]. A brief summary is given in the following.

1.1.1 Delays from electronics

Since the TF is measured below 1 kHz, the anti-image and anti-alias filters of the DAC (actuation) and ADC (sensing) are equivalent to pure delays ($\sim 180\,\mu$s and $\sim 75\,\mu$s respectively). They are not modeled in the calibration process. The TFs given for the actuation thus include these delays.

1.1.2 Delays from optical response

In the case of free swinging Michelson data, the optical response of the interferometer is described by a simple propagation time of the laser beam. In the following, the propagation times inside the central building are neglected (~ 70 ns for 20 m). For the NE and WE mirrors, the beam propagates into the 3-km arm and then goes to the detection bench: this induces a delay of $10\,\mu$s. For the NI and WI mirrors, the propagation time is negligible.

For the BS mirror, two paths are possible as shown in the figure 1.2. The BS motion is seen by the beam when it is reflected. It has no effect when the beam is transmitted.

- the beam that is transmitted to the north cavity "sees" the BS motion after its trip back and forth in the cavity, when it is reflected on BS to the detection bench: the propagation time from the BS mirror to the detection is negligible.
- the beam that is reflected to the west cavity "sees" the BS motion before it goes back and forth inside the cavity. The propagation time is thus $20\,\mu$s if the beam goes up to the WE mirror, and is negligible if the beam goes up to the WI mirror.

The delay due to the optical response free swinging Michelson configurations is thus: no delay if the WE mirror is not used (configurations WI-NI and WI-NE) ; 10 μs if the WE mirror is used (configurations WE-NI and WE-NE), since two beams with delays 0 and 20 μs are recombined to the detection bench. This was checked performing SIESTA simulations of the different configurations. In the TFs given for the BS mirror actuation, the optical response delays are corrected.

To conclude about the optical response delays that are included in the mirror actuation TFs given in this note:

- no delay for the NI, WI and BS mirror TFs,
- 10 μs for the NE and WE mirror TFs.

1.1.3 Pendulum mechanical response

The mirror actuation TFs given in this note are corrected for the mirror pendulum mechanical response. For all suspensions, it is assumed to be a second order low pass filter[1] with a cut-off frequency of 0.6 Hz and a quality factor of 1000.

1.2 Marionnette actuation transfer function

The controls of the WE and NE mirrors in the mid-frequency range (1-50 Hz) are not sent directly to the mirrors. They are sent to the marionettes of the suspensions. The effect of the marionette control signals (i.e. channel Sc_WE_zM) on the mirror movement needs to be taken into account in the h-reconstruction in order to reconstruct the h-amplitude properly below ~50 Hz.

[1] 2nd order low pass filter: $TF(f) = -\frac{f_0^2(f^2-f_0^2) - \mathrm{i}\, f_0^3 f/Q}{(f^2-f_0^2)^2 + (f f_0/Q)^2}$

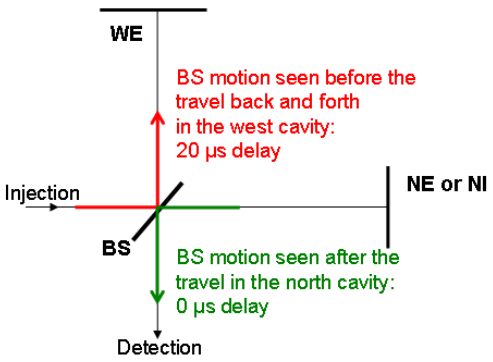

Figure 1.2: ***Optical response of the free swinging Michelson to the BS motion.***

The main marionette calibration stream is the following:

- **The ratio of the marionette actuation TF to the mirror actuation TF in LN mode is measured from 1 to 100 Hz from white noise injections in step 12.**
- **The absolute marionette actuation TF is then computed from 1 to 100 Hz multiplying the ratio by the calibrated mirror actuation in LN mode.**

As the mirror actuation TF (corrected for the mechanical pendulum response) is used in the process, the same delays from electronics and optical response as for the mirror actuation TF are included in the results.

1.3 Pendulum mechanical response

The conversion of the marionette control signal to the mirror movement includes the two-stage pendulum mechanical response [8]. In the results given in this note, the marionette actuation TF have been corrected for a simplified model mechanical response: the modulus is assumed to evolve as $\left(\frac{1\ \mathrm{Hz}}{f}\right)^4$ and the phase assumed to be 0.

Chapter 2

Calibration of the mirror actuators

The mirror actuation calibration results are shown separately for every suspensions from section 2.1 to 2.5. The data configurations and computation methods are given in the first part, about the WE mirror actuator. The sections about the other mirrors only contain comments when they are different from the WE ones.

The measurements of the PR mirror actuation, in HP mode, are different and described in section 2.6.

Other calibration data and methods have been used in order to measure the mirror actuator TFs. They are described in the section 2.7 along with the estimation of the systematic errors.

2.1 WE mirror actuator calibration

2.1.1 Mirror actuator gain in HP mode

The mirror actuator gain in HP mode are measured with the ITF in free swinging Michelson configurations, injecting a few lines on the actuators in HP mode. The injected signal is sent to the U and D coils.

The data

Data were taken in three different configurations: asymmetric WE-NI and NE-WI and short NI-WI free swinging Michelson. During VSR1, data in asymmetric configurations were taken every two weeks. More data were taken during post-VSR1 calibration in order to check that the saturation of the actuator electronic channelss occurs at amplitudes higher than the usual ones. Data are higher frequencies were also taken.

The ITF is re-aligned (step 1). It is then unlocked and set in one of the free swinging Michelson configurations. Then, a dataset consists in $\sim$5 minutes of line injections. A few lines are injected in every datasets. The ITF is then re-aligned. Data can then be taken in another configuration.

Saturation of the actuator electronic channels

During the post-VSR1 calibration, the lines have been injected with different amplitudes in order to estimate the saturation level of the actuator electronic channels.

For a single injected line, the saturation of the electronics would appear as a decrease of the measured actuator gain as the frequency increases. As different lines are injected at the same time, the signature of the saturation is less clear and depends not on the line amplitude but on the total amplitude of all the simultaneous lines. For a given frequency, the actuator gain (normalized to its non-saturated value) is computed as function of the sum of the amplitudes of the lines injected in *zCorr*. The figure 2.1 shows the evolution obtained at the different frequencies. The normalized gain is flat below 1.2 V. At 1.7 V, saturation is visible for the low frequency lines (below ∼30 Hz) only. The saturation is clearly visible for all frequencies above 2 V.

For these points indicating saturation at 1.7 V, the low frequency lines below 30 Hz were injected with a very low amplitude at the same time as a line at a few hundred Hz with an amplitude closed to the allowed dynamic. The signal is thus clipped only at the maximum and minimum of the high frequency lines, while it is clipped several times during the period of the low frequency lines. This must explain that the saturation is visible for the low frequency lines only.

In the following analysis, the GPS times of the data that show electronic saturation have been excluded. The main part of the data, coming from the VSR1 monitoring data, have injected amplitudes of the order of 1 V, well below saturation. They can be used to monitor the gain stability.

The results

All the non-saturated data with coherence between the mirror movement ΔL and the injected signal zCorr higher than 70% were then used to check the stability of the TF within time. The figures 2.2, 2.3 and 2.4 give the WE mirror actuation modulus and phase evolution from May to November 2007 at the different measured frequencies. The individual errors are estimated from the coherence of the measurements as:

$$\frac{\Delta M}{M} = \alpha \sqrt{\frac{1-C}{C}} \frac{1}{\sqrt{n_{call}}} \tag{2.1}$$

$$\Delta P = \beta \sqrt{\frac{1-C}{C}} \frac{1}{\sqrt{n_{call}}} \tag{2.2}$$

where M and P are the modulus and the phase of the TF respectively, C the coherence, n_{call} the number of averages performed on the TF, α and β two constants respectively estimated to 0.85 and 0.88.

The gain variations are of the order of 1%. The phase variations are of the order of 0.01 rad (∼1°). We note a step in the modulus evolution in the range 60-450 Hz: the gain has decreased

by 1% in the beginning of July. This must be linked with the addition of de-emphasis filters in the WE actuation electronic channels in LN mode on July 11th. The emphasis filters were also set in the DSP. They have pole and zero around 15 and 85 Hz. The modification should have affected the LN TF only. However, the coil driver electronics have been uplugged and modified. A slight modification of the HP TF related to this work cannot be excluded.

The variations of the mirror actuation TF during VSR1 being of the order of 1% for the gain and 1° for the phase, they can be considered as constant in relation with the aimed calibration error.

The averaged gain and phase in HP mode as function of frequency for the WE mirror actuator have thus been computed using the non-saturated datasets. The figure 2.5(a) shows the measurements of the different datasets. The figure 2.5(b) shows the time-averaged transfer function. The table 2.1 gives the average gain and phase as function of the frequency for the WE actuator in HP mode. For a given parameter M, the measurements of the N datasets are noted $M_i \pm \Delta M_i$ $(i = 1..N)$. The average value and its error are estimated as:

$$< M > = \frac{\sum_{i=1}^{N} \frac{M_i}{\Delta M_i}}{\sum_{i=1}^{N} \frac{1}{\Delta M_i}} \tag{2.3}$$

$$\Delta < M > = \frac{\sqrt{\sum_{i=1}^{N} \Delta M_i^2}}{N} \tag{2.4}$$

The χ^2/ndof for the constant gain and phase hypothesis are also given. It confirms that the TF did not evolve during VSR1, except in the range 60-450 Hz where the $\chi 2$ are larger due to the step of July 11th, 2007.

The statistical errors from the free Michelson measurements on the WE mirror actuation TF in HP mode are of the order of 0.1% on the gain and 1° on the phase. A 1% systematic error on the gain has to be added since the modification of July 11th 2007 is neglected.

The frequency dependence of the mirror actuation should a priori be flat. The observed variations must be explained by the presence of Eddy current induced by the coil current into the reference mass. This in return reduces the coil current, the effect increasing with frequency due to skin effects.

2.1.2 Mirror actuator: LN/HP transfer function

The mirror actuator TF in LN mode cannot be measured directly. It is thus necessary to measure the ratio of the TF LN/HP. Different methods were used. The more direct and more precise method uses direct electronics measurements of the coil drivers.

The other methods use the level of injected lines in the dark fringe during the lock acquisition. They are less precise and cover a lower frequency range and are thus use to check the results consistency and estimate systematic errors (see section 2.7.2).

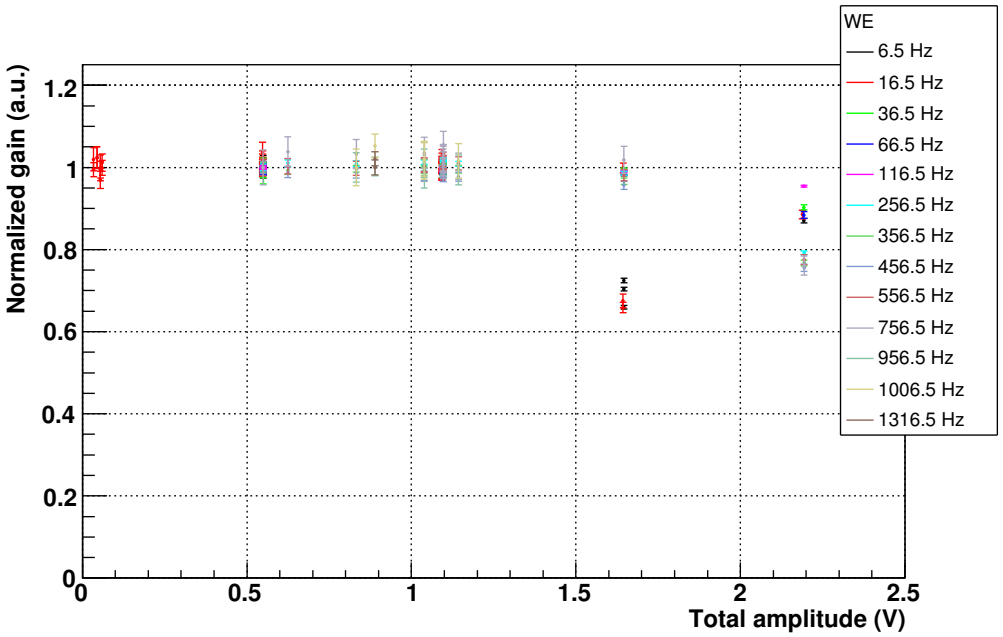

Figure 2.1: ***WE mirror actuator gain vs the amplitude*** *of the injected signal on zCorr. The gain is flat for injected signal up to 1.2 V. For higher amplitudes, the measured gain decreases, indicating a saturation of the electronics of the WE actuation.*

Frequency (Hz)	Gain (μm/V)	χ^2/ndf	Phase (rad)	χ^2/ndf
6.5	10.789 ± 0.009	47.1/40	3.1030 ± 0.0008	49.1/40
16.5	10.762 ± 0.022	33.5/39	3.0497 ± 0.0021	58.8/39
36.5	10.525 ± 0.022	24.3/16	2.9543 ± 0.0022	28.9/16
66.5	10.156 ± 0.008	94.0/16	2.8288 ± 0.0008	41.1/16
116.5	9.678 ± 0.004	240.2/16	2.6493 ± 0.0004	20.7/16
256.5	8.916 ± 0.005	60.1/14	2.1923 ± 0.0006	16.7/14
356.5	8.621 ± 0.008	34.7/11	1.8740 ± 0.0010	13.3/11
456.5	8.392 ± 0.011	31.6/11	1.5588 ± 0.0014	17.3/11
556.5	8.193 ± 0.016	8.6/11	1.2391 ± 0.0021	10.2/11
756.5	7.719 ± 0.028	19.7/11	0.6240 ± 0.0038	5.3/11
956.5	7.581 ± 0.054	1.5/ 4	-0.0218 ± 0.0074	5.4/ 4
1006.5	7.456 ± 0.061	17.5/ 4	-0.1922 ± 0.0086	13.6/ 4
1316.5	7.069 ± 0.041	3.3/ 1	-1.1485 ± 0.0060	3.6/ 1

Table 2.1: ***Time-average actuation TF of the WE mirror in HP mode****. All the good quality data from May 2007 were used. The χ^2 test for a constant value as function of time was performed for the gain and the phase.*

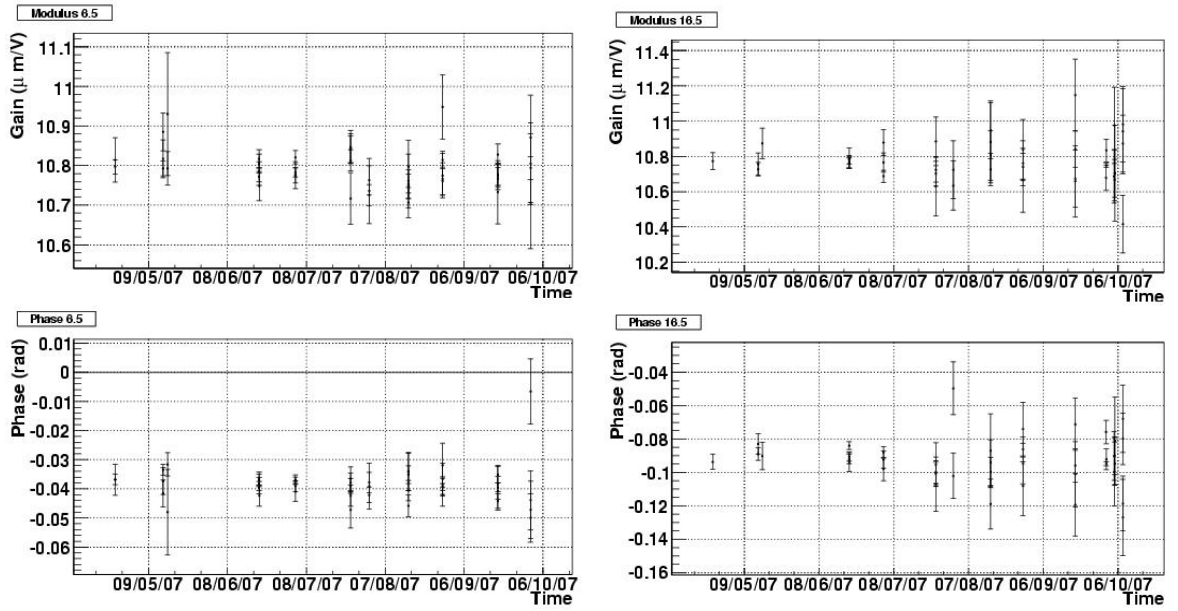

(a) 6.5 Hz

(b) 16.5 Hz

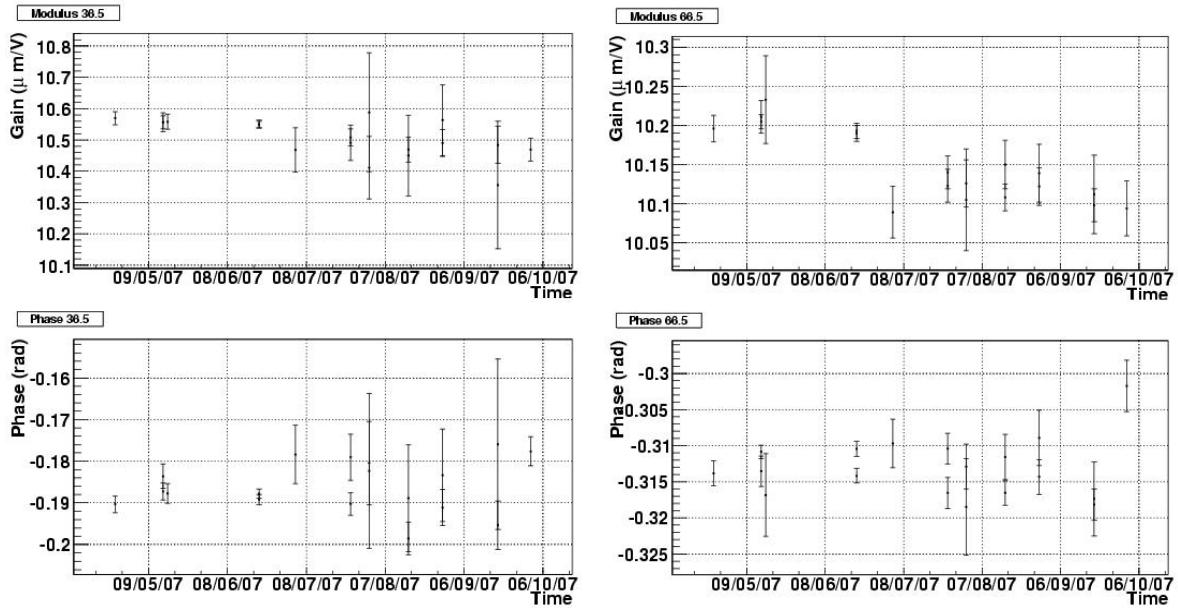

(c) 36.5 Hz

(d) 66.5 Hz

Figure 2.2: ***WE mirror actuation TF vs time.*** *Modulus and phase as function of time (May to October 2007) at 6.5 Hz (a), 16.5 Hz (b), 36.5 Hz (c) and 66.5 Hz (d).*

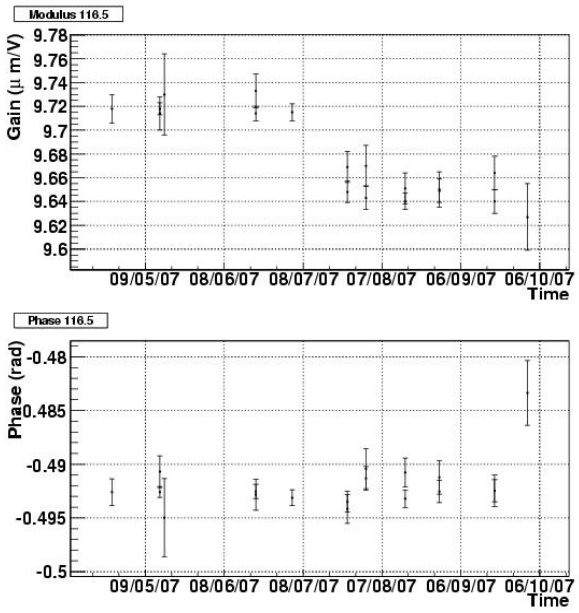

(a) 116.5 Hz

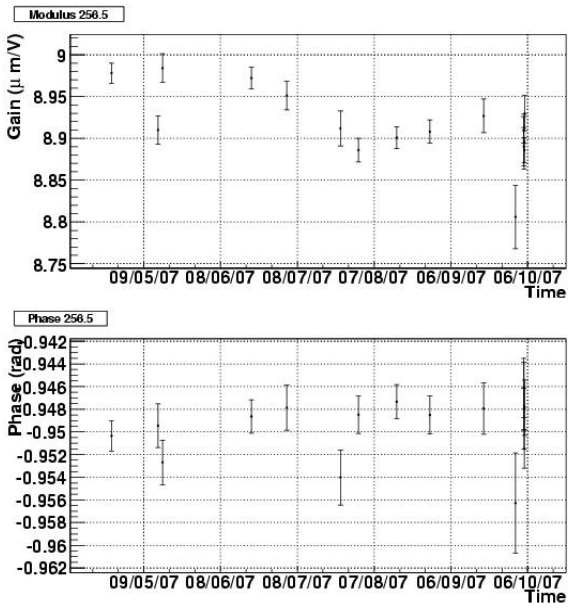

(b) 256.5 Hz

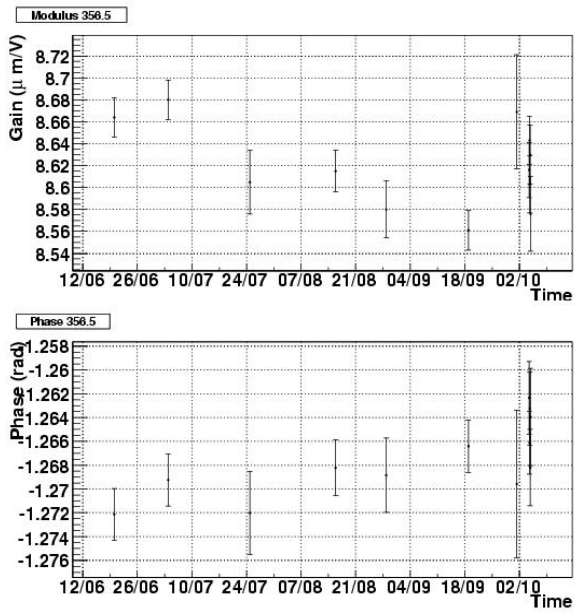

(c) 356.5 Hz

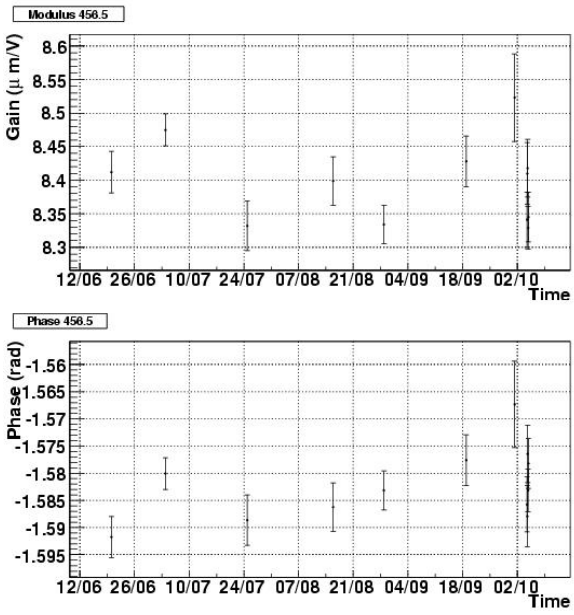

(d) 456.5 Hz

Figure 2.3: ***WE mirror actuation TF vs time.*** *Modulus and phase as function of time (May to October 2007) at 116.5 Hz (a), 256.5 Hz (b), 356.5 Hz (c) and 456.5 Hz (d).*

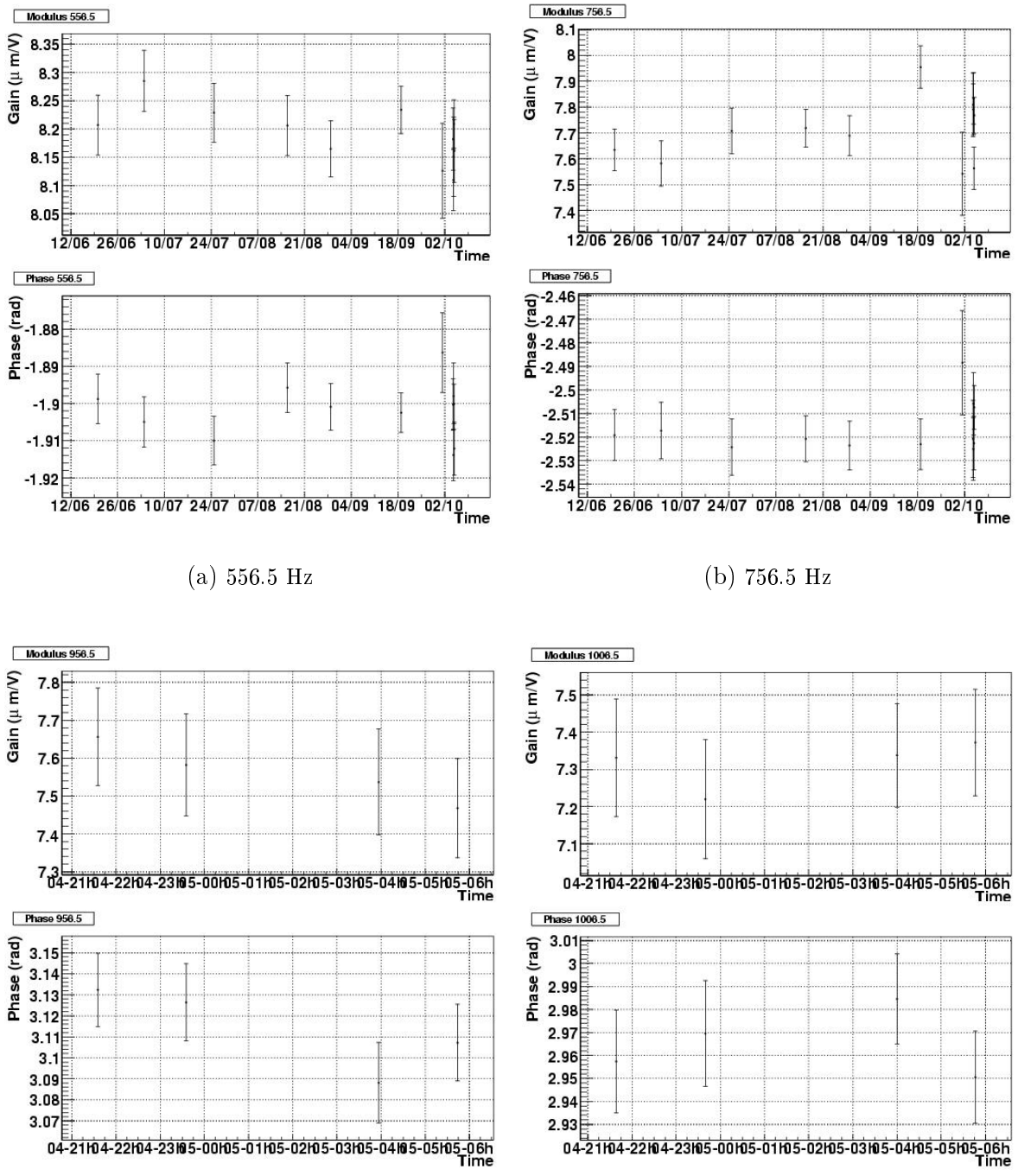

(a) 556.5 Hz

(b) 756.5 Hz

(c) 956.5 Hz

(d) 1006.5 Hz

Figure 2.4: ***WE mirror actuation TF vs time.*** *Modulus and phase as function of time (May to October 2007) at 556.5 Hz (a), 756.5 Hz (b), 956.5 Hz (c) and 1006.5 Hz (d).*

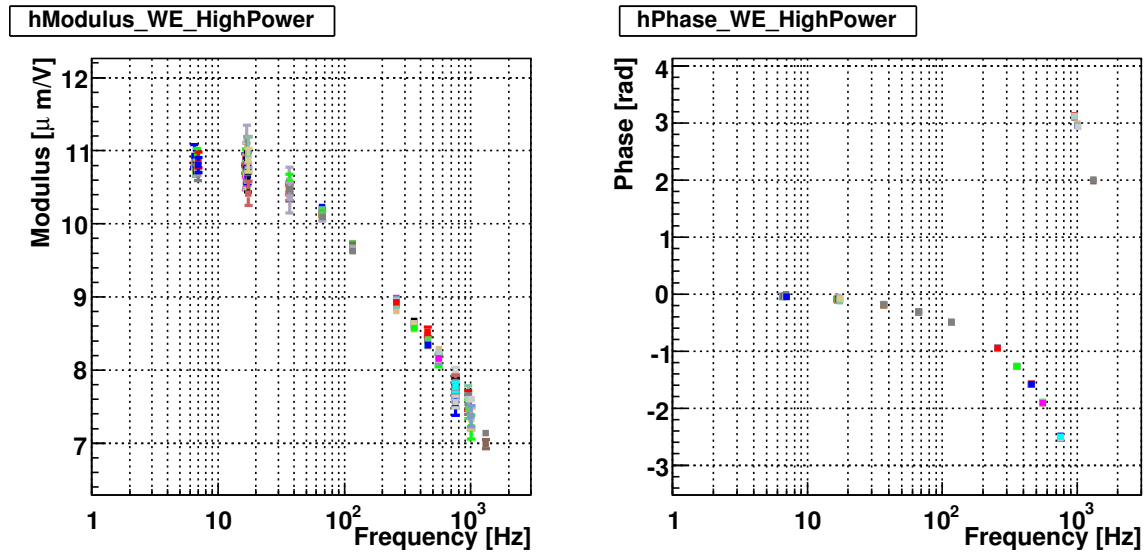

(a) WE TF in HP mode

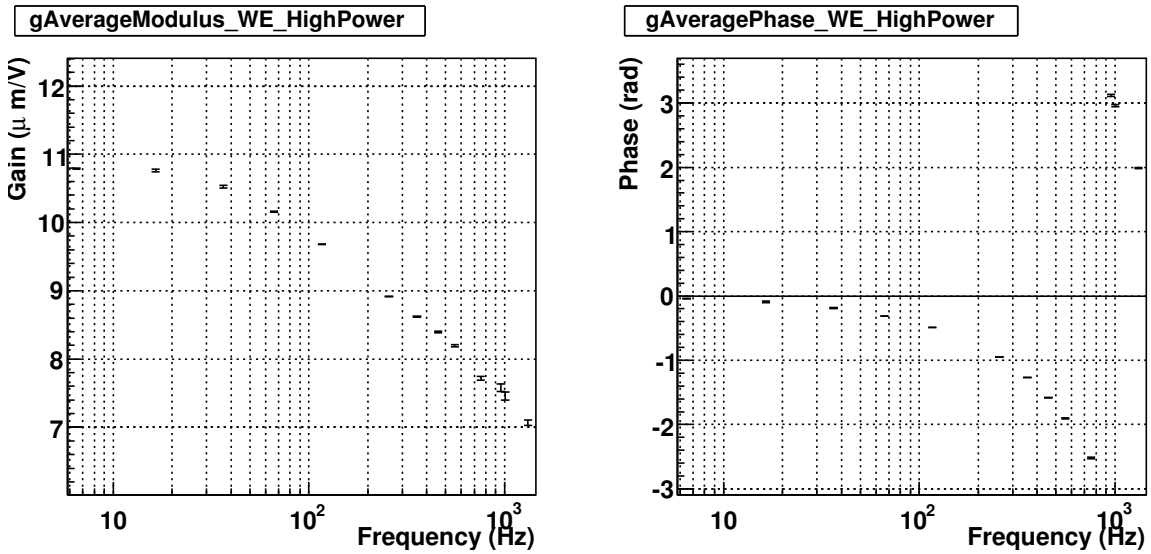

(b) WE averaged-TF in HP mode

Figure 2.5: ***WE mirror actuation TF in HP mode.*** *(a) Measurements from the different datasets (colors) from May to October 2007. (b) Average TF.*

Direct measurements from electronics

Electronic measurements were performed during the post-VSR1 calibration shifts in October and November 2007. They allow to measure precisely the LN/HP gain ratio of the actuation channels. The setup is described in the note [2].

The coil current is measured through a resistor and with the same sensing setup while the coil is switched from HP to LN mode. White noise is injected to the coil DSP through the LoopIn signal. The level of the injected noise is adapted to the actuation dynamic.

The figure 2.6 gives the LN/HP gain ratio obtained from the measurements for both actuators (up and down) of the WE mirror. The coherence between the signals is very high from a few Hz to 4 kHz. The LN/HP gain ratio is flat from a few Hz to a few hundreds of Hz, with values of the order of 1.15. The gain ratio and phase difference at the same frequencies as where the HP TF has been measured are given in the table 2.2.

The measurements have been performed only once, after the end of VSR1. The time variation of the TF ratio has not been monitored. A possible variation of a few % is expected due the coil driver modification of July 11th 2007 in particular.

2.1.3 Mirror actuator TF in LN mode

The mirror actuator TF in LN mode can be derived mutliplying the TF in HP mode and the LN/HP TF ratio. The table 2.3 gives the actuator gain and phase in LN mode for the WE tower.

The TF (modulus and phase) has been fit with different models. The DAC anti-alias filter [4] (p.65) (see fig. 2.10) has not been included in the models since its effect on the modulus is lower than 1% below 2 kHz. Its effect on the phase below 2 kHz is equivalent to a $177 \pm 5\mu$s delay. It is thus included in the fitted delay.

Three types of models were tested:

- model 1: a pole[1] and a zero[2],
- model 2: two poles and a zero,
- model 3: two poles and two zeros.

They have been fit on the modulus and phase simultaneously, with a free gain and delay. The fit parameters are given in the table 2.4.

The different fits of the WE mirror actuation in LN mode are shown on the figures 2.7, 2.8 and 2.9. The modulus in HP mode is also shown. For each fit, the phase has been corrected for the fitted delay in order to show the effect of the poles and zeros only. The red curves are the corresponding modulus and phase fit. The fit residuals are given in the right column. They are defined as:

[1] Simple pole: $TF(f) = \frac{1-\mathrm{i}\times x}{1+x^2}$, where $x = f/f_p$

[2] Simple zero: $TF(f) = 1 + \mathrm{i} \times \frac{f}{f_0}$

Freq (Hz)	Up channel		Down channel		Average	
	$\frac{g_{LN}}{g_{HP}}$	$\Phi_{LN} - \Phi_{HP}$ (rad)	$\frac{g_{LN}}{g_{HP}}$	$\Phi_{LN} - \Phi_{HP}$ (rad)	$\frac{g_{LN}}{g_{HP}}$	$\Phi_{LN} - \Phi_{HP}$ (rad)
6.5	1.171 ± 0.013	-0.007 ± 0.011	1.138 ± 0.016	-0.007 ± 0.014	1.155 ± 0.014	-0.007 ± 0.013
16.5	1.163 ± 0.007	-0.002 ± 0.007	1.143 ± 0.010	0.015 ± 0.009	1.153 ± 0.009	0.007 ± 0.008
36.5	1.152 ± 0.005	0.009 ± 0.004	1.144 ± 0.006	0.028 ± 0.006	1.148 ± 0.005	0.019 ± 0.005
66.5	1.152 ± 0.004	0.015 ± 0.003	1.149 ± 0.005	0.039 ± 0.005	1.151 ± 0.004	0.027 ± 0.004
116.5	1.146 ± 0.003	0.038 ± 0.003	1.163 ± 0.004	0.054 ± 0.004	1.154 ± 0.004	0.046 ± 0.004
256.5	1.153 ± 0.003	0.083 ± 0.003	1.159 ± 0.004	0.101 ± 0.003	1.156 ± 0.003	0.092 ± 0.003
356.5	1.152 ± 0.003	0.121 ± 0.003	1.158 ± 0.004	0.139 ± 0.003	1.155 ± 0.004	0.130 ± 0.003
456.5	1.153 ± 0.003	0.156 ± 0.003	1.169 ± 0.004	0.173 ± 0.004	1.161 ± 0.004	0.164 ± 0.003
556.5	1.165 ± 0.010	0.191 ± 0.009	1.169 ± 0.008	0.212 ± 0.007	1.167 ± 0.009	0.202 ± 0.008
756.5	1.178 ± 0.004	0.262 ± 0.004	1.190 ± 0.005	0.296 ± 0.004	1.184 ± 0.005	0.279 ± 0.004
956.5	1.229 ± 0.063	0.283 ± 0.053	1.205 ± 0.046	0.362 ± 0.039	1.217 ± 0.054	0.323 ± 0.046
1006.5	1.118 ± 0.062	0.371 ± 0.057	1.199 ± 0.089	0.453 ± 0.076	1.158 ± 0.075	0.412 ± 0.067
1316.5	1.276 ± 0.019	0.452 ± 0.015	1.314 ± 0.026	0.490 ± 0.020	1.295 ± 0.022	0.471 ± 0.018

Table 2.2: ***LN/HP TF ratio of the WE mirror actuators.*** *The gain ratio and phase difference of the LN/HP TF ratio are given for the up and down coil actuators. The average gain ratio is also given. Its error is set to the maximum value between the average error and the half of the difference of the up and down ratio.*

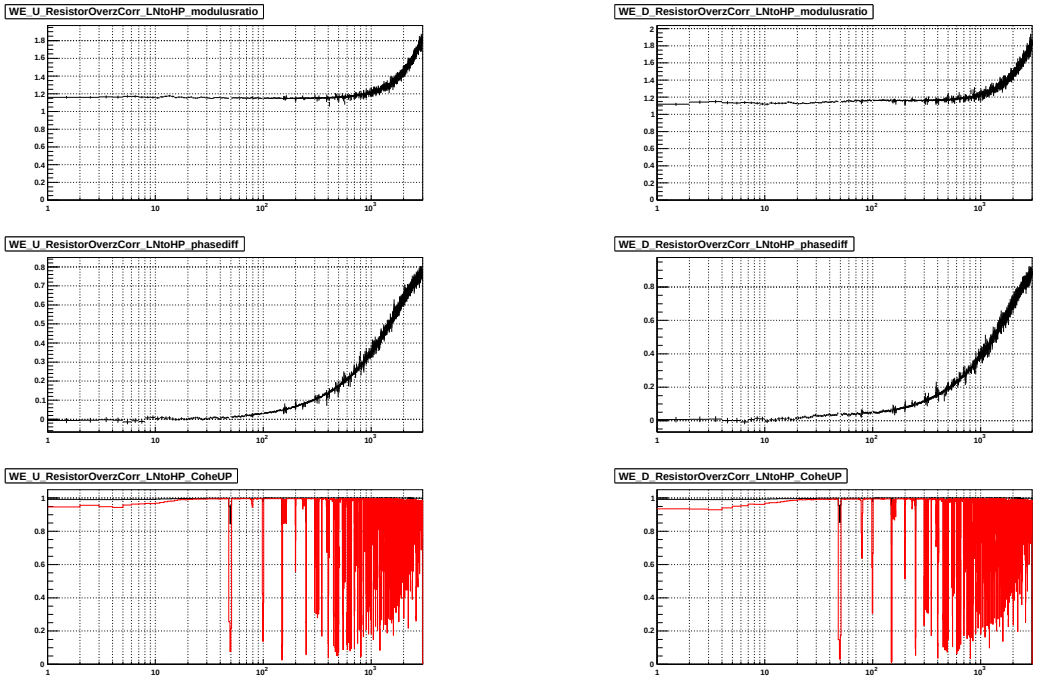

(a) WE up (b) WE down

Figure 2.6: ***LN/HP TF ratio of the WE actuators*** *obtained from direct electronic measurements. For both channels (up and down), the gain ratio and the phase difference are shown where both coherence were higher than 70%. The last figures show the coherence between zCorr and the coil current measurements both in HP (red) and LN (black) mode.*

Frequency (Hz)	Gain (μm/V)	Phase (rad)
6.5	12.458 ± 0.165	-0.046 ± 0.017
16.5	12.407 ± 0.118	-0.086 ± 0.020
36.5	12.083 ± 0.082	-0.167 ± 0.012
66.5	11.686 ± 0.054	-0.286 ± 0.007
116.5	11.173 ± 0.042	-0.446 ± 0.005
256.5	10.306 ± 0.037	-0.857 ± 0.005
356.5	9.956 ± 0.040	-1.137 ± 0.006
456.5	9.745 ± 0.045	-1.418 ± 0.008
556.5	9.558 ± 0.090	-1.700 ± 0.015
756.5	9.140 ± 0.068	-2.238 ± 0.017
956.5	9.225 ± 0.478	-2.845 ± 0.062
1006.5	8.636 ± 0.630	-2.912 ± 0.085
1316.5	9.156 ± 0.209	2.463 ± 0.026

Table 2.3: ***TF of the WE mirror actuation in LN mode.***

- the modulus residual is given in percentage: $100 \times \frac{g_{\rm data} - g_{\rm fit}}{g_{\rm data}}$
- the phase residual is given is rad: $\phi_{\rm data} - \phi_{\rm fit}$

The χ^2 probabilities show that only the model with two poles and two zeros is consistent with the data. However, the difference between the model and the data is less than 5% on the modulus and less than 3° on the phase for all the models below 1 kHz.

For comparison, the parametrisation used online during VSR1 is shown as the blue curve. Its shape consists in a pole at 100 Hz and a zero at 125 Hz. The used DC gain was 11.5 μm/V. The WE modulus was underestimated by about 10%. Also, the shape is somewhat different than the true mirror actuator TF.

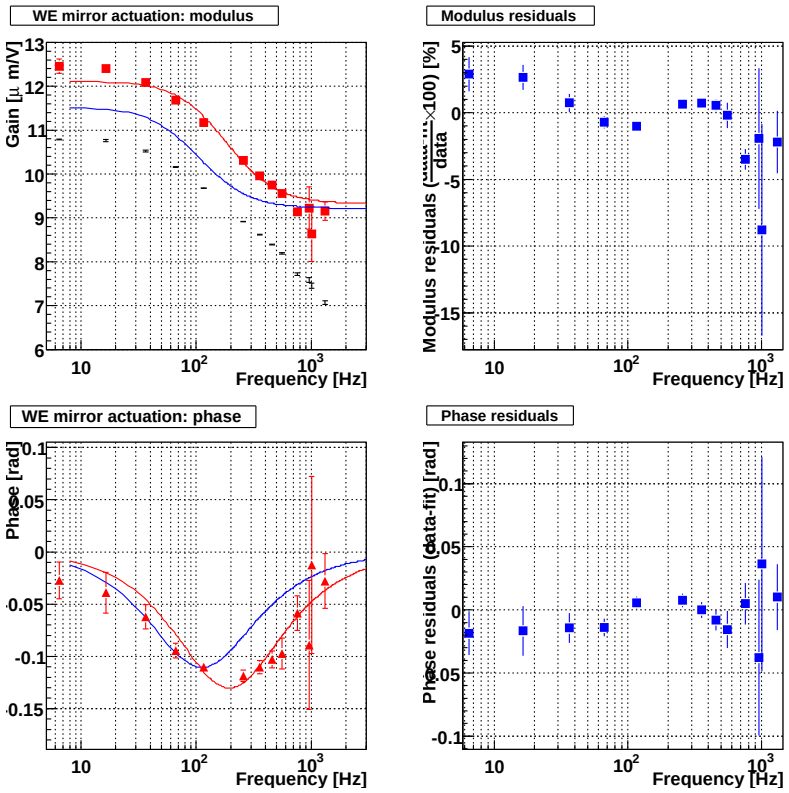

Figure 2.7: ***TF of the WE mirror actuation in LN mode fitted with one pole and one zero.*** *Left column: modulus and phase in LN mode. Right column: modulus and phase residuals of the fit. Black point: modulus in HP mode. Red squares: modulus in LN mode. Blue curve: parametrisation of the LN TF during VSR1. Red triangles: phase in LN mode, corrected for the fitted delay. Red curve: fit of the LN TF.*

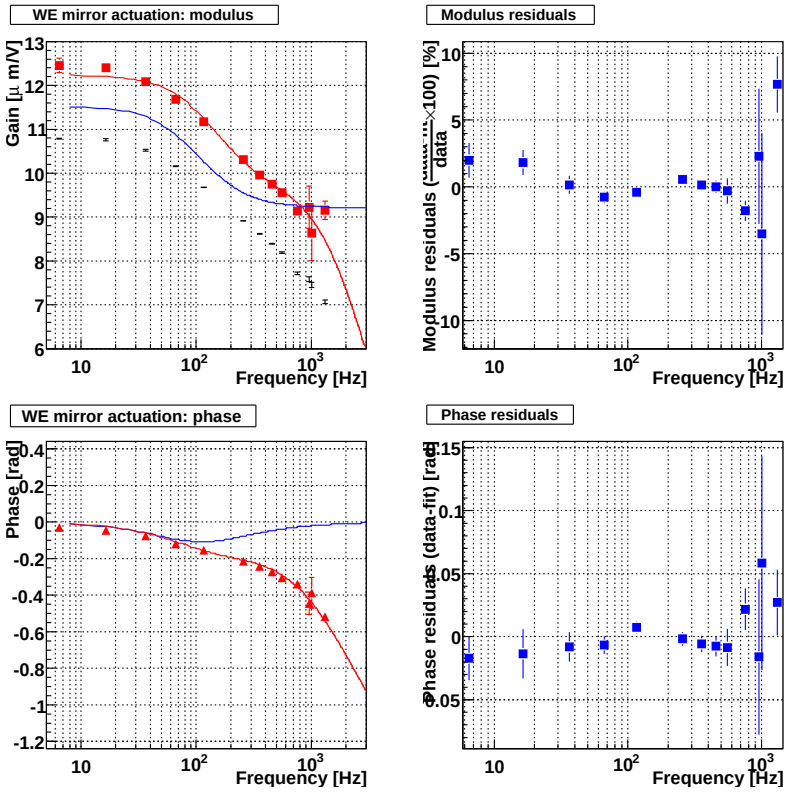

Figure 2.8: ***TF of the WE mirror actuation in LN mode fitted with two poles and one zero.*** *Left column: modulus and phase in LN mode. Right column: modulus and phase residuals of the fit. Black point: modulus in HP mode. Red squares: modulus in LN mode. Blue curve: parametrisation of the LN TF during VSR1. Red triangles: phase in LN mode, corrected for the fitted delay. Red curve: fit of the LN TF (phase corrected for the delay).*

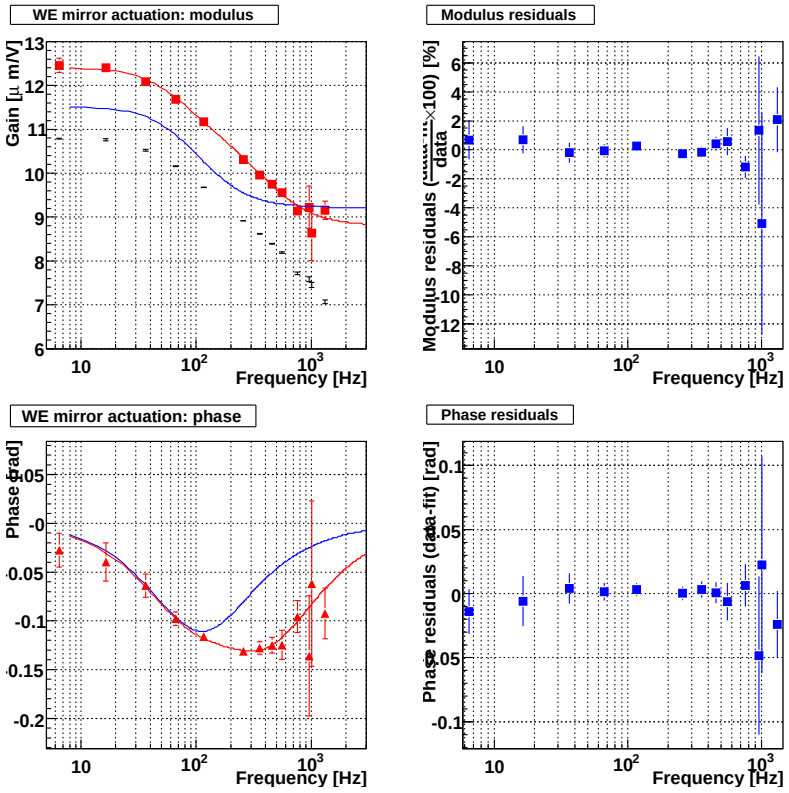

Figure 2.9: ***TF of the WE mirror actuation in LN mode fitted with two poles and two zeros.*** *Left column: modulus and phase in LN mode. Right column: modulus and phase residuals of the fit. Black point: modulus in HP mode. Red squares: modulus in LN mode. Blue curve: parametrisation of the LN TF during VSR1. Red triangles: phase in LN mode, corrected for the fitted delay. Red curve: fit of the LN TF (phase corrected for the delay).*

Model 1	Model 2	Model 3
$g = 12.10 \pm 0.04\,\mu$m/V	$g = 12.21 \pm 0.05\,\mu$m/V	$g = 12.39 \pm 0.08\,\mu$m/V
$t_d = 458.5 \pm 1.7\,\mu$s	$t_d = 399.3 \pm 5.5\,\mu$s	$t_d = 450.7 \pm 2.3\,\mu$s
$\phi_0 = 0$	$\phi_0 = 0$	$\phi_0 = 0$
$f_p = 170.2 \pm 6.6$ Hz	$f_p = 137.4 \pm 8.5$ Hz	$f_p = 81.2 \pm 15.6$ Hz
$f_0 = 221.4 \pm 9.0$ Hz	$f_0 = 173 \pm 11$ Hz	$f_0 = 93.7 \pm 20.1$ Hz
-	$f_p = 2312 \pm 239$ Hz	$f_p = 390 \pm 84$ Hz
-	-	$f_0 = 476 \pm 98$ Hz
$P(\chi^2) \sim 10^{-4}\%$	$P(\chi^2) \sim 0.7\%$	$P(\chi^2) \sim 96\%$

Table 2.4: ***Fit results of the mirror actuation TF of WE in LN mode*** *for the three different simple pole and zero models discussed in the text. The last line indicates the χ^2 probability of the fit.*

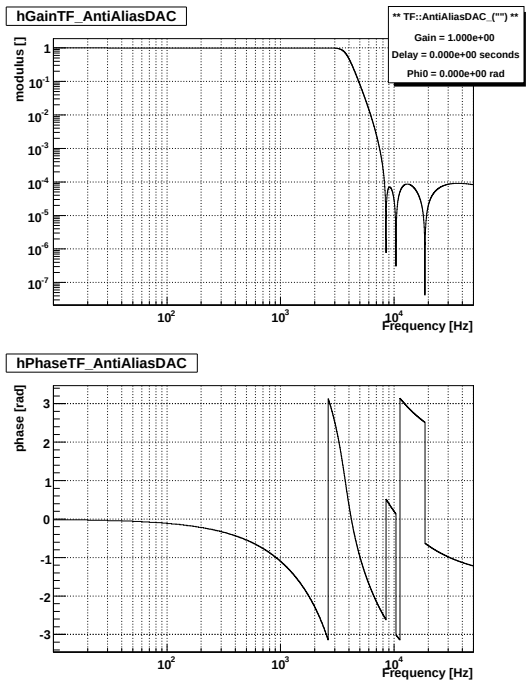

Figure 2.10: ***Parametrisation of the TF of the DAC anti-alias filter*** *of an actuation channel.*

2.2 NE mirror actuator calibration

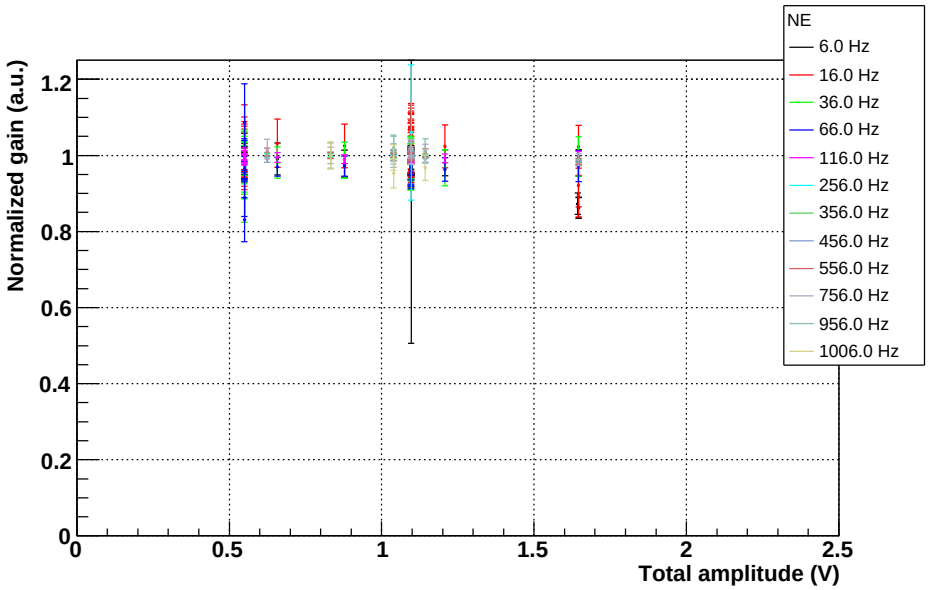

Figure 2.11: ***NE mirror actuation TF vs the amplitude*** *of the injected signal on zCorr. The gain is flat for injected signal up to 1.5 V.*

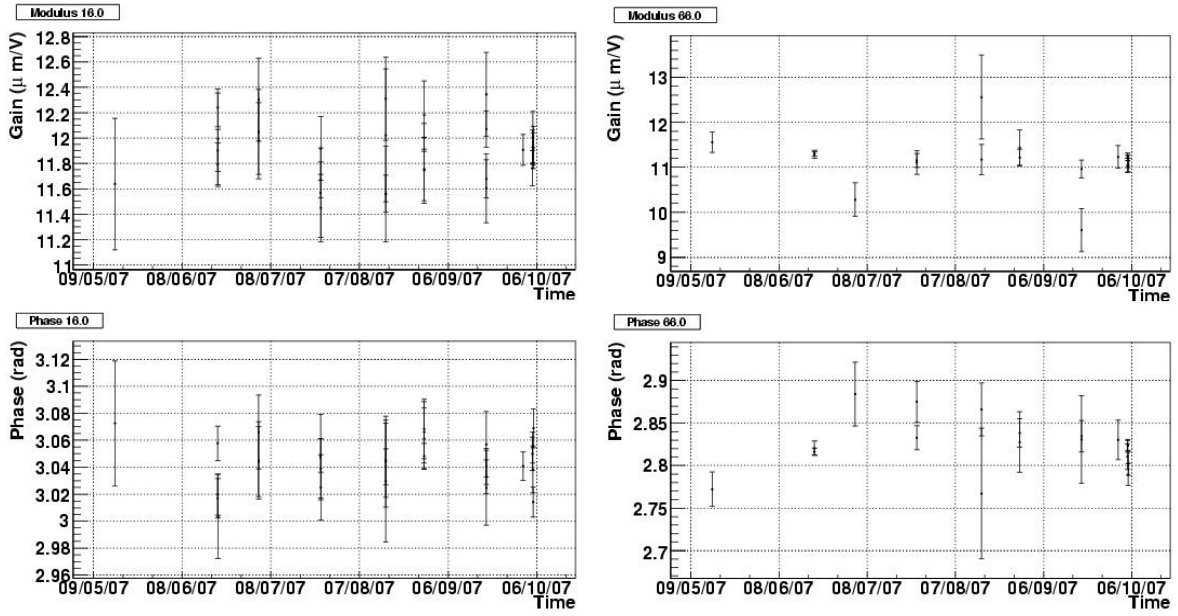

(a) 16.0 Hz

(b) 66.0 Hz

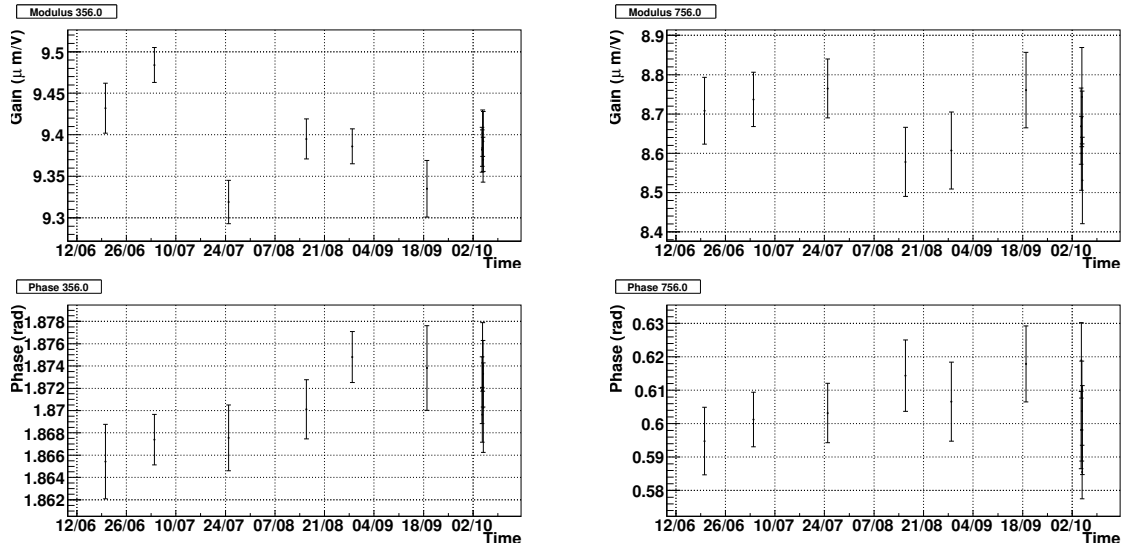

(c) 356.0 Hz

(d) 756.0 Hz

Figure 2.12: ***NE mirror actuation TF vs time.*** *Modulus and phase as function of time (May to October 2007) at 16.0 Hz (a), 66.0 Hz (b), 356.0 Hz (c) and 756.0 Hz (d).*

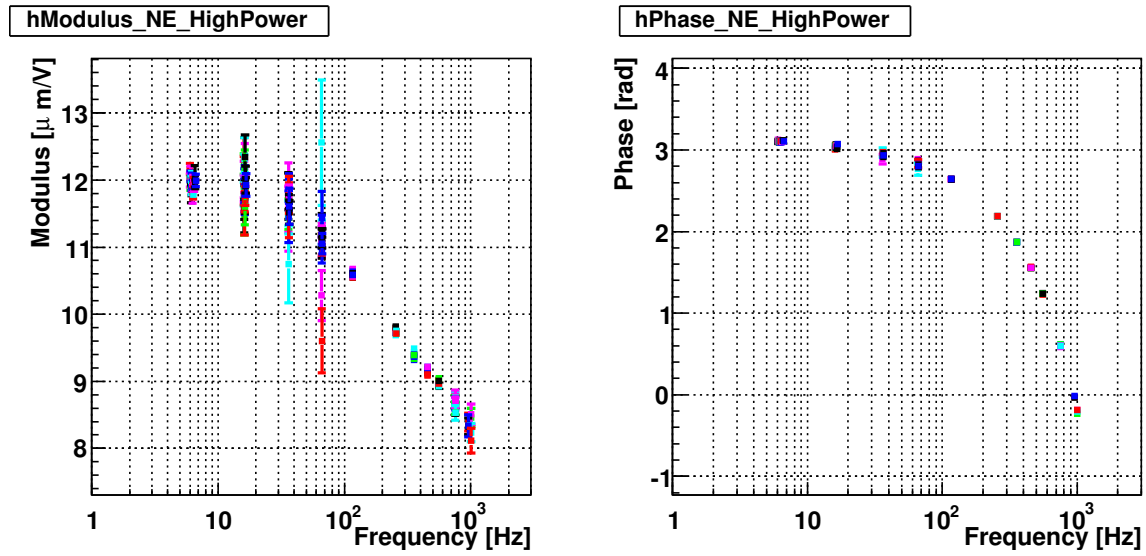

(a) NE TF in HP mode

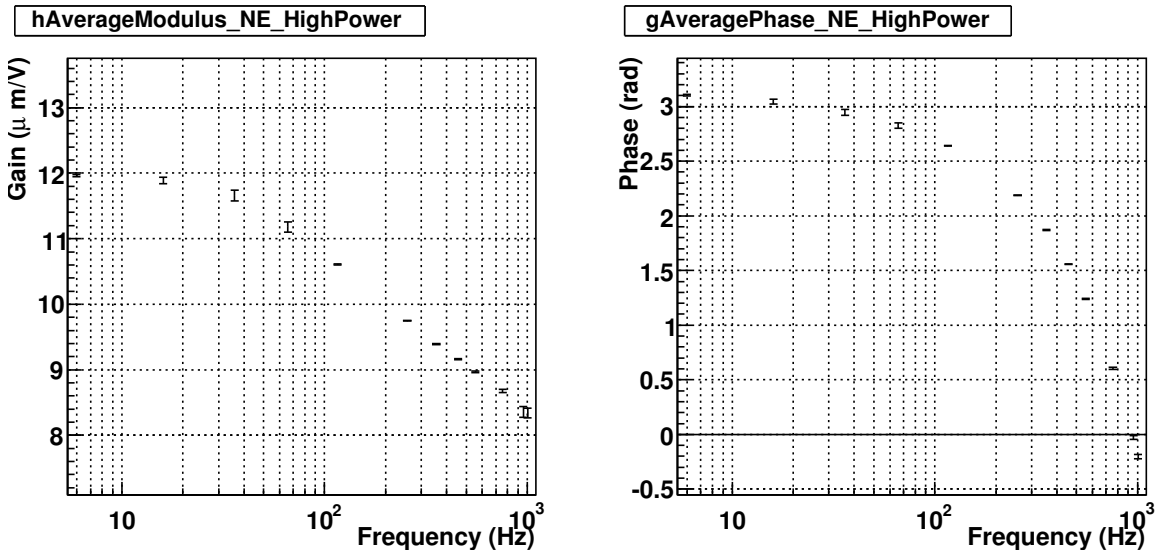

(b) NE averaged-TF in HP mode

Figure 2.13: ***NE mirror actuation TF in HP mode.*** *(a) Measurements from the different datasets (colors) from May to October 2007. (b) Average TF.*

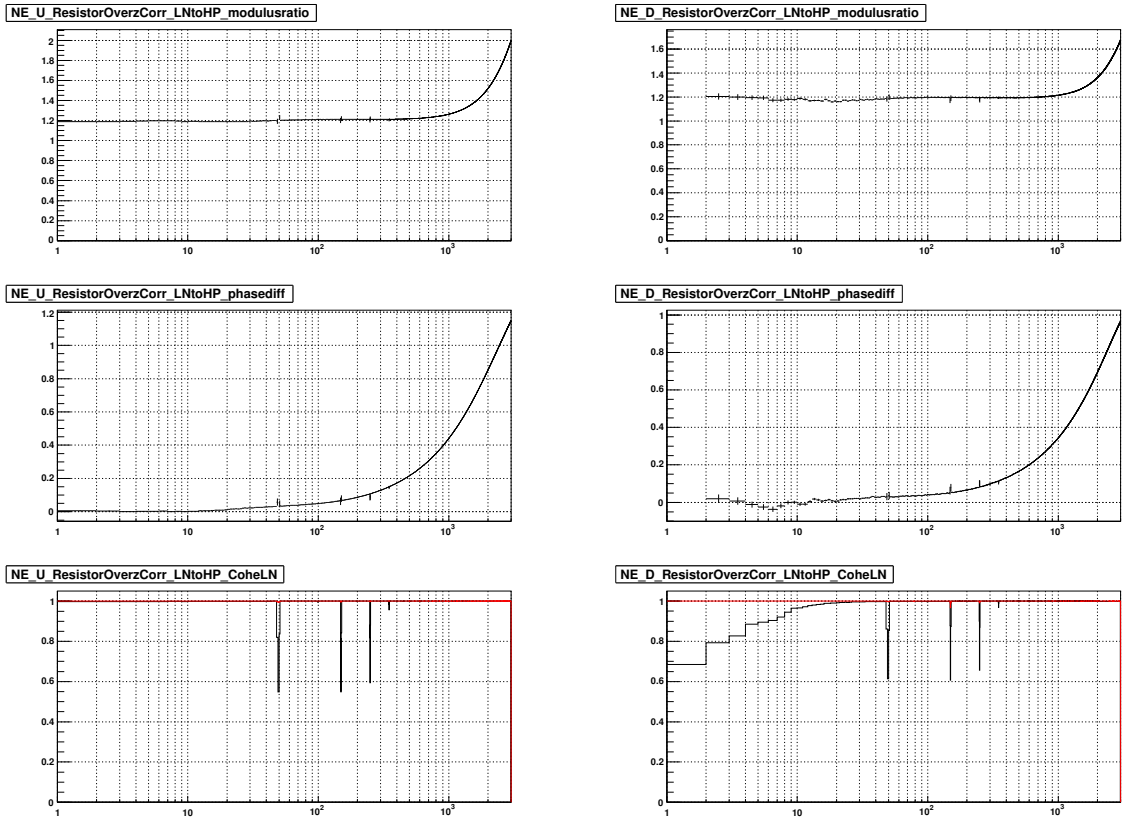

(a) NE up

(b) NE down

Figure 2.14: ***LN/HP TF ratio of the NE actuators*** *obtained from direct electronic measurements. For both channels (up and down), the gain ratio and the phase difference are shown where both coherence were higher than 70%. The last figures show the coherence between zCorr and the coil current measurements both in HP (red) and LN (black) mode.*

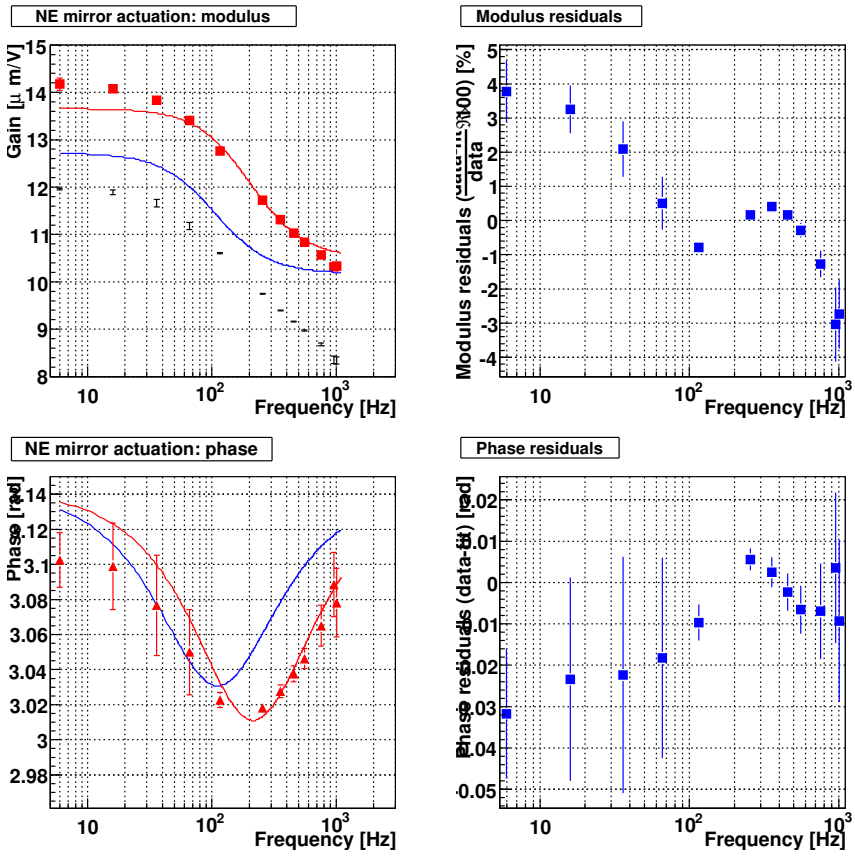

Figure 2.15: ***TF of the NE mirror actuation in LN mode fitted with one pole and one zero.*** *Left column: modulus and phase in LN mode. Right column: modulus and phase residuals of the fit. Black point: modulus in HP mode. Red squares: modulus in LN mode. Blue curve: parametrisation of the LN TF during VSR1. Red triangles: phase in LN mode, corrected for the fitted delay. Red curve: fit of the LN TF.*

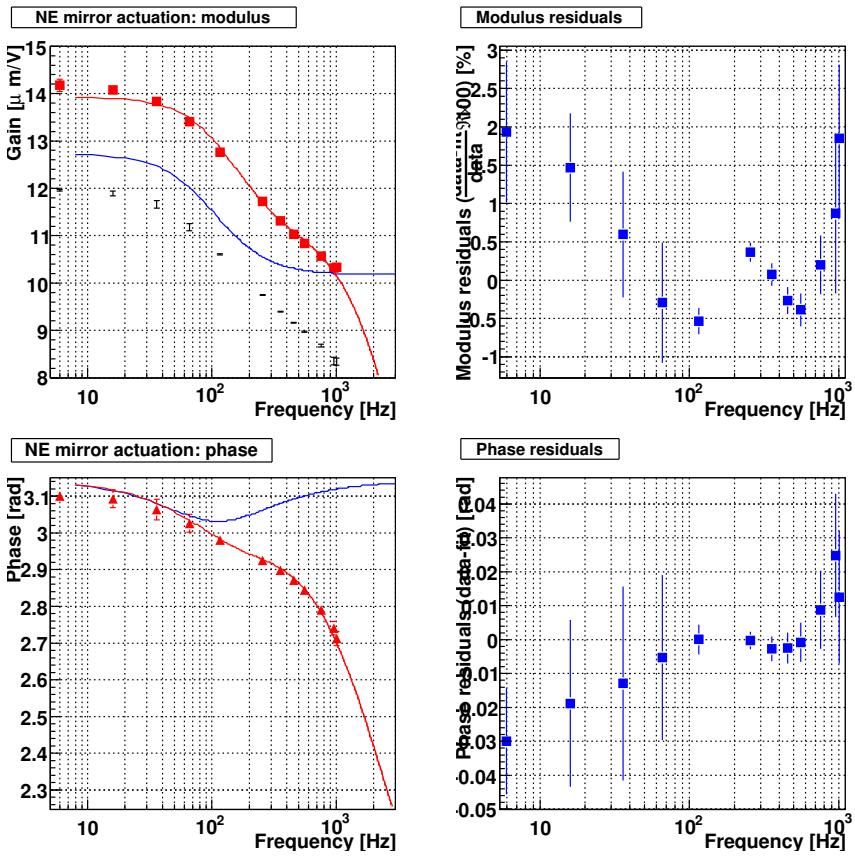

Figure 2.16: ***TF of the NE mirror actuation in LN mode fitted with two poles and one zero.*** *Left column: modulus and phase in LN mode. Right column: modulus and phase residuals of the fit. Black point: modulus in HP mode. Red squares: modulus in LN mode. Blue curve: parametrisation of the LN TF during VSR1. Red triangles: phase in LN mode, corrected for the fitted delay. Red curve: fit of the LN TF (phase corrected for the delay).*

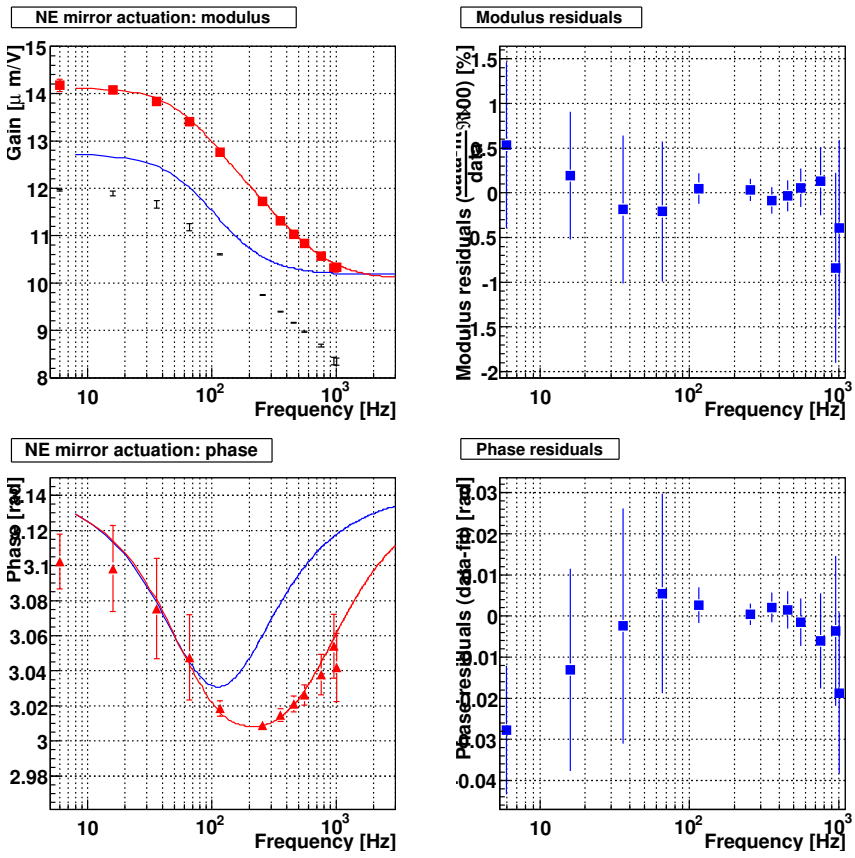

Figure 2.17: ***TF of the NE mirror actuation in LN mode fitted with two poles and two zeros.*** *Left column: modulus and phase in LN mode. Right column: modulus and phase residuals of the fit. Black point: modulus in HP mode. Red squares: modulus in LN mode. Blue curve: parametrisation of the LN TF during VSR1. Red triangles: phase in LN mode, corrected for the fitted delay. Red curve: fit of the LN TF (phase corrected for the delay).*

Frequency (Hz)	Gain (μm/V)	χ^2/ndf	Phase (rad)	χ^2/ndf
6.0	11.960 ± 0.017	41.0/35	3.1037 ± 0.0014	36.2/35
16.0	11.889 ± 0.049	32.2/29	3.0431 ± 0.0043	26.8/29
36.0	11.658 ± 0.078	9.0/17	2.9455 ± 0.0071	19.3/17
66.0	11.179 ± 0.076	34.6/17	2.8216 ± 0.0069	28.6/17
116.0	10.606 ± 0.010	32.4/17	2.6405 ± 0.0009	14.1/17
256.0	9.747 ± 0.006	59.6/10	2.1871 ± 0.0006	7.2/10
356.0	9.392 ± 0.008	32.8/10	1.8708 ± 0.0009	12.6/10
456.0	9.160 ± 0.011	16.2/10	1.5566 ± 0.0012	11.1/10
556.0	8.969 ± 0.014	8.6/10	1.2385 ± 0.0016	15.8/10
756.0	8.677 ± 0.028	7.6/10	0.6032 ± 0.0034	10.8/10
956.0	8.353 ± 0.082	0.1/ 2	-0.0283 ± 0.0102	0.8/ 2
1006.0	8.340 ± 0.076	4.2/ 3	-0.2035 ± 0.0095	4.6/ 3

Table 2.5: ***Time-average actuation TF of the NE suspension in HP mode****. All the good quality data from May 2007 were used. The χ^2 test for a constant value as function of time was performed for the gain and the phase.*

Freq (Hz)	Up channel		Down channel		Average	
	$\frac{g_{LN}}{g_{HP}}$	$\Phi_{LN} - \Phi_{HP}$ (rad)	$\frac{g_{LN}}{g_{HP}}$	$\Phi_{LN} - \Phi_{HP}$ (rad)	$\frac{g_{LN}}{g_{HP}}$	$\Phi_{LN} - \Phi_{HP}$ (rad)
6.0	1.197 ± 0.002	0.003 ± 0.002	1.174 ± 0.016	-0.036 ± 0.014	1.185 ± 0.009	-0.016 ± 0.008
16.0	1.189 ± 0.002	0.009 ± 0.001	1.179 ± 0.005	0.010 ± 0.005	1.184 ± 0.004	0.009 ± 0.003
36.0	1.195 ± 0.001	0.027 ± 0.0009	1.178 ± 0.003	0.028 ± 0.002	1.187 ± 0.002	0.027 ± 0.002
66.0	1.205 ± 0.0008	0.039 ± 0.0007	1.194 ± 0.002	0.033 ± 0.001	1.199 ± 0.001	0.036 ± 0.001
116.0	1.211 ± 0.0006	0.055 ± 0.0006	1.196 ± 0.001	0.045 ± 0.001	1.203 ± 0.0010	0.050 ± 0.0008
256.0	1.211 ± 0.0005	0.109 ± 0.0004	1.194 ± 0.001	0.085 ± 0.0010	1.203 ± 0.0008	0.097 ± 0.0007
356.0	1.212 ± 0.0004	0.153 ± 0.0004	1.196 ± 0.001	0.119 ± 0.0009	1.204 ± 0.0007	0.136 ± 0.0006
456.0	1.215 ± 0.0004	0.196 ± 0.0004	1.193 ± 0.001	0.150 ± 0.0009	1.204 ± 0.0007	0.173 ± 0.0006
556.0	1.220 ± 0.0005	0.241 ± 0.0004	1.195 ± 0.001	0.186 ± 0.0009	1.208 ± 0.0007	0.213 ± 0.0006
756.0	1.234 ± 0.0004	0.330 ± 0.0004	1.202 ± 0.001	0.256 ± 0.0009	1.218 ± 0.0007	0.293 ± 0.0006
956.0	1.257 ± 0.0006	0.421 ± 0.0005	1.213 ± 0.001	0.327 ± 0.001	1.235 ± 0.0009	0.374 ± 0.0008
1006.0	1.263 ± 0.0005	0.443 ± 0.0004	1.214 ± 0.001	0.346 ± 0.0009	1.239 ± 0.0008	0.395 ± 0.0007

Table 2.6: ***LN/HP TF ratio of the NE mirror actuators.*** *The gain ratio and phase difference of the LN/HP TF ratio are given for the up and down coil actuators. The average gain ratio is also given.*

Frequency (Hz)	Gain (μm/V)	Phase (rad)
6.0	14.175 ± 0.132	3.085 ± 0.016
16.0	14.081 ± 0.101	3.053 ± 0.025
36.0	13.835 ± 0.114	2.974 ± 0.029
66.0	13.407 ± 0.105	2.861 ± 0.024
116.0	12.762 ± 0.022	2.690 ± 0.004
256.0	11.725 ± 0.015	2.284 ± 0.003
356.0	11.310 ± 0.017	2.007 ± 0.004
456.0	11.031 ± 0.019	1.730 ± 0.005
556.0	10.832 ± 0.023	1.452 ± 0.006
756.0	10.569 ± 0.040	0.897 ± 0.012
956.0	10.314 ± 0.108	0.347 ± 0.018
1006.0	10.332 ± 0.101	0.193 ± 0.020

Table 2.7: ***TF of the NE mirror actuation in LN mode.***

Model 1	Model 2	Model 3
$g = 13.64 \pm 0.04\,\mu$m/V	$g = 13.91 \pm 0.06\,\mu$m/V	$g = 14.11 \pm 0.07\,\mu$m/V
$t_d = 456.5 \pm 0.9\,\mu$s	$t_d = 398.6 \pm 3.0\,\mu$s	$t_d = 450.7 \pm 1.4\,\mu$s
$\phi_0 = \pi$	$\phi_0 = \pi$	$\phi_0 = \pi$
$f_p = 189.7 \pm 4.7$ Hz	$f_p = 146.0 \pm 5.7$ Hz	$f_p = 101.7 \pm 8.9$ Hz
$f_0 = 246.7 \pm 61$ Hz	$f_0 = 185.2 \pm 7.3$ Hz	$f_0 = 121.0 \pm 12.2$ Hz
-	$f_p = 2353 \pm 134$ Hz	$f_p = 423 \pm 63$ Hz
-	-	$f_0 = 498 \pm 70$ Hz
$P(\chi^2) \sim 10^{-14}\%$	$P(\chi^2) \sim 0.05\%$	$P(\chi^2) \sim 98\%$

Table 2.8: ***Fit results of the mirror actuation TF of NE in LN mode*** *for the three different models discussed in the text. The last line indicates the χ^2 probability of the fit.*

2.3 WI mirror actuator calibration

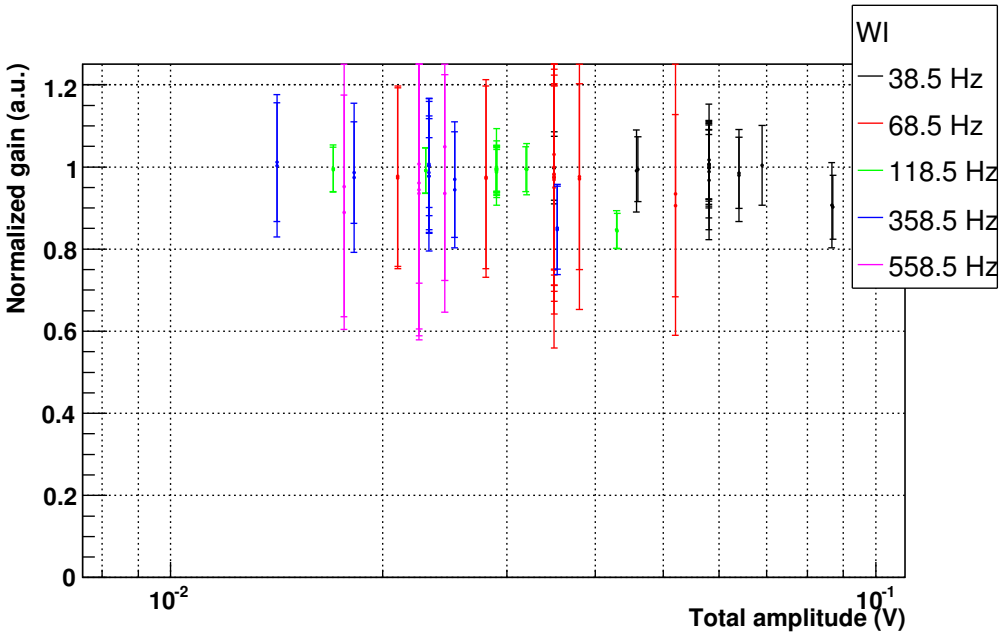

Figure 2.18: ***WI mirror actuator gain vs the amplitude*** *of the injected signal on zCorr for the data from August 2007. End of July 2007, emphasis filters have been added on the HP channels, before the DAC of the input mirror actuators. The maximum non-saturated amplitude thus decreases when the frequency increases. A slight effect can be seen at 38 and 118 Hz.*

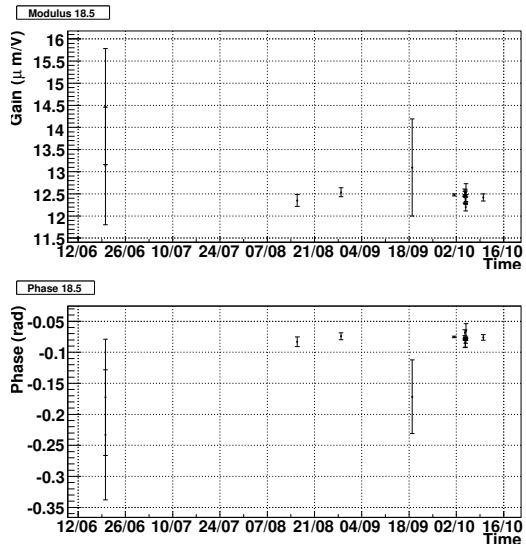

(a) 18.5 Hz

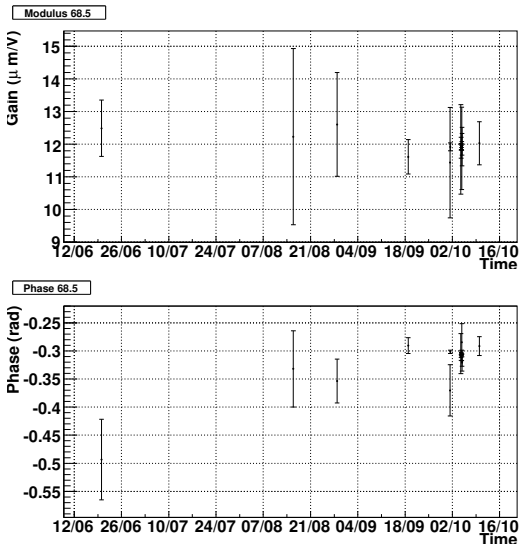

(b) 68.5 Hz

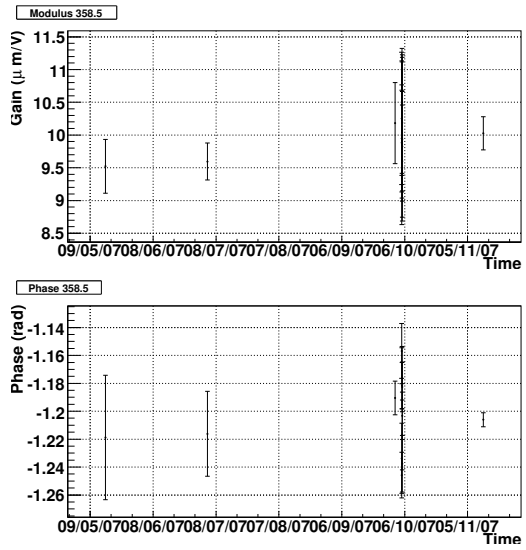

(c) 358.5 Hz

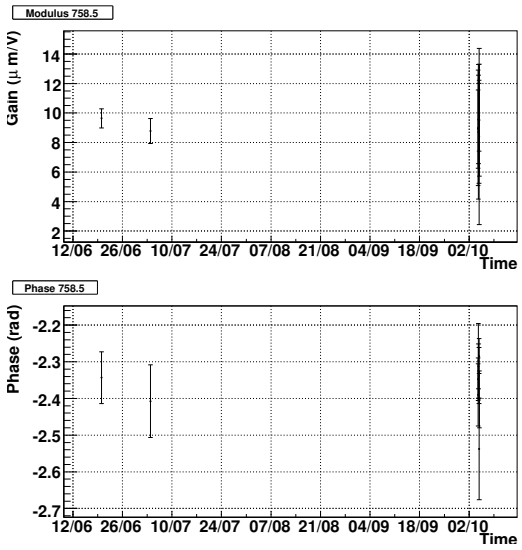

(d) 758.5 Hz

Figure 2.19: ***WI mirror actuation vs time.*** *Modulus and phase as function of time (May to October 2007) at 18.5 Hz (a), 68.5 Hz (b), 358.5 Hz (c) and 758.5 Hz (d).*

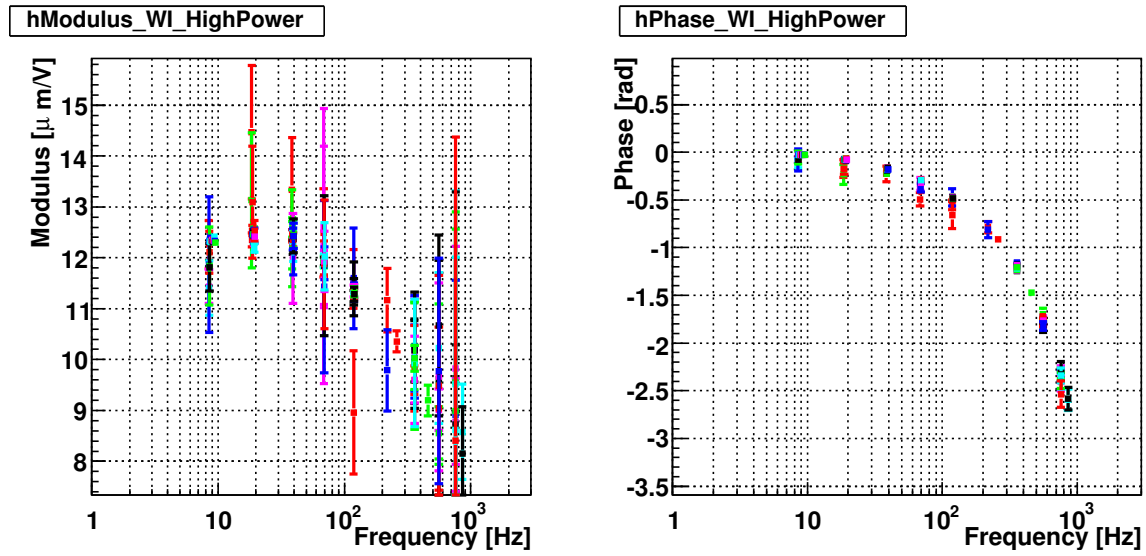

(a) WI TF in HP mode

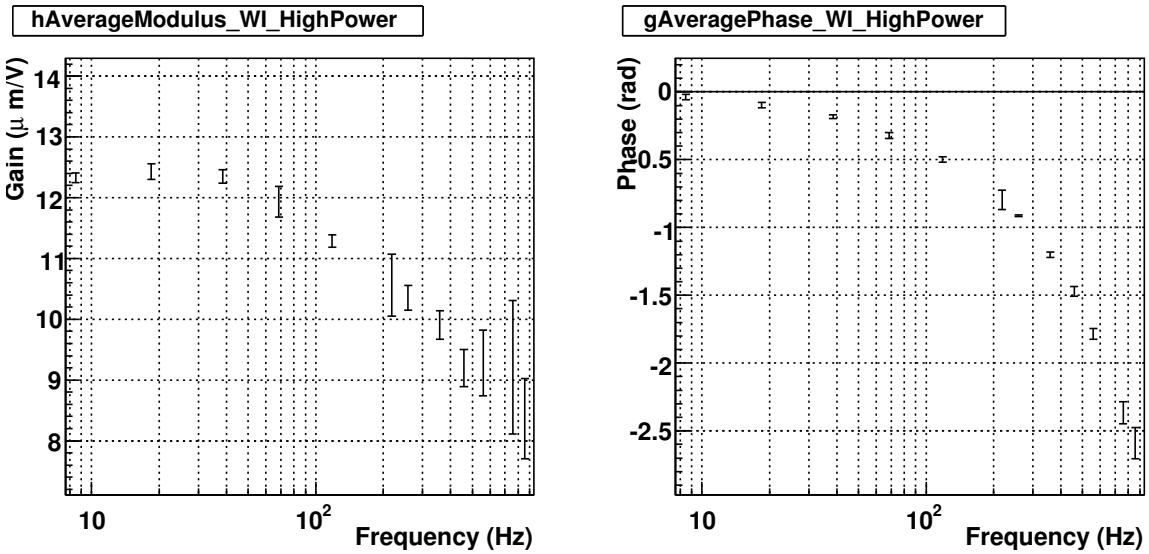

(b) WI averaged-TF in HP mode

Figure 2.20: ***WI mirror actuation TF in HP mode.*** *(a) Measurements from the different datasets (colors) from March to October 2007. (b) Average TF.*

Frequency (Hz)	Gain (μm/V)	χ^2/ndf	Phase (rad)	χ^2/ndf
8.5	12.326 ± 0.082	243.2/23	-0.04 ± 0.02	19705.5/23
18.5	12.430 ± 0.129	82.2/16	-0.10 ± 0.02	1650.0/16
38.5	12.351 ± 0.112	7.2/16	-0.18 ± 0.01	104.5/16
68.5	11.933 ± 0.251	1.6/16	-0.32 ± 0.02	462.2/16
118.5	11.283 ± 0.102	12.3/17	-0.50 ± 0.02	510.4/17
218.5	10.562 ± 0.508	1.9/ 1	-0.80 ± 0.07	0.07/ 1
258.5	10.354 ± 0.206	0./ 0	-0.91 ± 0.004	0./ 0
358.5	9.905 ± 0.231	3.1/13	-1.20 ± 0.02	30.8/13
458.5	9.198 ± 0.303	0./ 0	-1.47 ± 0.03	0./ 0
558.5	9.282 ± 0.541	3.6/ 9	-1.78 ± 0.04	12.6/ 9
758.5	9.211 ± 1.098	0.8/ 9	-2.37 ± 0.08	6.5/ 9
858.5	8.364 ± 0.657	0.1/ 1	-2.59 ± 0.12	0.003/ 1

Table 2.9: ***Time-average actuation TF of the WI mirror in HP mode****. All the good quality data from May 2007 were used. The χ^2 test for a constant value as function of time was performed for the gain and the phase.*

2.4 NI mirror actuator calibration

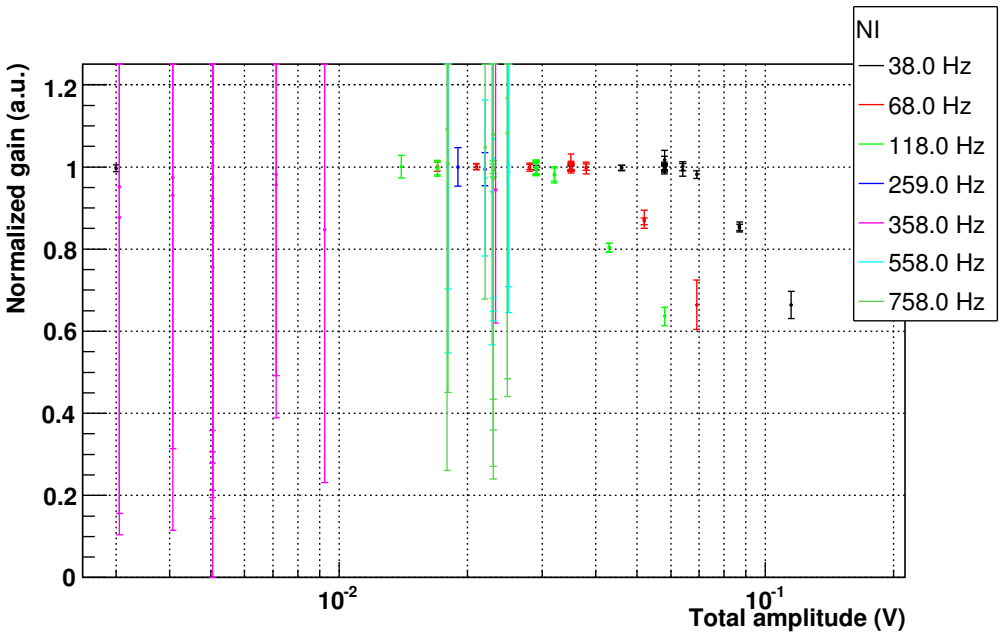

Figure 2.21: ***NI mirror actuation gain vs the amplitude*** *of the injected signal on zCorr for the data from August 2007. End of July 2007, emphasis filters have been added on the HP channels, before the DAC of the input mirror actuators. The maximum non-saturated amplitude thus decreases when the frequency increases as seen on the figure.*

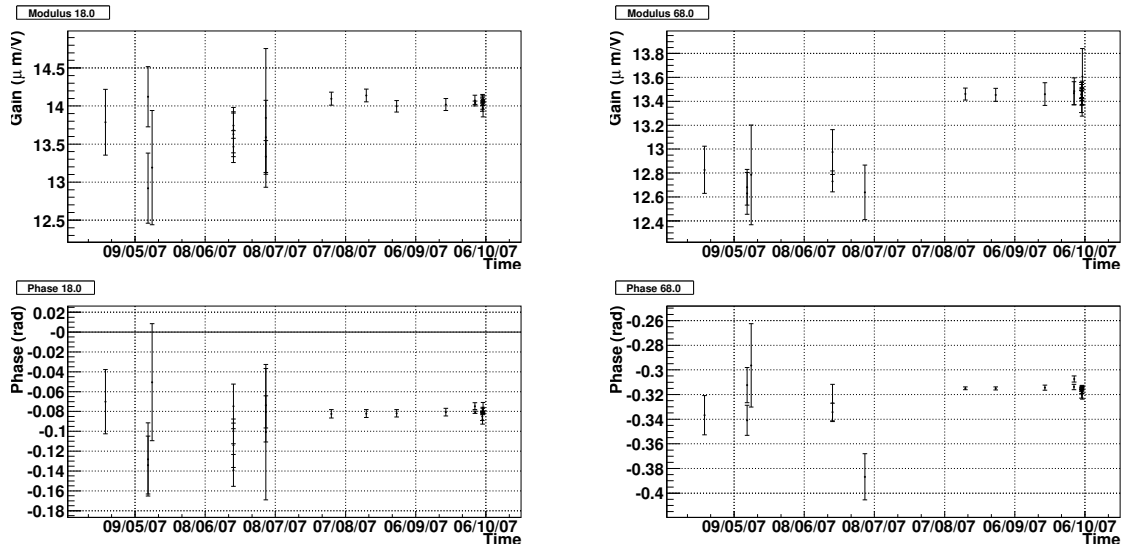

(a) 18.0 Hz

(b) 68.0 Hz

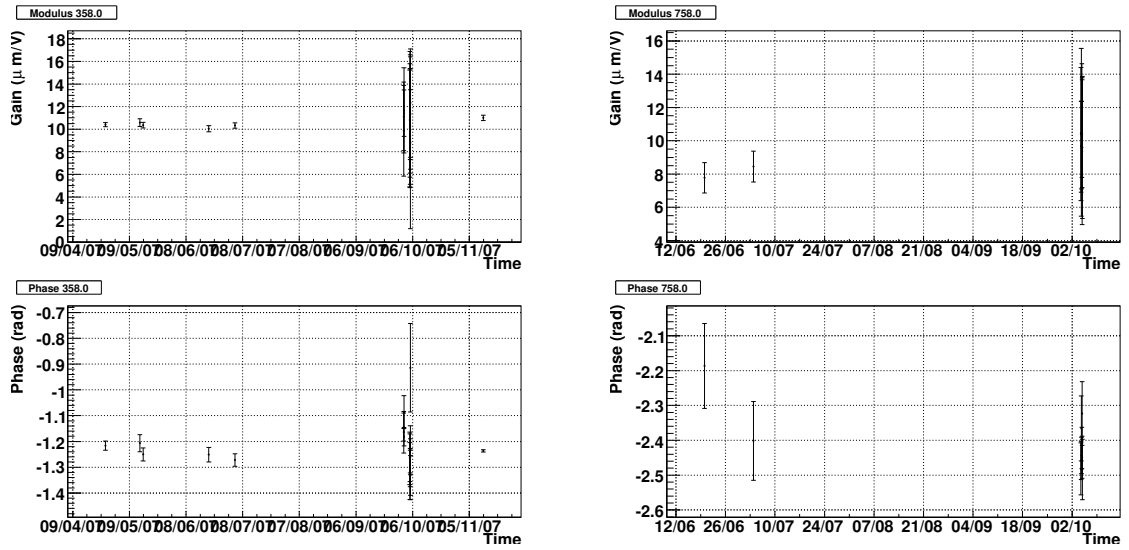

(c) 358.0 Hz

(d) 758.0 Hz

Figure 2.22: ***NI mirror actuation TF vs time.*** *Modulus and phase as function of time (May to October 2007) at 18.0 Hz (a), 68.0 Hz (b), 358.0 Hz (c) and 758.0 Hz (d).*

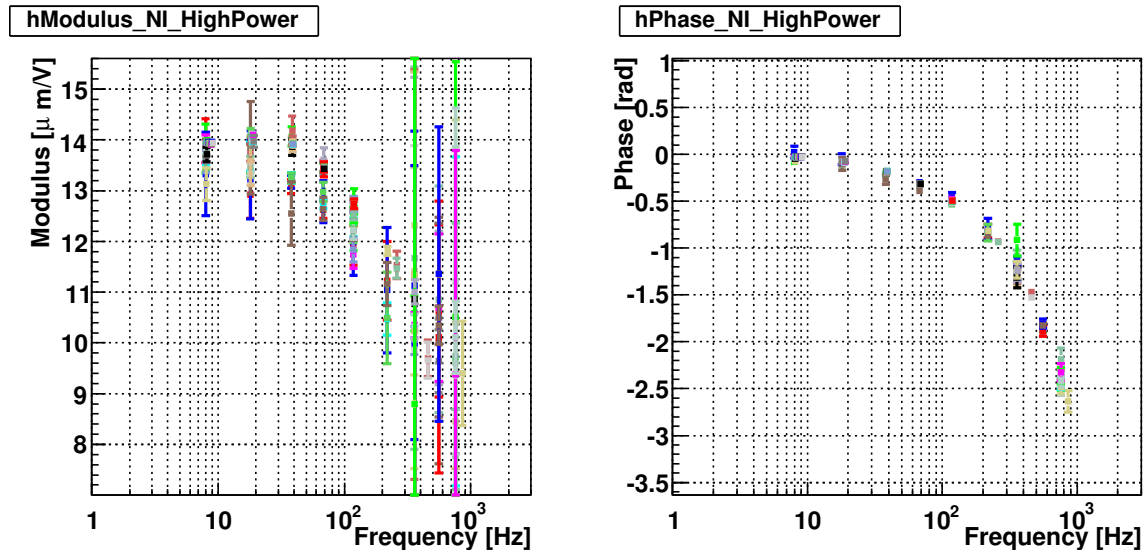

(a) NI TF in HP mode

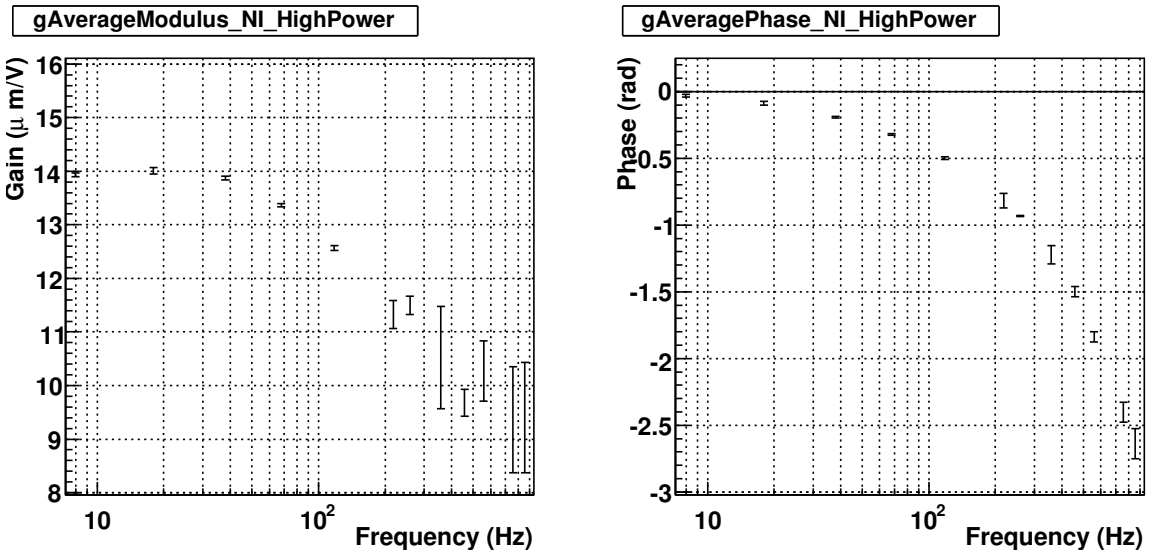

(b) NI averaged-TF in HP mode

Figure 2.23: ***NI mirror actuation TF in HP mode.*** *(a) Measurements from the different datasets (colors) from May to October 2007. (b) Average TF.*

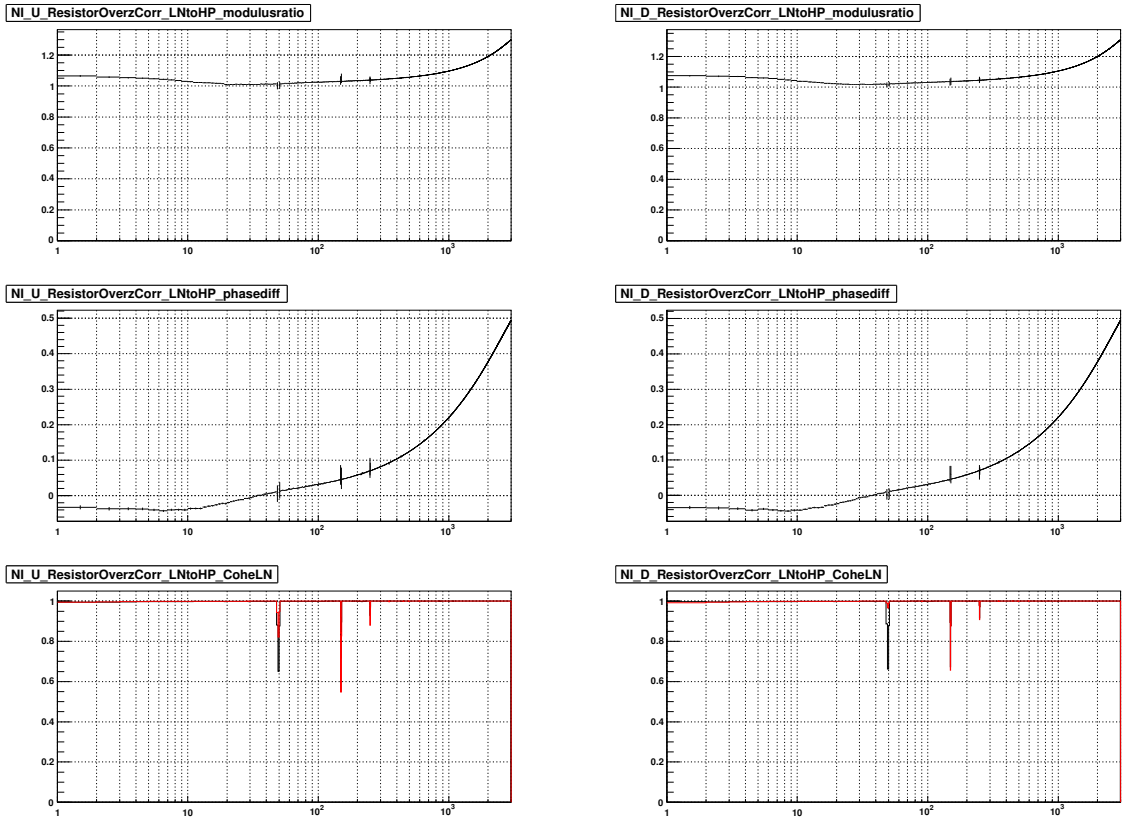

(a) NI up

(b) NI down

Figure 2.24: ***LN/HP TF ratio of the NI mirror actuators*** *obtained from direct electronic measurements. For both channels (up and down), the gain ratio and the phase difference are shown where both coherence were higher than 70%. The last figures show the coherence between zCorr and the coil current measurements both in HP (red) and LN (black) mode.*

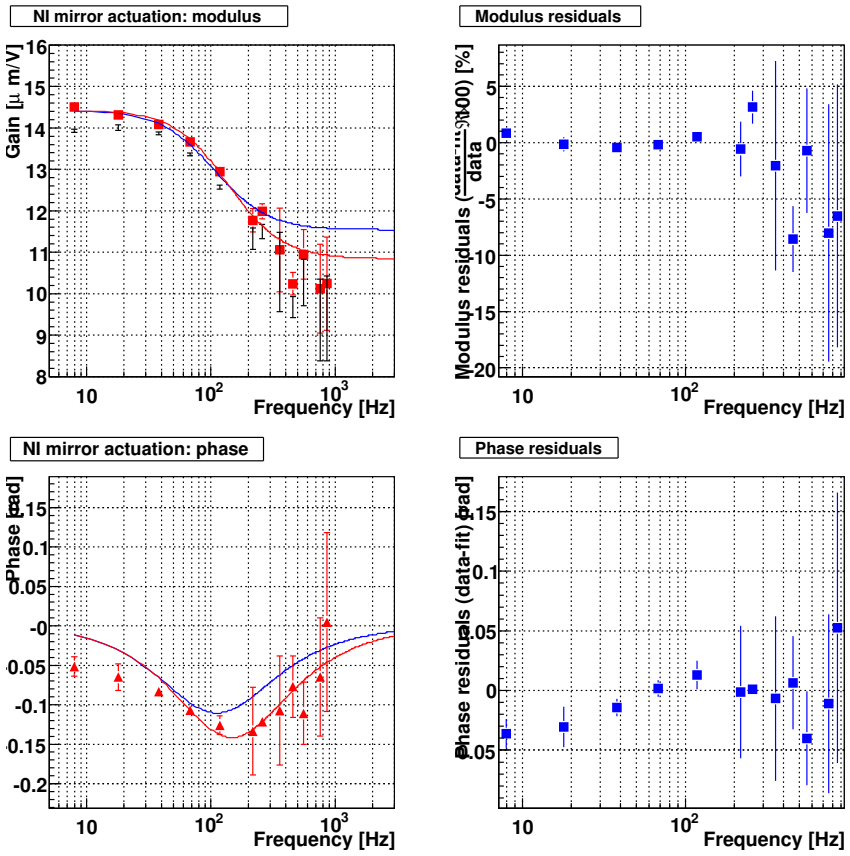

Figure 2.25: ***TF of the NI mirror actuation in LN mode fitted with one pole and one zero.*** *Left column: modulus and phase in LN mode. Right column: modulus and phase residuals of the fit. Black point: modulus in HP mode. Red squares: modulus in LN mode. Blue curve: parametrisation of the LN TF during VSR1. Red triangles: phase in LN mode, corrected for the fitted delay. Red curve: fit of the LN TF.*

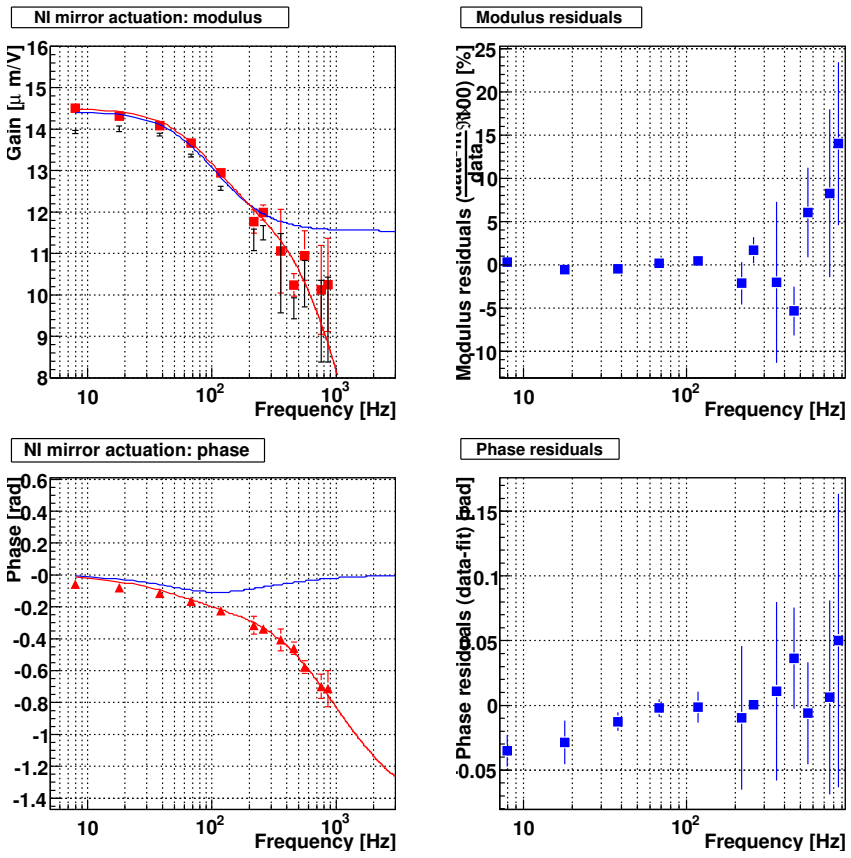

Figure 2.26: ***TF of the NI mirror actuation in LN mode fitted with two poles and one zero.*** *Left column: modulus and phase in LN mode. Right column: modulus and phase residuals of the fit. Black point: modulus in HP mode. Red squares: modulus in LN mode. Blue curve: parametrisation of the LN TF during VSR1. Red triangles: phase in LN mode, corrected for the fitted delay. Red curve: fit of the LN TF (phase corrected for the delay).*

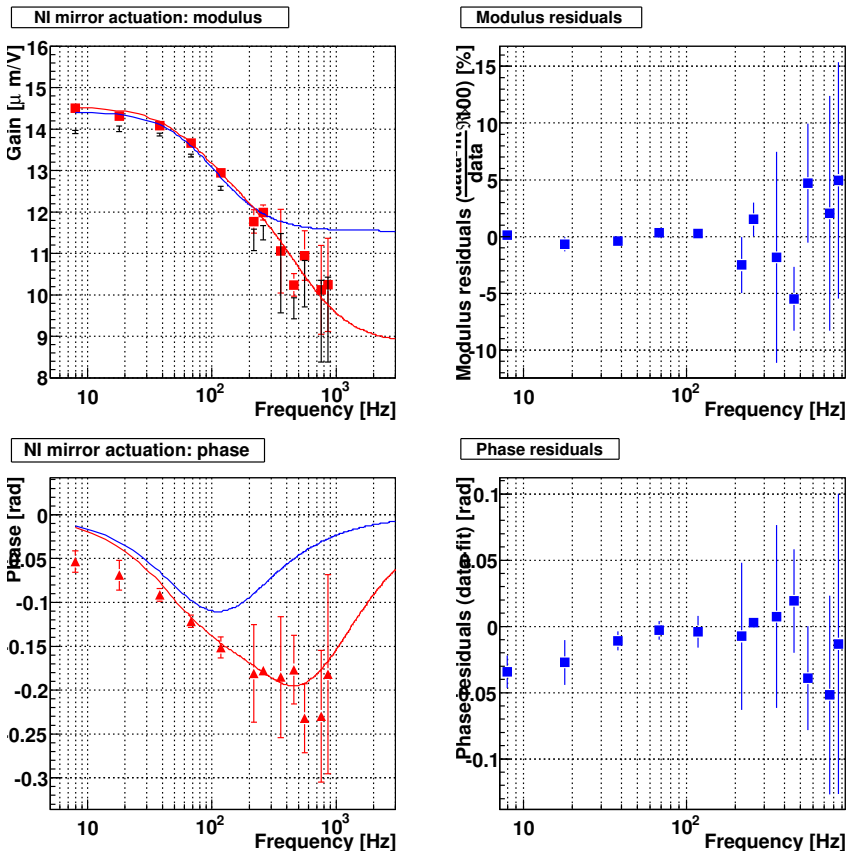

Figure 2.27: ***TF of the NI mirror actuation in LN mode fitted with two poles and two zeros.*** *Left column: modulus and phase in LN mode. Right column: modulus and phase residuals of the fit. Black point: modulus in HP mode. Red squares: modulus in LN mode. Blue curve: parametrisation of the LN TF during VSR1. Red triangles: phase in LN mode, corrected for the fitted delay. Red curve: fit of the LN TF (phase corrected for the delay).*

Frequency (Hz)	Gain (μm/V)	χ^2/ndf	Phase (rad)	χ^2/ndf
8.0	13.934 ± 0.039	122.8/31	-0.0325 ± 0.0096	6515.1/31
18.0	14.008 ± 0.064	54.8/23	-0.0886 ± 0.0150	363.1/23
38.0	13.872 ± 0.034	212.3/23	-0.1924 ± 0.0060	1910.6/23
68.0	13.365 ± 0.033	149.7/20	-0.3203 ± 0.0061	292.3/20
118.0	12.570 ± 0.045	69.3/24	-0.4989 ± 0.0113	57.1/24
218.0	11.329 ± 0.261	40.4/ 6	-0.8188 ± 0.0545	27.5/ 6
259.0	11.499 ± 0.168	0.04/ 1	-0.9321 ± 0.0041	0.9/ 1
358.0	10.525 ± 0.955	8.9/17	-1.2225 ± 0.0685	34.5/17
458.0	9.678 ± 0.256	0.005/ 1	-1.4994 ± 0.0387	1.1/ 1
558.0	10.273 ± 0.561	1.8/10	-1.8384 ± 0.0390	8.9/10
758.0	9.363 ± 0.986	5.7/10	-2.4017 ± 0.0746	8.5/10
858.0	9.403 ± 1.027	0./ 0	-2.6360 ± 0.1130	0./ 0

Table 2.10: ***Time-average actuation TF of the NI mirror in HP mode****. All the good quality data from May 2007 were used. The χ^2 test for a constant value as function of time was performed for the gain and the phase.*

Freq (Hz)	Up channel		Down channel		Average	
	$\frac{g_{LN}}{g_{HP}}$	$\Phi_{LN} - \Phi_{HP}$ (rad)	$\frac{g_{LN}}{g_{HP}}$	$\Phi_{LN} - \Phi_{HP}$ (rad)	$\frac{g_{LN}}{g_{HP}}$	$\Phi_{LN} - \Phi_{HP}$ (rad)
8.0	1.035 ± 0.003	-0.040 ± 0.003	1.047 ± 0.003	-0.044 ± 0.003	1.041 ± 0.003	-0.042 ± 0.003
18.0	1.018 ± 0.002	-0.026 ± 0.002	1.025 ± 0.002	-0.029 ± 0.002	1.022 ± 0.002	-0.028 ± 0.002
38.0	1.012 ± 0.001	0.002 ± 0.001	1.018 ± 0.001	-0.0005 ± 0.001	1.015 ± 0.001	0.0008 ± 0.001
68.0	1.020 ± 0.0009	0.020 ± 0.0009	1.025 ± 0.0008	0.019 ± 0.0008	1.022 ± 0.0008	0.020 ± 0.0008
118.0	1.027 ± 0.0007	0.037 ± 0.0007	1.033 ± 0.0006	0.036 ± 0.0006	1.030 ± 0.0007	0.037 ± 0.0007
218.0	1.035 ± 0.002	0.065 ± 0.002	1.043 ± 0.0005	0.063 ± 0.0005	1.039 ± 0.001	0.064 ± 0.001
259.0	1.039 ± 0.0006	0.072 ± 0.0006	1.046 ± 0.0005	0.072 ± 0.0005	1.042 ± 0.0006	0.072 ± 0.0006
358.0	1.047 ± 0.0005	0.094 ± 0.0005	1.054 ± 0.0004	0.095 ± 0.0004	1.050 ± 0.0005	0.094 ± 0.0005
458.0	1.054 ± 0.0004	0.116 ± 0.0004	1.062 ± 0.0004	0.117 ± 0.0004	1.058 ± 0.0004	0.117 ± 0.0004
558.0	1.062 ± 0.0004	0.136 ± 0.0004	1.070 ± 0.0004	0.137 ± 0.0004	1.066 ± 0.0004	0.137 ± 0.0004
758.0	1.077 ± 0.0004	0.175 ± 0.0004	1.085 ± 0.0004	0.176 ± 0.0003	1.081 ± 0.0004	0.176 ± 0.0004
858.0	1.085 ± 0.0004	0.194 ± 0.0004	1.093 ± 0.0003	0.195 ± 0.0003	1.089 ± 0.0004	0.195 ± 0.0004

Table 2.11: ***LN/HP TF ratio of the NI mirror actuators.*** *The gain ratio and phase difference of the LN/HP TF ratio are given for the up and down coil actuators. The average gain ratio is also given. Its error is set to the maximum value between the average error and the half of the difference of the up and down ratio.*

Frequency (Hz)	Gain (μm/V)	Phase (rad)
8.0	14.505 ± 0.079	-0.074 ± 0.012
18.0	14.314 ± 0.091	-0.116 ± 0.017
38.0	14.081 ± 0.051	-0.192 ± 0.007
68.0	13.665 ± 0.044	-0.301 ± 0.007
118.0	12.947 ± 0.055	-0.462 ± 0.012
218.0	11.771 ± 0.284	-0.755 ± 0.056
259.0	11.986 ± 0.182	-0.860 ± 0.005
358.0	11.056 ± 1.008	-1.128 ± 0.069
458.0	10.240 ± 0.274	-1.383 ± 0.039
558.0	10.948 ± 0.602	-1.702 ± 0.039
758.0	10.122 ± 1.069	-2.226 ± 0.075
858.0	10.242 ± 1.122	-2.441 ± 0.113

Table 2.12: ***TF of the NI mirror actuation in LN mode.***

Model 1	Model 2	Model 3
$g = 14.40 \pm 0.04\,\mu$m/V	$g = 14.47 \pm 0.05\,\mu$m/V	$g = 14.50 \pm 0.06\,\mu$m/V
$t_d = 453.8 \pm 6.4\,\mu$s	$t_d = 320 \pm 19\,\mu$s	$t_d = 419.2 \pm 21\,\mu$s
$\phi_0 = 0$	$\phi_0 = 0$	$\phi_0 = 0$
$f_p = 128 \pm 7$ Hz	$f_p = 97.7 \pm 12$ Hz	$f_p = 83.8 \pm 14$ Hz
$f_0 = 170 \pm 12$ Hz	$f_0 = 119 \pm 17$ Hz	$f_0 = 98.4 \pm 19$ Hz
-	$f_p = 944 \pm 163$ Hz	$f_p = 459 \pm 201$ Hz
-	-	$f_0 = 643 \pm 374$ Hz
$P(\chi^2) \sim 0.6\%$	$P(\chi^2) \sim 6.6\%$	$P(\chi^2) \sim 9.5\%$

Table 2.13: ***Fit results of the NI LN TF*** *for the three different models discussed in the text. The last line indicates the χ^2 probability of the fit.*

2.5 BS mirror actuator calibration

The BS mirror actuation TF can be measured in all the free Michelson configurations. It thus allows to compare the different measurements and to estimate systematics.

The figure 2.29 shows the evolution of the gain as function of the total amplitude of the Sc_BS_zCorr signal obtained at the different frequencies. The normalized gain is flat up to the maximum injected amplitude of 2 V.

2.5.1 Effect of optical response

Different delays, offset by 10 μs, are expected to be observed in the BS mirror actuation TF as function of the different free swinging Michelson configurations as described in section 1.1.2. The difference is shown in the figure 2.28 and fit to a delay of 10.58 $\pm$ 0.34μs.

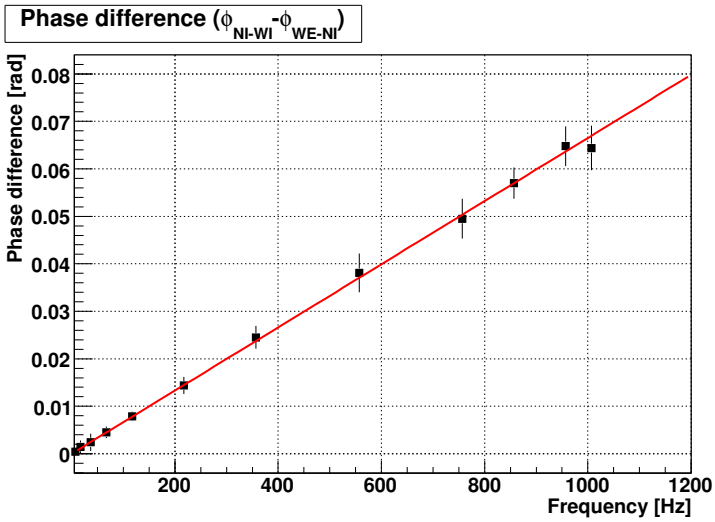

Figure 2.28: ***Optical response of the free swinging Michelson to the BS motion:*** *the phase of the data in WE-NI configuration is different from the phase of the data in NI-WI and WE-NI configurations. The difference can be fit by a delay of* 10.58 $\pm$ 0.34μs.

2.5.2 BS mirror actuator calibration

In the following, the phase measured from data in WE-NI configurations is corrected for a 10 μs delay in order to be combined with the data from other configurations.

The figure 2.30 shows the modulus and phase of the BS mirror actuation as function of time for some fixed frequencies. Some time variations of the phase are visible while the modulus look constant. The average modulus and phase are given in the table 2.14. The χ^2/ndf are rather high for the modulus and phase averages It indicates the presence of systematics.

The distribution of the modulus, weighted by the statistical errors, have been computed. The 1-sigma width of the modulus distribution, used as an estimation of the systematic error on the measurements, is of the order of $0.1\,\mu$m/V ($\sim$ 2%). From the time variations, the systematic errors on the phase are estimated to ~ 0.005 rad.

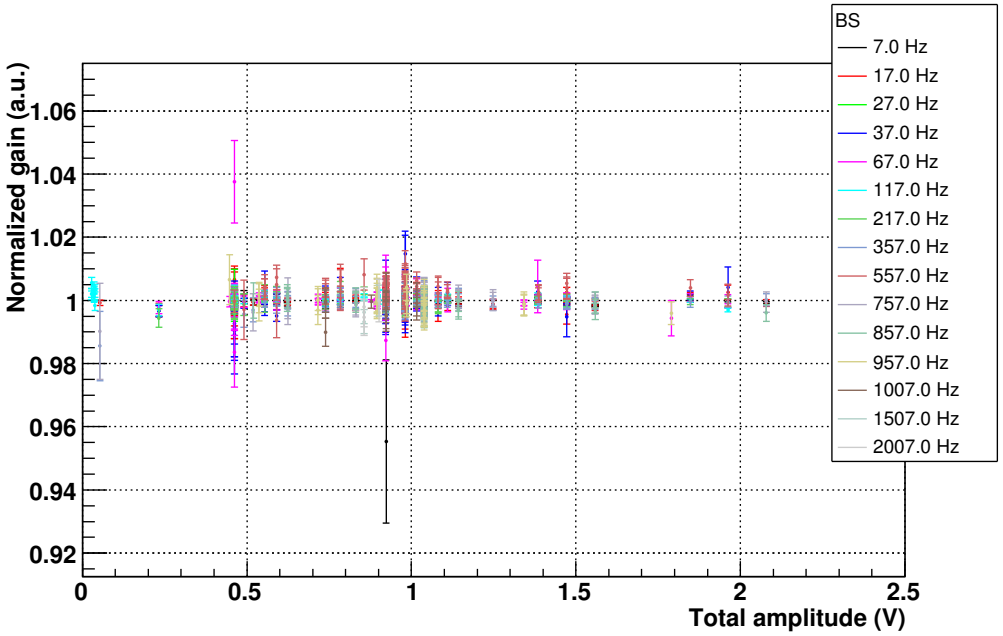

Figure 2.29: ***BS mirror actuation gain vs the amplitude*** *of the injected signal on zCorr. The gain is flat for injected signal up to the maximum injected amplitude of 2 V.*

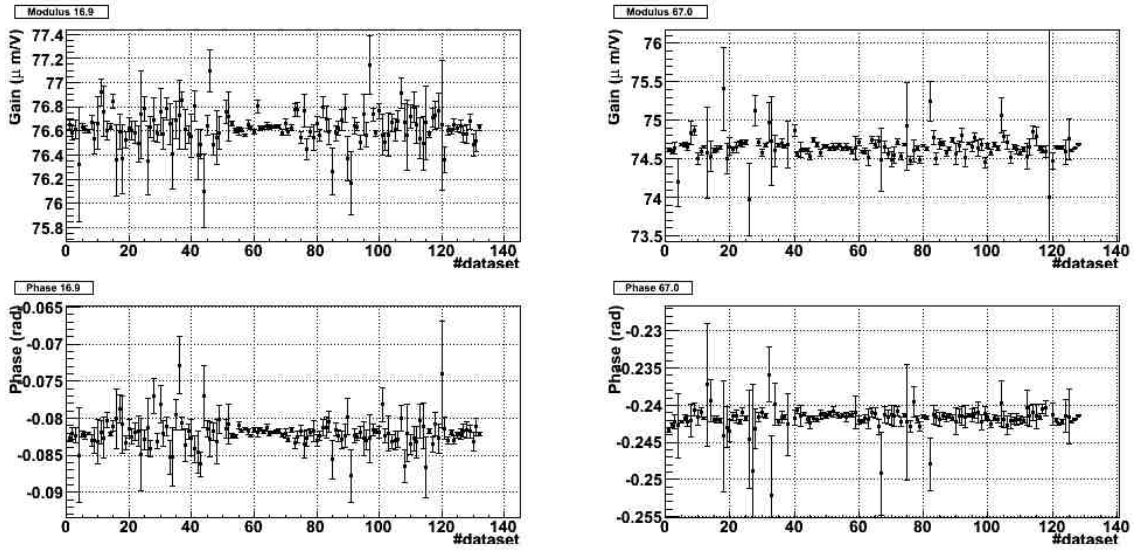

(a) 17.0 Hz

(b) 67.0 Hz

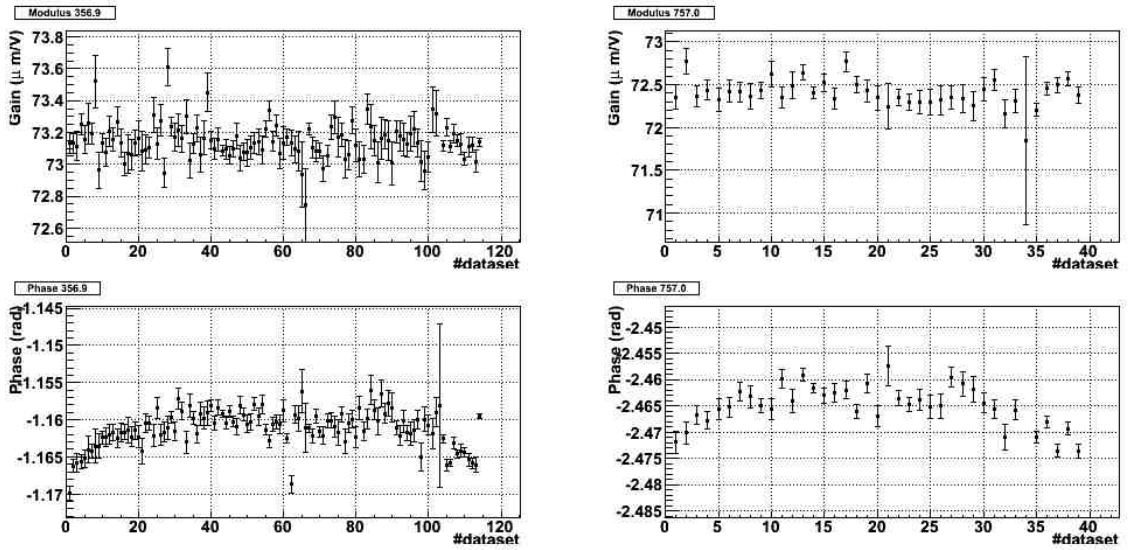

(c) 357.0 Hz

(d) 757.0 Hz

Figure 2.30: ***BS mirror actuation TF vs time in HP mode.*** *Modulus and phase as function of time (May to October 2007) at 17.0 Hz (a), 67.0 Hz (b), 357.0 Hz (c) and 757.0 Hz (d).*

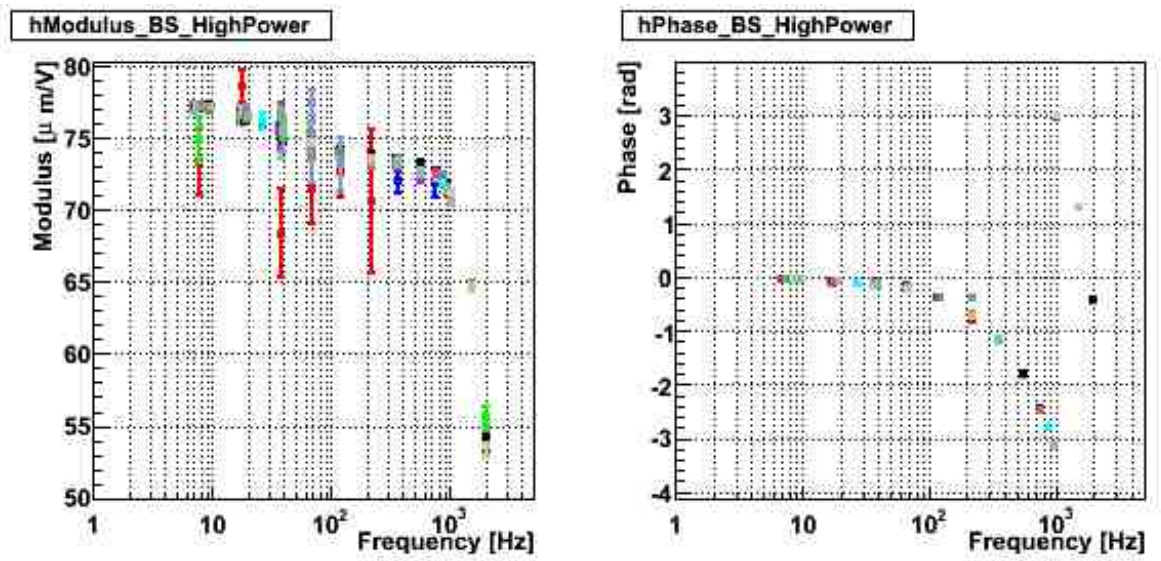

(a) BS TF in HP mode

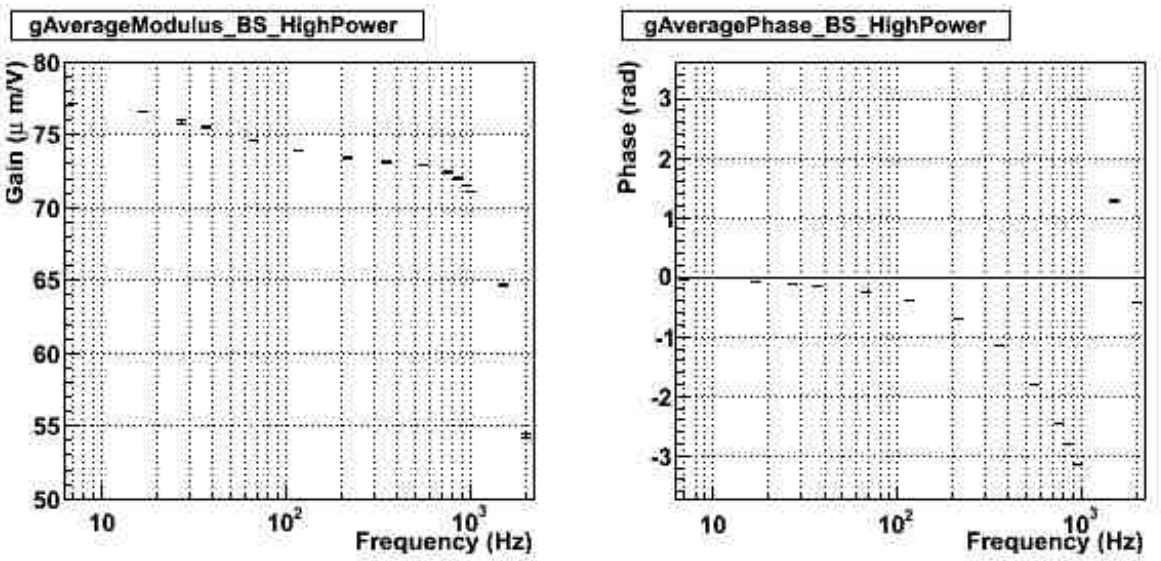

(b) BS averaged-TF in HP mode

Figure 2.31: ***BS mirror actuation TF in HP mode.***
(a) Measurements from the different datasets (colors) from May to December 2007.
(b) Average TF.

Frequency (Hz)	Gain (μm/V)	χ^2/ndf	Phase (rad)	χ^2/ndf
7.0	77.153 ± 0.0157	2542.7/181	-0.04026 ± 0.0002192	144.1/181
16.9	76.626 ± 0.0154	242.5/131	-0.08205 ± 0.0002068	154.9/131
26.9	75.928 ± 0.139	0.2/ 3	-0.1161 ± 0.001886	0.3/ 3
37.0	75.515 ± 0.0460	143.7/88	-0.1474 ± 0.0006680	80.2/88
67.0	74.651 ± 0.0290	380.6/127	-0.2417 ± 0.0004105	206.6/127
117.0	73.943 ± 0.0247	381.2/108	-0.3979 ± 0.0003501	414.5/108
216.9	73.448 ± 0.110	3656.0/93	-0.7129 ± 0.0007986	700.3/93
356.9	73.141 ± 0.0110	152.2/113	-1.1615 ± 0.0001568	732.5/113
557.0	72.887 ± 0.0200	81.2/75	-1.8080 ± 0.0002841	481.7/75
757.0	72.418 ± 0.0326	49.5/38	-2.4653 ± 0.0004689	245.3/38
857.0	72.021 ± 0.0211	57.9/34	-2.7975 ± 0.0003031	356.6/34
957.0	71.494 ± 0.0279	58.5/33	-3.1313 ± 0.0004039	147.7/33
1007.0	71.081 ± 0.0524	17.8/12	2.9869 ± 0.0007641	72.0/12
1507.0	64.664 ± 0.0684	4.9/ 2	1.2816 ± 0.001096	99.5/ 2
2007.0	54.381 ± 0.150	19.2/14	-0.4195 ± 0.002858	31.1/14

Table 2.14: ***Time-average actuation TF of the BS mirror in HP mode****, using the free Michelson configurations from May to December 2007, with coherence higher than 70%.. The χ^2 test for a constant value as function of time was performed for the gain and the phase.*

Freq (Hz)	UL channel		UR channel	
	$\frac{g_{LN}}{g_{HP}}$	$\Phi_{LN} - \Phi_{HP}$ (rad)	$\frac{g_{LN}}{g_{HP}}$	$\Phi_{LN} - \Phi_{HP}$ (rad)
7.0	1.243 ± 0.00338	0.0118 ± 0.00282	1.097 ± 0.00276	0.0005395 ± 0.00260
16.9	1.243 ± 0.00245	0.00514 ± 0.00204	1.105 ± 0.00210	0.0187 ± 0.00196
26.9	1.238 ± 0.00206	0.00751 ± 0.00172	1.113 ± 0.00178	0.0232 ± 0.00165
37.0	1.238 ± 0.00182	0.0132 ± 0.00152	1.118 ± 0.00154	0.0285 ± 0.00143
67.0	1.230 ± 0.00143	0.0289 ± 0.00121	1.121 ± 0.00135	0.0379 ± 0.00124
117.0	1.228 ± 0.00134	0.0526 ± 0.00113	1.123 ± 0.00114	0.0588 ± 0.00105
216.9	1.222 ± 0.00117	0.102 ± 0.0009952	1.119 ± 0.00106	0.105 ± 0.0009786
356.9	1.214 ± 0.00110	0.176 ± 0.0009417	1.110 ± 0.0009978	0.175 ± 0.0009310
557.0	1.193 ± 0.00116	0.282 ± 0.00101	1.093 ± 0.0009821	0.283 ± 0.0009304
757.0	1.177 ± 0.00106	0.398 ± 0.0009348	1.079 ± 0.0009711	0.398 ± 0.0009313
857.0	1.169 ± 0.00119	0.460 ± 0.00105	1.073 ± 0.00118	0.460 ± 0.00114
957.0	1.163 ± 0.00109	0.522 ± 0.0009734	1.067 ± 0.00100	0.524 ± 0.0009738
1007.0	1.161 ± 0.00170	0.552 ± 0.00152	1.065 ± 0.00180	0.559 ± 0.00174
1507.0	1.172 ± 0.00118	0.904 ± 0.00104	1.082 ± 0.00107	0.912 ± 0.00103
2007.0	1.264 ± 0.00152	1.244 ± 0.00124	1.184 ± 0.00142	1.262 ± 0.00124

Table 2.15: ***LN/HP TF ratio of the BS mirror up actuators.*** *The gain ratio and phase difference of the LN/HP TF ratio are given for the up and down coil actuators.*

Freq (Hz)	DL channel		DR channel		Average (4 coils)	
	$\frac{g_{LN}}{g_{HP}}$	$\Phi_{LN} - \Phi_{HP}$ (rad)	$\frac{g_{LN}}{g_{HP}}$	$\Phi_{LN} - \Phi_{HP}$ (rad)	$\frac{g_{LN}}{g_{HP}}$	$\Phi_{LN} - \Phi_{HP}$ (rad)
7.0	1.099 ± 0.006	0.0141 ± 0.0059	1.149 ± 0.0035	0.0005 ± 0.0032	1.124 ± 0.0050	0.007254 ± 0.0045
17.0	1.097 ± 0.0039	0.0186 ± 0.0037	1.147 ± 0.0026	0.010 ± 0.0024	1.122 ± 0.0033	0.01429 ± 0.0030
27.0	1.103 ± 0.0032	0.0233 ± 0.0030	1.154 ± 0.0023	0.012 ± 0.0021	1.128 ± 0.0028	0.01781 ± 0.0025
37.0	1.111 ± 0.0028	0.0282 ± 0.0026	1.157 ± 0.0019	0.016 ± 0.0017	1.134 ± 0.0024	0.02197 ± 0.0022
67.0	1.121 ± 0.0024	0.0337 ± 0.0022	1.161 ± 0.0016	0.021 ± 0.0014	1.141 ± 0.0020	0.02744 ± 0.0018
117.0	1.127 ± 0.0020	0.0402 ± 0.0018	1.160 ± 0.0012	0.030 ± 0.0011	1.143 ± 0.0016	0.03496 ± 0.0014
217.0	1.125 ± 0.0017	0.0662 ± 0.0016	1.156 ± 0.0013	0.054 ± 0.0011	1.141 ± 0.0015	0.06006 ± 0.0013
357.0	1.119 ± 0.0017	0.104 ± 0.0016	1.147 ± 0.0011	0.090 ± 0.0010	1.133 ± 0.0014	0.09699 ± 0.0013
557.0	1.111 ± 0.0016	0.167 ± 0.0015	1.136 ± 0.0012	0.15 ± 0.0011	1.123 ± 0.0014	0.1583 ± 0.0013
757.0	1.101 ± 0.0014	0.239 ± 0.0013	1.126 ± 0.0010	0.22 ± 0.0010	1.114 ± 0.0012	0.2291 ± 0.0011
857.0	1.101 ± 0.0015	0.281 ± 0.0015	1.123 ± 0.0018	0.25 ± 0.0016	1.112 ± 0.0017	0.2667 ± 0.0015
957.0	1.099 ± 0.0015	0.323 ± 0.0015	1.121 ± 0.0010	0.29 ± 0.0010	1.110 ± 0.0013	0.3081 ± 0.0012
1007.0	1.106 ± 0.0021	0.344 ± 0.0020	1.121 ± 0.0021	0.31 ± 0.0019	1.113 ± 0.0021	0.3288 ± 0.0019
1507.0	1.164 ± 0.0016	0.572 ± 0.0014	1.169 ± 0.0012	0.53 ± 0.0011	1.166 ± 0.0014	0.5526 ± 0.0013
2007.0	1.351 ± 0.0022	0.778 ± 0.0017	1.339 ± 0.0018	0.73 ± 0.0014	1.345 ± 0.0020	0.7548 ± 0.0015

Table 2.16: ***LN/HP TF ratio of the BS mirror down actuators.*** *The gain ratio and phase difference of the LN/HP TF ratio are given for the up and down coil actuators. The average gain ratio (of the four coils) is also given.*

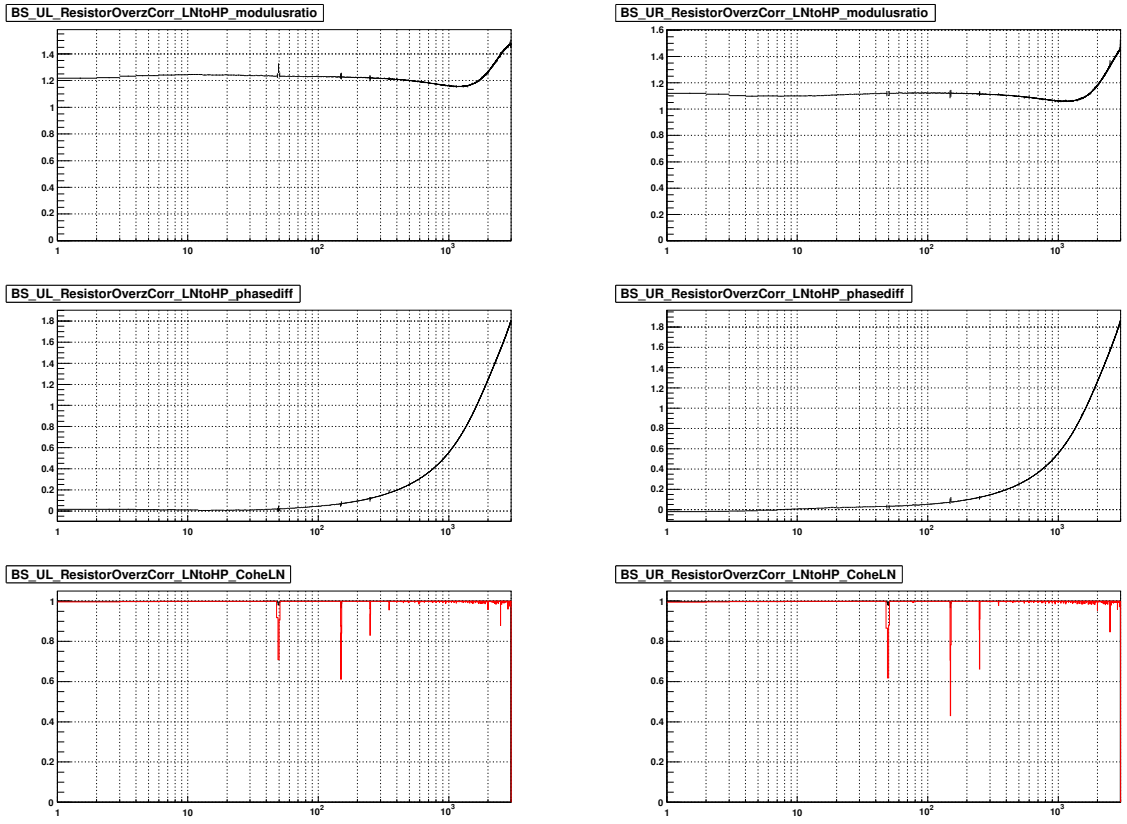

(a) BS UL (b) BS UR

Figure 2.32: ***LN/HP TF ratio of the BS UL and UR actuators*** *obtained from direct electronic measurements. For both channels (up-left and up-right), the gain ratio and the phase difference are shown where both coherence were higher than 70%. The last figures show the coherence between zCorr and the coil current measurements both in HP (red) and LN (black) mode.*

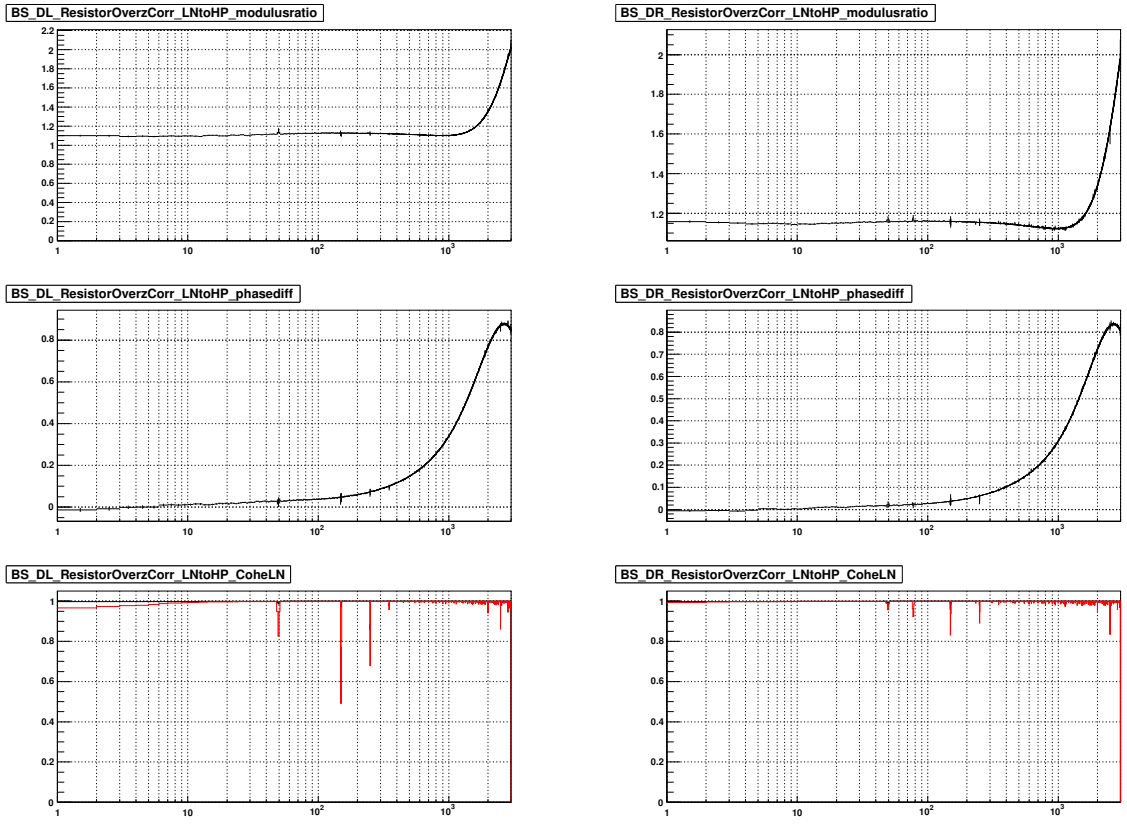

(a) BS DL (b) BS DR

Figure 2.33: ***LN/HP TF ratio of the BS DL and DR actuators*** *obtained from direct electronic measurements. For both channels (down-left and down-right), the gain ratio and the phase difference are shown where both coherence were higher than 70%. The last figures show the coherence between zCorr and the coil current measurements both in HP (red) and LN (black) mode.*

Frequency (Hz)	Gain (μm/V)	Phase (rad)
7.0	88.482 ± 0.0180	-0.03355 ± 0.0038
16.9	87.968 ± 0.0178	-0.06895 ± 0.0027
26.9	87.466 ± 0.160	-0.09955 ± 0.0040
37.0	87.289 ± 0.0533	-0.1260 ± 0.0025
67.0	86.487 ± 0.0337	-0.2113 ± 0.0019
117.0	85.714 ± 0.0286	-0.3526 ± 0.0016
216.9	84.880 ± 0.127	-0.6311 ± 0.0020
356.9	83.921 ± 0.0126	-1.0253 ± 0.0013
557.0	82.601 ± 0.0227	-1.5876 ± 0.0014
757.0	81.179 ± 0.0366	-2.1517 ± 0.0015
857.0	80.408 ± 0.0236	-2.4344 ± 0.0016
957.0	79.540 ± 0.0311	-2.7156 ± 0.0015
1007.0	79.125 ± 0.0584	-2.8542 ± 0.0026
1507.0	74.149 ± 0.0786	2.0118 ± 0.0022
2007.0	69.872 ± 0.193	0.5844 ± 0.0042

Table 2.17: ***TF of the BS mirror actuation LN mode.*** *The mirror actuation TF in HP mode that was used is derived using all the free Michelson configurations.*

BS model in LN Mode
$g = 88.339 \pm 0.014\,\mu$m/V
$t_d = 392.9 \pm 0.3\,\mu$s
$f_p = 71.4 \pm 1.2$ Hz
$f_0 = 74.6 \pm 1.3$ Hz
$f_p = 2634 \pm 8.5$ Hz
$\chi^2/ndf = 385./21$

Table 2.18: ***Fit results of the BS mirror actuation TF in LN mode*** *with two simple poles and a simple zero. The fit range was limited up to 1.1 kHz.*

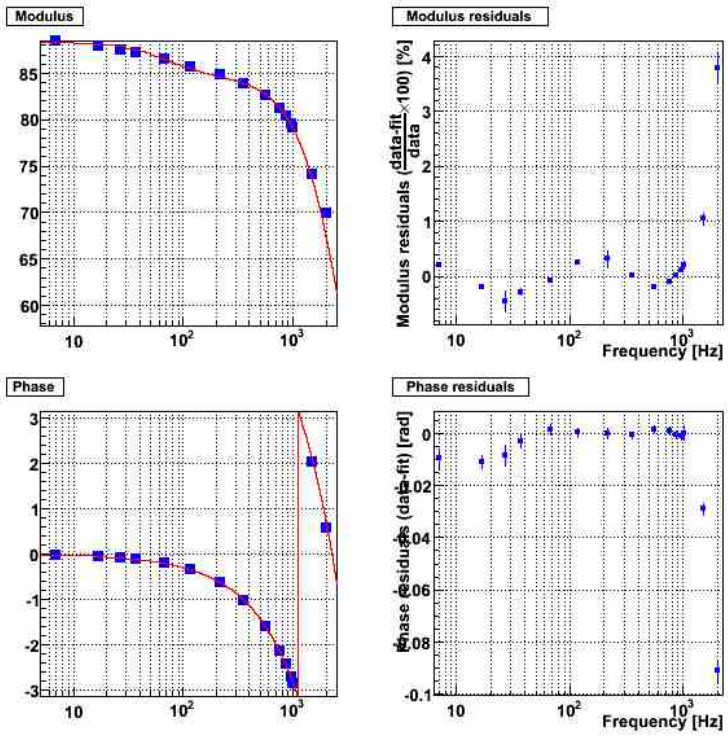

Figure 2.34: ***TF of the BS mirror actuation in LN mode fitted with two poles and a zero.*** *The fit was computed up to 1.1 kHz while the residuals are given up to 2 kHz.*
Left column: modulus and phase in LN mode. Blue squares: modulus in LN mode. Red curve: fit of the LN TF.
Right column: modulus and phase residuals of the fit.

2.6 PR mirror actuator calibration

The PR mirror was controlled through the up and down coils during VSR1. The reference mass is made of aluminum as the arm reference masses. The Eddy current effects should thus be similar, inducing a similar actuation response shape. The PR suspension was always used in HP mode only.

The TF of the PR mirror actuation has been measured relatively to the BS mirror actuation TF by the locking team. The data configuration and results have been already described in the note [6].

2.6.1 The data

The measurements were performed locking the PR-WI cavity: the BS is used as a folding mirror. A motion of PR, BS or WI has the effect of changing the length of the cavity. This can be seen by the photodiode used for locking (Pr_B1p_ACp).

Noise was injected on the BS and then on the PR mirrors through the CaRT server and the $LoopIn$ and $zCorr$ signals.

The photodiode signal is proportionnal to the injected signal multiplied by the mirror actuation response:

$$Pr\_B1p\_ACp \propto Sc\_BS\_LoopIn \times G_{BS} \quad \text{in the first dataset} \tag{2.5}$$
$$Pr\_B1p\_ACp \propto Sc\_PR\_LoopIn \times G_{PR} \quad \text{in the second dataset} \tag{2.6}$$

Two TFs are built and normalised by the calibration gain N applied between the injected $LoopIn$ signal and the $zCorr$ signal (i.e. $Sc\_PR\_Gain\_cal\_loop$ and $Sc\_PR\_Gain\_cal\_zCorr$):

$$TF_{BS} = \frac{Pr\_B1p\_ACp}{Sc\_BS\_LoopIn \times N_{BS}} \qquad TF_{PR} = \frac{Pr\_B1p\_ACp}{Sc\_PR\_LoopIn \times N_{PR}} \tag{2.7}$$

Their ratio gives the actuation TF ratio:

$$\frac{TF_{PR}}{TF_{BS}} = \frac{G_{PR}}{G_{BS}} \tag{2.8}$$

The ratio is then multiplied by the BS mirror actuation TF to extract the PR mirror actuation TF.

As the modulus of the BS mirror actuation calibrated using the Free Michelson data is an effective length variation (it does not take into account the $\sqrt{2}$ factor for the 45°angle of the BS mirror), this factor is not applied here neither.

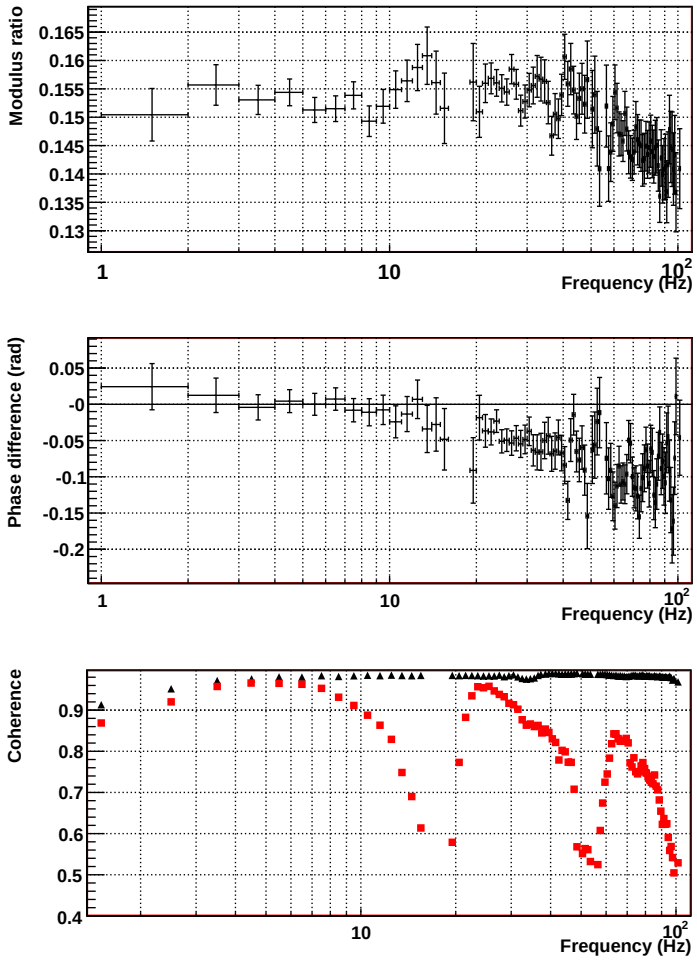

Figure 2.35: ***Ratio of PR (HP) to BS (LN) mirror actuation TFs.*** *The modulus ratio and phase difference are shown. The coherence are given (black: injection on PR, red: injection on BS).*

2.6.2 The results

The former TF ratio $\frac{G_{PR}}{G_{BS}}$ is shown on the figure 2.35. The coherences between the injected noise and the photodiode signal do not allow to measure the ratio above 100 Hz. The derived PR mirror actuation TF is given in the table 2.19.

Below 100 Hz, the shape of the PR mirror actuation looks closer to the arm mirror actuation than to the BS mirror actuation. This is confirmed since the PR reference mass is made of aluminium as the arm ones (while the BS reference mass is made of stainless steel). The frequency dependence due to the Eddy currents should thus be similar.

Frequency (Hz)	Gain (μm/V)	Phase (rad)
7.0	13.76 ± 0.21	-0.038 ± 0.020
17.0	13.77 ± 0.49	-0.042 ± 0.040
27.0	13.53 ± 0.23	-0.052 ± 0.020
37.0	13.66 ± 0.34	-0.078 ± 0.027
67.0	12.62 ± 0.31	-0.108 ± 0.027

Table 2.19: ***TF of the PR mirror actuation in HP mode.***

2.7 Estimation of the systematic errors

2.7.1 Systematic error in the free Michelson measurements

Possible origin of systematic errors

The fringes are observed using the Pr_B1p signals, before the output mode cleaner, instead of the Pr_B1 channels as when the ITF is locked. Different filters between the channels could induce some systematic effects.

Estimation ?

Observation of time variations

Time variation of the order of 1%, higher than the statistical errors have been observed on the modulus of the mirror actuation TF (see 2.1.1 (p. 8)).

2.7.2 LN/HP ratio: indirect measurements during lock acquisition

The electronic data described in section 2.1.2 (p. 9) give direct measurements of the LN/HP mirror actuator TF ratio.

An independent method has been developped in order to measure the LN/HP mirror actuation TF. It is based on the injection of a few lines through the mirror actuators during the lock acquisition before and after the suspensions are switched from HP to LN mode. It is described in the note [2].

The LN/HP gain ratio of mirror actuators derived using this method are given in the table 2.20 for NE and WE and in the table 2.21 for BS. The statistical errors are larger than with the direct electronic measurements: 1% to 5% errors instead of less than 1%. The LN/HP gain ratio derived from this method is compatible with the results of the main method.

Systematic errors of the lock acquisition method

The lock acquisition method assumes that the optical gain and loop coefficients are stable between both datasets, within $\sim$ 3 minutes. If the hypothesis is true, the gain ratio of the suspensions that were not switched between both datasets should be equal to 1. This criteria is used to check the hypothesis and estimate systematic errors of the method.

In the datasets used to measure the end mirror actuators ratio, the BS suspension was kept in HP mode. The method thus gives the BS HP/HP gain ratio, which should thus be 1 if the optical gain and loop factors are stable as assumed in the analysis. The last column of the table 2.20 gives the results for the BS HP/HP ratio. The points are compatible with 1. The average value is 0.992 ± 0.007.

In the datasets used to measure the BS mirror actuators ratio, the end suspensions was kept in LN mode. As before, the method thus gives the WE and NE LN/LN gain ratio, which should

thus be 1. The last columns of the table 2.21 give the results for the end mirrors LN/LN ratio. The points are compatible with 1 and the average values are 0.999 ± 0.017 and 0.993 ± 0.014.

These results confirm the hypothesis of the optical gain and loop coefficient stability int the different datasets. They do not show any systematic error of the method higher than 1% due to some possible time variation of the locking loop coefficients.

Systematic errors on the LN/HP ratio measurements

The LN/HP ratio R_{lock} obtained with the lock acquisition data have been compared to the ratio R_{main} obtained from the electronic measurements (see tables 2.2 (p. 16), 2.6 (p. 31) and 2.16 (p. 53)). The relative difference

$$\frac{R_{lock} - R_{main}}{R_{main}}$$

has been computed for the common frequency points (8-9 per suspension). The average values of the difference are $-2.45\% \pm 0.71\%$, $-3.07\% \pm 0.90\%$ and $-1.49\% \pm 0.19\%$ for the WE, NE and BS ratio respectively. A systematic difference of $\sim 2\%$ is derived from the comparison, the ratio from electronic measurements being higher than the current measurements.

Conclusions

Two independent methods, using datasets in completely different configurations have been used to measure the LN/HP mirror actuator TF modulus ratio. From their comparison, a systematic error of $^{+0\%}_{-2\%}$ can be estimated on the LN/HP ratio used in the main calibration stream.

2.7.3 LN/HP ratio: lack of monitoring data during VSR1

The LN/HP ratio has been measured only in October/November 2007, after the run. A hardware modification of the coil driver electronics occurred in July 2007. The added de-emphasis filters were measured and compensated in the DSP. But the compensation have a few % errors and the LN/HP TF ratio should thus have been modified by the same amount. The systematic error for the data before July 11th 2007 should thus be increased by a few %.

2.7.4 Measurements of the mirror actuation in LN mode from free Michelson data

Measurement of the BS and input mirror actuation TF in LN mode were possible at low frequency using the short free swinging Michelson configuration. Line injections were performed during datasets of $\sim 1 - 2$ hours in order to measure the TF.

The mirror actuation TF TF_{FM} of the BS, NI and WI suspensions in LN mode as measured using free Michelson data are given in the table 2.22.

WE mirror: LN/HP			NE mirror: LN/HP			BS mirror: HP/HP		
Freq (Hz)	HP/LN	χ^2/ndf	Freq (Hz)	HP/LN	χ^2/ndf	Freq (Hz)	HP/LN	χ^2/ndf
36.5	1.216 ± 0.110	0./ 0	36.0	1.366 ± 0.131	0./ 0	37.0	1.184 ± 0.163	0./ 0
66.5	1.118 ± 0.047	7.4/ 4	66.0	1.102 ± 0.047	4.6/ 4	67.0	1.016 ± 0.050	5.7/ 4
76.5	1.498 ± 0.885	2.8/ 3	76.0	0.762 ± 0.239	3.5/ 3	77.0	0.876 ± 0.343	2.9/ 3
116.5	1.103 ± 0.016	5.8/ 4	116.0	1.189 ± 0.023	3.9/ 4	117.0	0.999 ± 0.021	3.5/ 4
256.5	1.136 ± 0.008	3.1/ 4	256.0	1.172 ± 0.010	1.0/ 4	257.0	0.974 ± 0.025	1.5/ 4
356.5	1.107 ± 0.018	14.0/10	356.0	1.160 ± 0.019	19.3/10	357.0	1.011 ± 0.013	5.8/10
456.5	1.119 ± 0.022	19.3/10	456.0	1.172 ± 0.015	14.6/10	457.0	0.980 ± 0.014	19.1/10
556.5	1.160 ± 0.024	5.7/11	556.0	1.144 ± 0.020	4.5/11	557.0	0.984 ± 0.019	15.6/11
756.5	1.176 ± 0.051	9.3/11	756.0	1.190 ± 0.046	9.6/11	757.0	0.993 ± 0.028	5.8/11
856.5	1.145 ± 0.061	6.4/10	856.0	1.211 ± 0.055	8.7/10	857.0	0.954 ± 0.027	7.4/10
956.5	1.178 ± 0.065	4.9/11	956.0	1.177 ± 0.078	17.0/11	957.0	1.019 ± 0.046	8.0/11

Table 2.20: ***LN/HP gain ratio of the WE and NE mirror actuators from lock acquisition data.*** *The χ^2/ndf to test the hypothesis that the ratio is constant with time is given. The HP/HP gain ratio of the BS mirror actuator computed with the same datasets is given. It shows that systematics could be of the order of 5%. The ratio at frequencies below ∼100 Hz cannot be trusted since the marionnetta effect was not taken into account. The measurements from electronics can be found in the table 2.20.*

BS mirror: LN/HP			WE mirror: LN/LN			NE mirror: LN/LN		
Freq (Hz)	LN/HP	χ^2/ndf	Freq (Hz)	LN/LN	χ^2/ndf	Freq (Hz)	LN/LN	χ^2/ndf
37.0	1.223 ± 0.040	0./ 0	36.5	1.036 ± 0.035	0./ 0	36.0	1.081 ± 0.040	0./ 0
67.0	1.156 ± 0.011	0.6/ 4	66.5	0.990 ± 0.006	0.6/ 4	66.0	1.003 ± 0.006	2.2/ 4
77.0	1.332 ± 0.365	5.6/ 3	76.5	1.147 ± 0.181	7.8/ 3	76.0	0.991 ± 0.264	12.4/ 3
117.0	1.133 ± 0.007	68.2/ 4	116.5	0.998 ± 0.005	2.4/ 4	116.0	0.992 ± 0.004	11.7/ 4
257.0	1.144 ± 0.008	2.2/ 4	256.5	0.998 ± 0.003	6.3/ 4	256.0	0.998 ± 0.003	7.9/ 4
357.0	1.130 ± 0.004	11.7/10	356.5	0.998 ± 0.003	20.3/10	356.0	0.995 ± 0.003	19.3/10
457.0	1.127 ± 0.004	13.4/10	456.5	0.998 ± 0.003	14.4/10	456.0	0.998 ± 0.002	21.1/10
557.0	1.118 ± 0.005	35.1/11	556.5	0.998 ± 0.003	15.2/11	556.0	0.997 ± 0.002	28.8/11
757.0	1.104 ± 0.004	23.3/11	756.5	0.999 ± 0.003	14.8/11	756.0	0.999 ± 0.002	52.8/11
857.0	1.102 ± 0.004	14.1/10	856.5	1.001 ± 0.003	13.4/10	856.0	0.999 ± 0.003	14.5/10
957.0	1.096 ± 0.004	23.7/11	956.5	0.997 ± 0.003	26.9/11	956.0	0.998 ± 0.002	41.6/11

Table 2.21: ***LN/HP gain ratio of the BS mirror actuator from indirect measurements.*** *The χ^2/ndf to test the hypothesis that the ratio is constant with time is given. The LN/LN gain ratio of the WE and NE mirror actuators computed with the same datasets is given. The ratio at frequencies below ∼100 Hz cannot be trusted since the marionnetta effect was not taken into account. The measurements from electronics can be found in the table 2.21.*

Frequency (Hz)	Gain (μm/V)	Phase (rad)
BS mirror actuation		
7.0	88.063 ± 0.653	-0.0383 ± 0.0127
17.0	87.417 ± 0.037	-0.0704 ± 0.0004
37.0	86.541 ± 0.217	-0.1272 ± 0.0026
67.0	85.170 ± 0.772	-0.2154 ± 0.0094
117.0	82.714 ± 2.269	-0.3782 ± 0.0284
NI mirror actuation		
9.0	14.765 ± 0.0001	3.0871 ± 0.0012
19.0	14.510 ± 0.0004	3.0287 ± 0.0036
38.0	14.221 ± 0.002	2.9706 ± 0.0185
WI mirror actuation		
8.5	12.745 ± 0.0002	-0.0493 ± 0.0016
18.5	12.516 ± 0.0004	-0.1035 ± 0.0043
38.5	11.797 ± 0.002	-0.1522 ± 0.0224

Table 2.22: ***Time-average actuator gain in LN mode of the BS, NI and WI suspension, using the data in short Michelson in LN mode.*** *The data with coherence higher than 30% between the injected line and the reconstructed mirror movement were used.*

It has been compared to the TF TF_{main} obtained from the calibration main stream. The relative difference of the modulus and the difference of the phase

$$\frac{G_{FM} - G_{main}}{G_{main}}$$

$$\Phi_{FM} - \Phi_{main}$$

have been computed for the BS and NI data at every common frequency. The average modulus relative difference are $-1.04\% \pm 0.24\%$ and $+1.27\% \pm 0.28\%$ respectively. The average phase difference are -0.0010 ± 0.0035 rad and 0.016 ± 0.010 rad respectively. The phase difference evolution with frequency does not indicate any systematic time delay.

Conclusions

Systematic errors of the order of $\pm 1\%$ can be estimated on the modulus value. No systematic effect higher than 0.01 rad ($0.5°$) is seen on the phase. At 100 Hz, this indicates that a possible systematic delay would be lower than $15\,\mu$s. Note that systematic effects coming from the use of the channel Pr_B1p in the free Michelson data would not appear in this comparison.

2.8 Conclusions about the mirror actuation TFs

The main calibration stream in order to calibrate the mirror actuation in LN mode is the following:

- the mirror actuation TFs are computed in HP mode from free swinging Michelson data,
- the LN/HP ratio is computed from electronic measurements,
- the mirror actuation TFs are computed in LN mode combining the former ones.

The final results with the statistical errors are given in the tables 2.3 (p. 18), 2.7 (p. 32), 2.12 (p. 46) and 2.17 (p. 56) for the WE, NE, NI and BS mirrors respectively.

The BS and arm mirror TFs have been fitted (without systematic errors) within 1% in modulus and 0.05 rad in phase below 1 kHz. The fit parameters are given in the tables 2.4 (p. 22), 2.8 (p. 32), 2.13 (p. 46) and 2.18 (p. 56).

The PR mirror actuation is always used in HP mode. Its TF has been measured below 100 Hz relatively to the BS mirror actuation in LN mode using injections with a locked cavity PR-WI. The PR mirror actuation TF with the statistical errors are given in the table 2.19 (p. 60). Systematic errors

The shapes of the mirror actuator TFs in LN mode (PR in HP mode) are compared on the figure 2.36. The modulus have been normalized and the phases have been corrected for a 450 μs delay. The shapes of the gain and phase of the arm mirrors are very similar. A difference might be visible between the NI mirrors compared to the end mirrors above $\sim$ 200 Hz. However, the large NI statistical errors do not allow to conclude. The shapes of the BS actuator gain and phase are much flatter up to 1 kHz, and with different structures as function of frequency. The PR measurements indicate a frequency dependence close to the arm mirror actuator even if it not clear since the data are only below 100 Hz. The delay from PR to the dark fringe seems lower than for the other mirrors.

The frequency dependence of the mirror actuator is probably due to the Eddy current effects of the coil current into the reference mass. The BS reference mass is made of Aluminium [7] while the arm and PR reference masses are made of stainless steel.The Eddy currents are predicted to be higher in the stainless steel than in Aluminium. The frequency dependence of the mirror actuators is also higher in the arm mirrors than in the BS mirror. The geometry of the coil inside the reference mass is also in the direction on lower Eddy currents in the BS reference mass. Taking this into account, the PR mirror actuation should behave as the arm mirror. The shape in the h-reconstruction will thus be of this type.

Since all the arm mirrors have the same reference mass, the Eddy current effect is expected to have the same behaviour, inducing similar mirror actuation TFs. The data for the NI mirror

actuation have large errors, especially at frequencies of a few 100's Hz. The NI data are still compatible with the TFs obtained after renormalisation of the TFs of the NE and WE mirrors to the NI modulus. **It is thus reasonable to assume that the response of the NI mirror actuation is closer to the NE and WE models that to the best fit obtained in this note.**

The systematic errors have been estimated in the section 2.7 (p. 61). **The systematic errors on the mirror actuation TF modulus measured through the calibration main stream have been estimated as** $^{+2\%}_{-4\%}$ (from July 11th 2007 to October 1st 2007):

- $\pm 1\%$ from the measurements in free Michelson data,
- $^{+0\%}_{-2\%}$ from the LN/HP measurements,
- $\pm 1\%$ from the time variation of the modulus in HP mode.

The systematic errors on the phase of actuation TF has been estimated of the order of 0.05 rad from the fit residuals. No additional errors were observed comparing the other data.

A study to explain the delays measured in the mirror actuation given in this note is described in the note [3]. Additionnal phase systematics due to timing uncertainties are given.

Additionnal systematic errors of the order of 5% should be taken into account for the data before July 11th 2007 since the LN/HP mirror actuation TF ratio was not measured for this period.

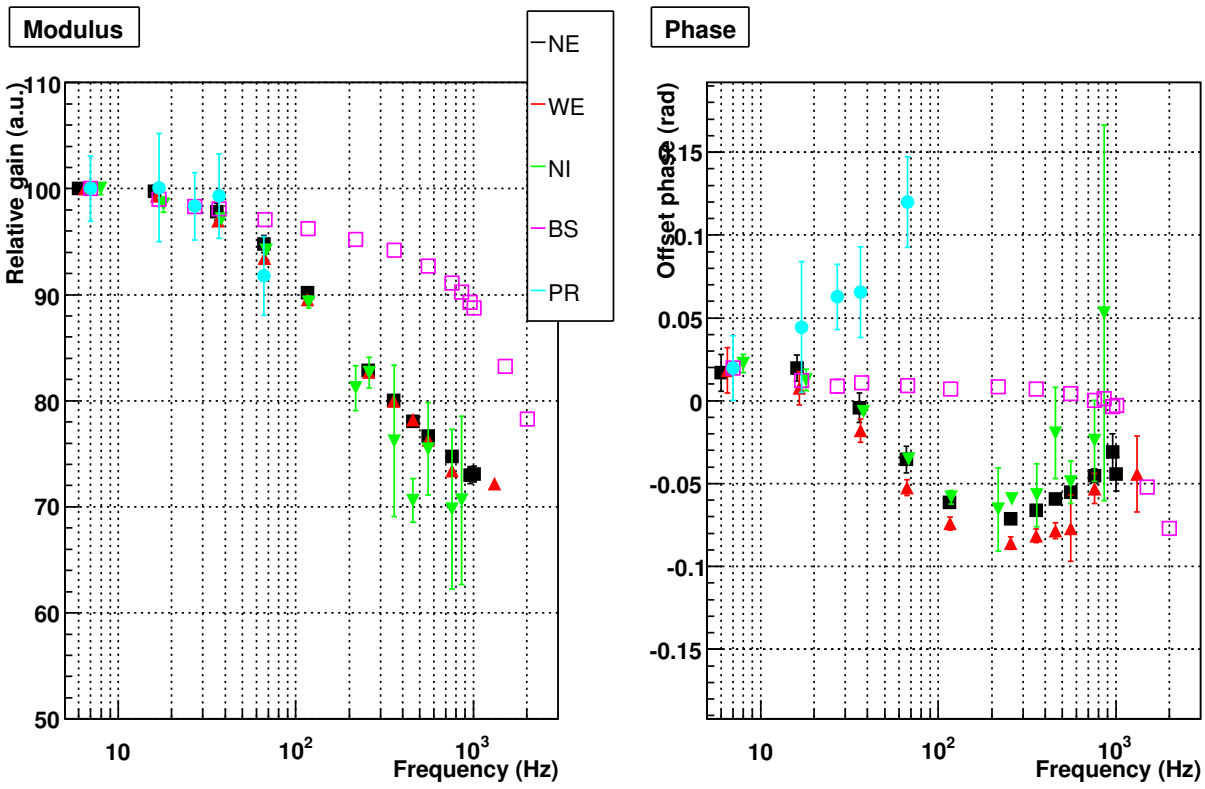

Figure 2.36: ***Mirror actuator TFs comparison in LN mode.*** *The relative modulus and the phase (offset so that the first points are 100 and 0 respectively) are shown for the WE, NE, NI and BS mirrors in LN mode and the PR mirror in HP mode. For visibility, the phase has been corrected for a delay of* $450\mu s$.

Chapter 3

Calibration of the NE and WE marionette actuations

Two measurements of the marionette actuation TFs are done:

- The ratio of the marionette actuation TF to the mirror actuation TF in LN mode is measured from 1 to 100 Hz from white noise injections in step 12. The absolute marionette actuation TF is then computed from 1 to 100 Hz multiplying the ratio by the calibrated mirror actuation in LN mode.
- The TF is measured directly from 1 to 10 Hz using free Michelson data with line injections at the level of the marionettes.

The first method allows to measure the marionette actuation TF in the interesting range for the h-reconstruction. The second one is used as a check of the measurements below 10 Hz and is used to estimate the systematic errors.

The details are given about the calibration of the WE marionette. Only additionnal remarques are given about the NE marionette calibration if necessary.

3.1 WE marionnette actuation calibration

3.1.1 Shape of the WE marionette actuation TF from 1 to 100 Hz

White noise has been injected on the mirror actuation and then on the marionette actuation with the ITF locked in step 12. In both cases, the injected noise is injected through the channel Sc_WE_LoopIn. It is added to Sc_WE_zCorr or Sc_WE_zM respectively in both datasets[1].

The TFs of the dark fringe signal Pr_B1_ACp over the injected noise Sc_WE_LoopIn were computed in both cases. They are referenced as TF_{mir} and TF_{mar} in the following for the

[1] GPS times: injection on the WE mirror from 882264782 to 882265085, injection of the WE marionette from 882265136 to 882265454.

Frequency (Hz)	Modulus ratio	Phase difference (rad)
1.40	0.071 ± 0.019	-0.031 ± 0.28
2.90	0.0429 ± 0.0016	-0.233 ± 0.039
2.10	0.0506 ± 0.0022	-0.160 ± 0.045
3.00	0.0427 ± 0.0019	-0.231 ± 0.045
4.00	0.03929 ± 0.00090	-0.256 ± 0.024
5.00	0.03920 ± 0.00051	-0.339 ± 0.013
6.00	0.03696 ± 0.00032	-0.3921 ± 0.0090
6.50	0.03686 ± 0.00038	-0.420 ± 0.011
8.90	0.03430 ± 0.00017	-0.5464 ± 0.0050
11.90	0.03139 ± 0.00013	-0.6644 ± 0.0043
16.50	0.02778 ± 0.00037	-0.783 ± 0.014
36.50	0.02457 ± 0.00015	-0.9460 ± 0.0065
66.50	0.03432 ± 0.00025	-1.3081 ± 0.0075
116.50	0.0438 ± 0.0042	-1.797 ± 0.099

Table 3.1: ***WE marionette to mirror actuation TF ratio.*** *Modulus ratio and phase difference of the ratio of the TFs at some frequencies. The ratio has been corrected for the pendulum mechanical response models given in the text. The errors are statistical.*

injections on the mirror and the marionette respectively. Their ratio has been corrected for the different model of pendulum mechanical response. The mirror pendulum P_{mir} is assumed to be a second order low-pass filter with $f_0 = 0.6$ Hz and $Q = 1000$. For the marionette pendulum P_{mar}, the model is a $\left(\frac{1\,\mathrm{Hz}}{f}\right)^4$ modulus and no phase effect. The final ratio is the following:

$$\frac{TF_{mar}}{TF_{mir}} \times \frac{P_{mir}}{P_{mar}} \tag{3.1}$$

It gives the ratio of the marionette actuation to mirror actuation TFs. The ratio as function of frequency is given in the figure 5. The table 3.1 gives the values of the ratio at some frequencies.

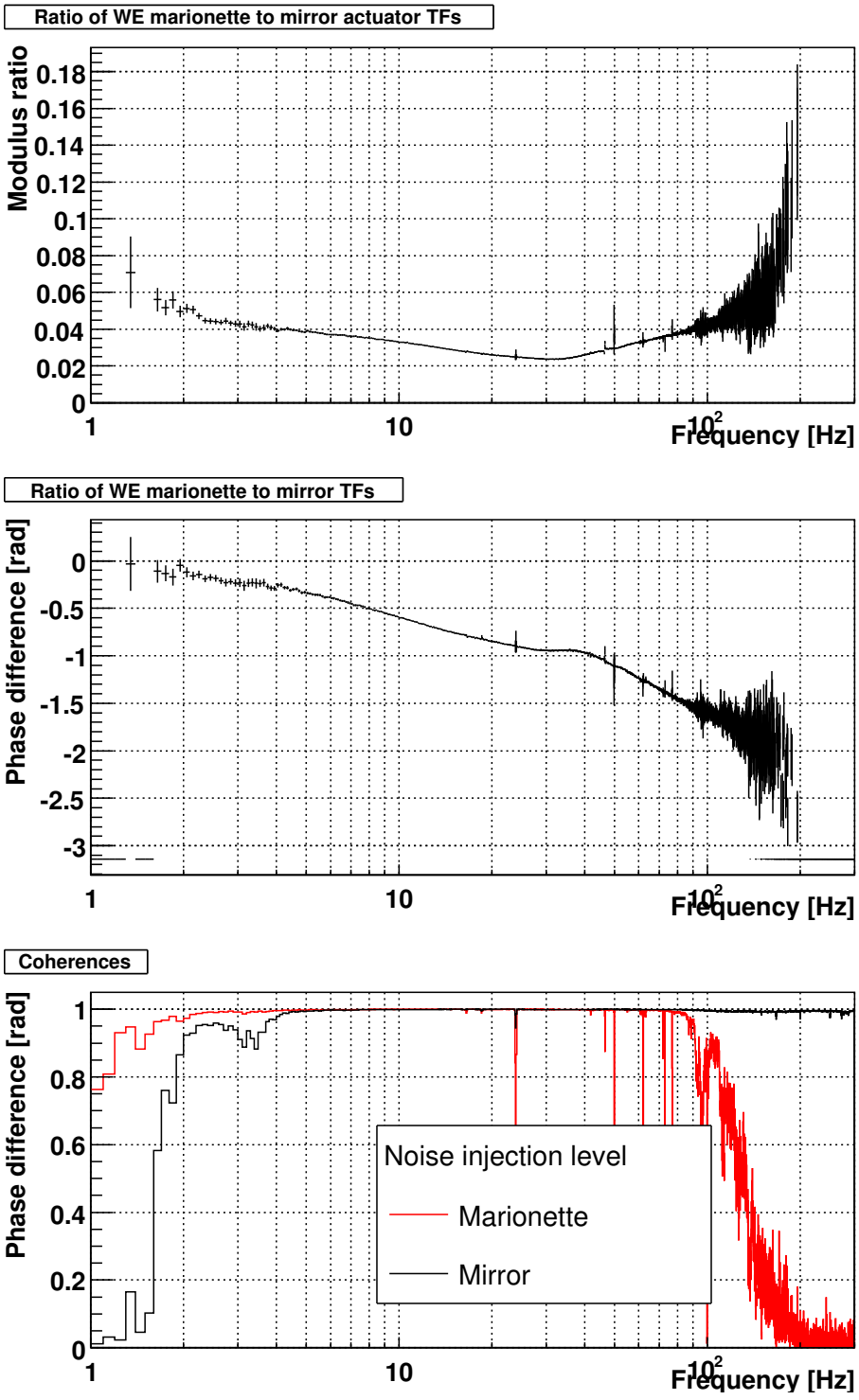

Figure 3.1: ***WE marionette to mirror actuation TF ratio.*** *Modulus ratio and phase difference of the ratio of the TFs. The ratio has been corrected for the pendulum mechanical response models given in the text. All points with coherence higher than 70% were used. The errors are computed from the coherence value. The coherences of the dark fringe with the noise injected on* Sc_WE_LoopIn *are shown for both datasets.*

Frequency (Hz)	Gain G_R ($\mu m/V$)	Phase Φ_R (rad)
1.40	0.88 ± 0.24	-0.038 ± 0.28
1.90	0.615 ± 0.039	-0.057 ± 0.067
2.10	0.626 ± 0.027	-0.170 ± 0.045
3.00	0.529 ± 0.023	-0.246 ± 0.045
4.00	0.487 ± 0.011	-0.276 ± 0.024
5.00	0.4854 ± 0.0062	-0.364 ± 0.013
6.00	0.4575 ± 0.0040	-0.4219 ± 0.0090
6.50	0.4563 ± 0.0047	-0.453 ± 0.011
8.90	0.4243 ± 0.0021	-0.5905 ± 0.0050
11.90	0.3879 ± 0.0016	-0.7231 ± 0.0043
16.50	0.3424 ± 0.0046	-0.864 ± 0.014
36.50	0.2976 ± 0.0019	-1.1173 ± 0.0065
66.50	0.4014 ± 0.0029	-1.5957 ± 0.0075
116.50	0.488 ± 0.047	-2.246 ± 0.099

Table 3.2: ***WE marionette actuation TF*** *computed assuming the model with two poles and two zeros for the WE mirror actuation TF in LN mode. Modulus and phase of the marionette assuming a pendulum mechanical response equal to f^{-4} in modulus and no phase effect.*

3.1.2 WE marionette actuation TF from 1 to 100 Hz

The marionette actuation TF (G_R and Φ_R) is computed multiplying the ratio of the marionette to mirror actuation TFs and the mirror actuation TF in LN mode. The model 3 of the table 2.4 has been used for the mirror actuation TF. The results are shown in the figure 3.2 and given in the table 3.2.

The marionette TF has been fit using simple poles and zeros, and complex poles[2] and zeros[3]. The fit parameters are given in the table 3.3. In order not to have any divergency at high frequency, a pole has been arbitrarily set 150 Hz. The fit superposed to the data and the fit residuals are shown on the the figure 3.3 Note that a simple zero with negative frequency was needed to match the phase properly.

The model matches the modulus within $\pm 2\%$ and the phase within ± 0.03 rad ($1.7°$) between 5 and 70 Hz. This might increase up to $\pm 5\%$ and ± 0.05 rad at 100 Hz.

3.1.3 WE marionette actuation TF from 1 to 10 Hz - Comparison

During the post-VSR1 calibration, data were taken in WE-NI asymmetric free swinging Michelson configuration, with lines injected to the WE marionette. The mirror movement $\Delta L(t)$ is

[2] Complex pole (2nd order low pass filter): $TF(f) = -\frac{f_0^2(f^2-f_0^2) - \mathrm{i}\, f_0^3 f/Q}{(f^2-f_0^2)^2 + (f f_0/Q)^2}$

[3] Complex zero: $TF(f) = -\frac{f_0^2(f^2-f_0^2) + \mathrm{i}\, f_0^3 f/Q}{(f^2-f_0^2)^2 + (f f_0/Q)^2}$

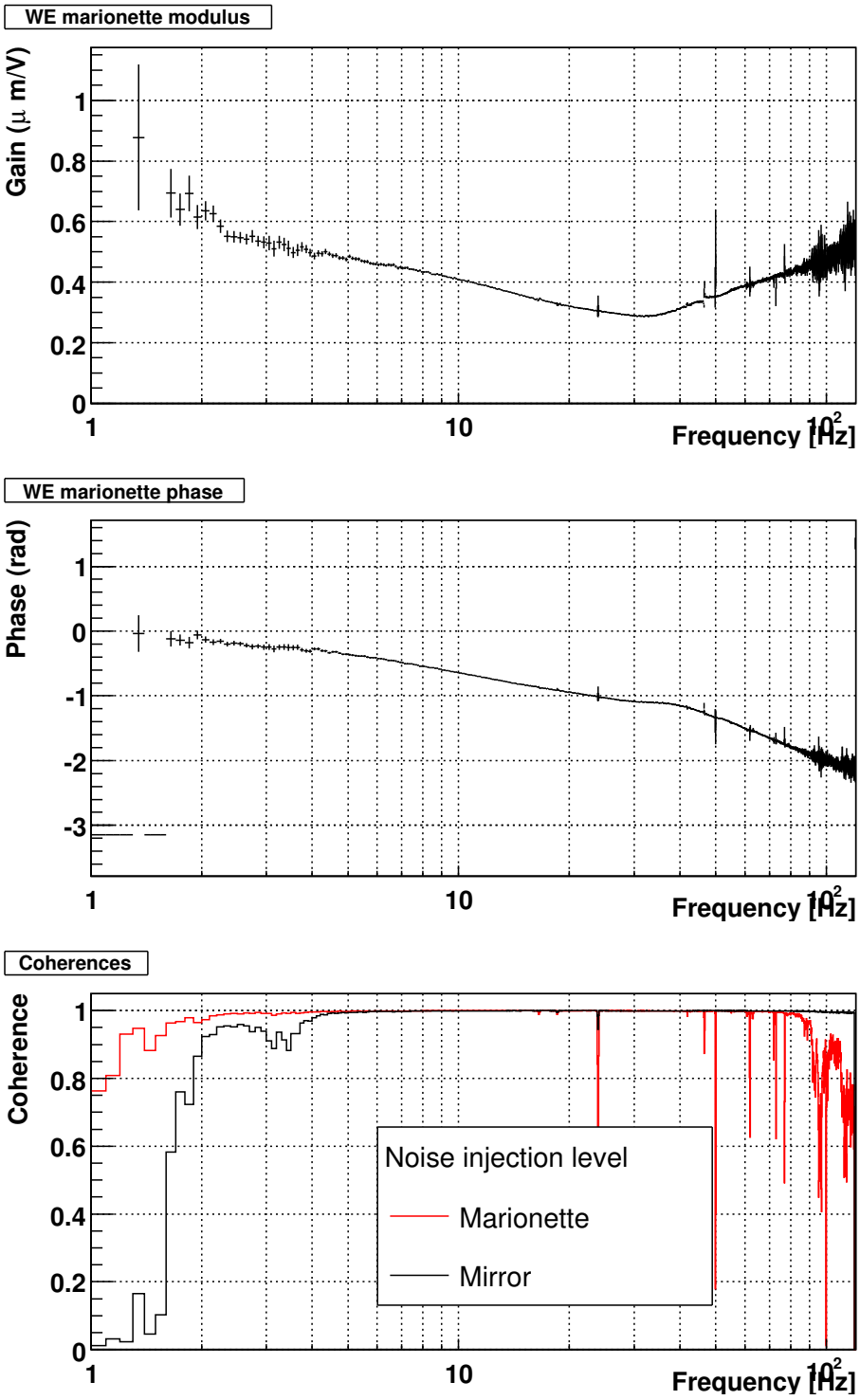

Figure 3.2: ***WE marionette actuation TF.*** *Modulus and phase of the marionette assuming a pendulum mechanical response equal to f^{-4} in modulus and no phase effect.*

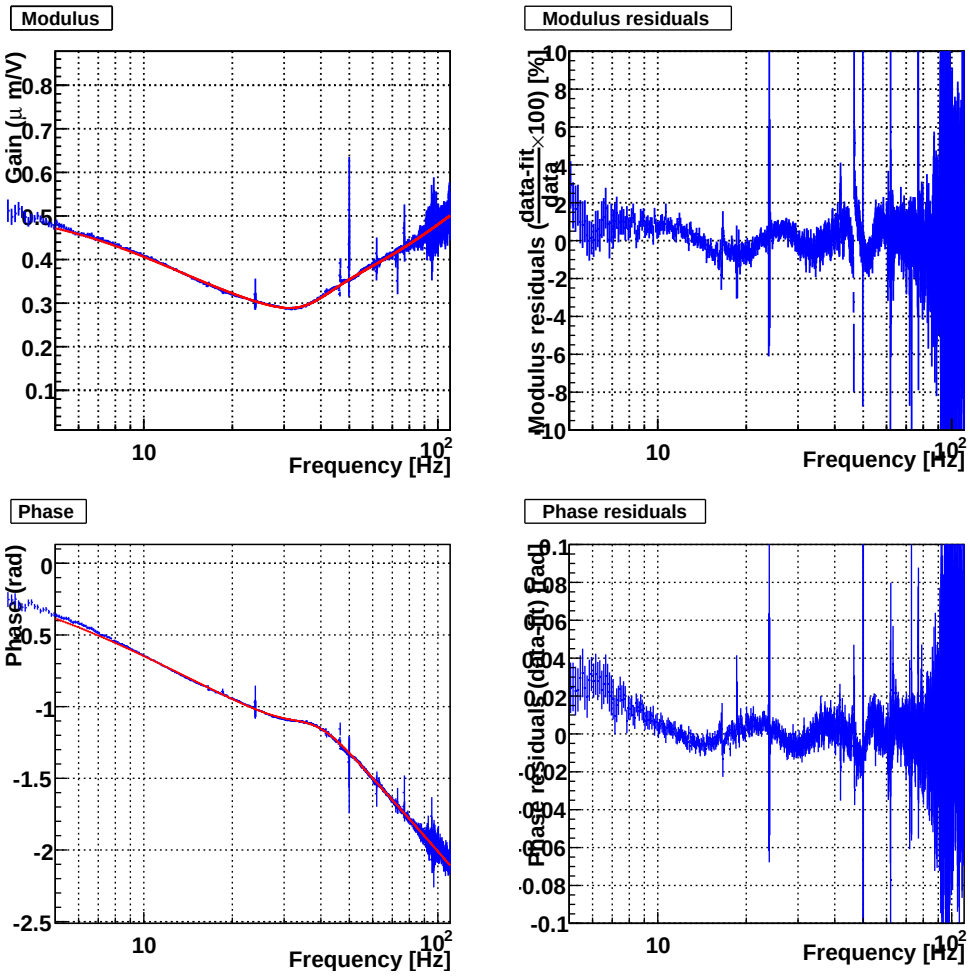

Figure 3.3: ***Fit of the WE marionette actuation TF.*** *The data (modulus and phase) and superposed fit function are given on the left column. The fit residuals are shown on the right column.*

$g = 0.51410 \pm 0.00058\,\mu$m/V
$t_d = 0.356 \pm 0.0036$ ms
$f_p = 7.75 \pm 0.026$ Hz
$f_p = 14.175 \pm 0.094$ Hz
$f_p = 39.02 \pm 0.15$ Hz, $Q = 1.379 \pm 0.010$
$f_p = 150$ Hz
$f_0 = 9.224 \pm 0.020$ Hz
$f_0 = -49.810 \pm 0.051$ Hz
$f_0 = 27.75 \pm 0.26$ Hz
$f_0 = 36.68 \pm 0.10$ Hz, $Q = 1.379 \pm 0.010$

Table 3.3: ***Parameters of the WE marionette TF fit*** *with two simple poles, a complex pole, three simple zeros and a complex zero.*

reconstructed as described here [2]. The data with a coherence between ΔL and the injected signa Sc_WE_zM higher than 15% are used. The marionette TF (G_{FM} and Φ_{FM}) is extracted at the injected frequencies from the TF of ΔL over Sc_WE_zM. Lines were injected from 1.4 to 11.9 Hz. The TF modulus is then corrected by a f^4 factor to approximate the two pendulum stages. The phase is not corrected.

The figure 3.4(a) shows the measurements of the different datasets. The table 3.4 and the figure 3.4(b) give the WE marionette TF as function of frequency.

Comparison of both methods below 10 Hz

The two independent methods used to measure the WE marionette TF are compared in the range 1 to 10 Hz in the table 3.4. The relative modulus difference and the phase difference between both methods are given.

No systematic effects is visible above the statistical uncertainties. The systematic errors are thus determine to be less than 4% on the modulus and less than 0.05 rad (2.5°) on the phase.

3.2 NE marionnette actuation calibration

3.2.1 Shape of the NE marionette actuation TF from 1 to 100 Hz

The white noise was injected on NE mirror from 882263747 to 882264049 and on NE marionette from 882264243 to 882264544.

3.2.2 NE marionette actuation TF from 1 to 100 Hz

The ratio has been corrected using the model 3 from table 2.8 for the mirror actuation TF in LN mode.

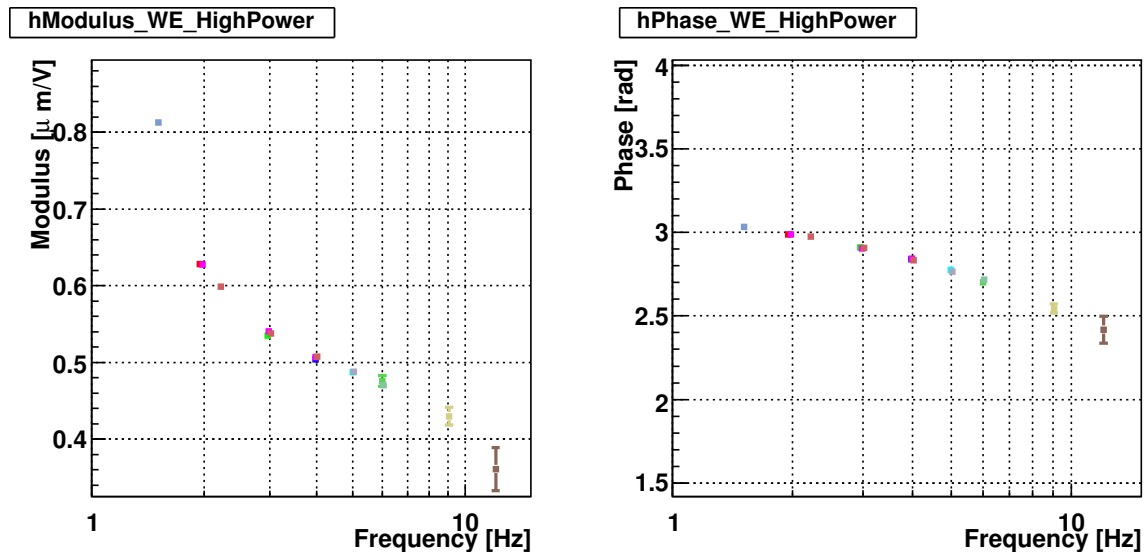

(a) WE marionette TF.

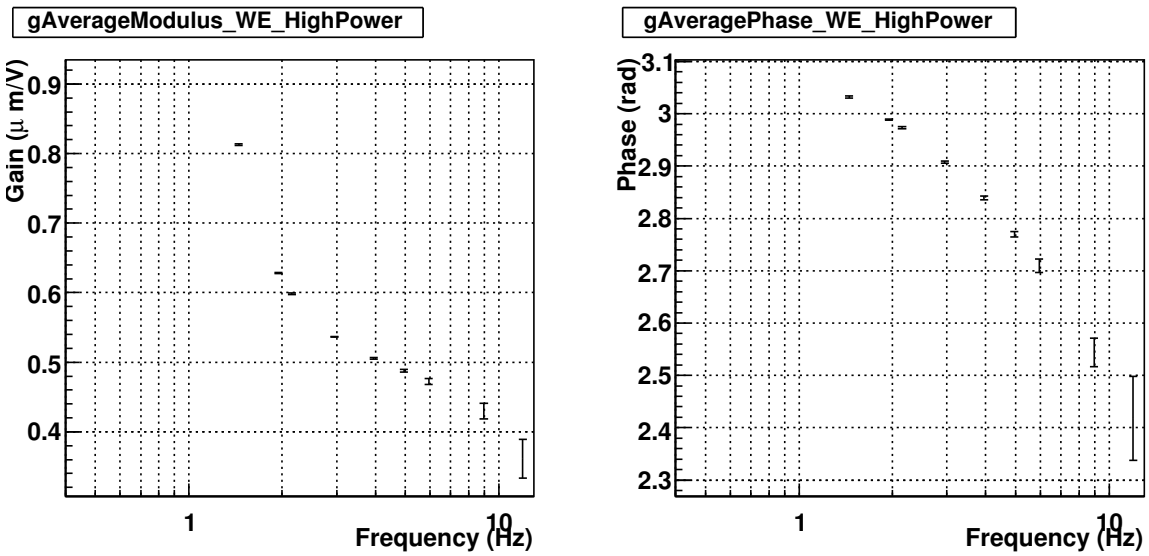

(b) WE time-averaged marionette TF.

Figure 3.4: ***WE marionette actuation TF.*** *(a) Measurements from the different datasets (colors) (October-December 2007). (b) Time-averaged modulus and phase as function of frequency. The modulus is corrected for a f^4 factor for the 2-stage mechanical pendulum response.*

Freq. (Hz)	Gain G_{FM} (μm/V)	Phase Φ_{FM} (rad)	$\frac{G_{FM}-G_R}{G_R}$ (%)	$\Phi_{FM} - \Phi_R$ (rad)
1.4	0.813 ± 0.001	3.0318 ± 0.0019	-7 ± 30	-0.07 ± 0.29
1.9	0.628 ± 0.0005	2.9889 ± 0.0012	2.2 ± 7	-0.096 ± 0.068
2.1	0.599 ± 0.001	2.9732 ± 0.0022	-4.4 ± 4	0.002 ± 0.048
3.0	0.536 ± 0.0006	2.9075 ± 0.0017	1.3 ± 5	0.012 ± 0.047
4.0	0.506 ± 0.001	2.8388 ± 0.0036	4.0 ± 3	-0.027 ± 0.027
5.0	0.488 ± 0.002	2.7700 ± 0.0050	0.5 ± 2	-0.007 ± 0.018
6.0	0.472 ± 0.004	2.7099 ± 0.0128	3.2 ± 2	-0.010 ± 0.022
8.9	0.430 ± 0.011	2.5440 ± 0.0276	1.3 ± 3	-0.007 ± 0.033
11.9	0.361 ± 0.028	2.4183 ± 0.0803	-6.9 ± 8	-0.000 ± 0.085

Table 3.4: ***Time-average actuation TF of the WE marionette****. First two columns: modulus and phase of the WE marionette. The modulus is corrected for a f^4 factor for the 2-stage mechanical pendulum response. All data with coherence higher than 15% were used. Last two columns: comparison of the modulus and phase measured with the two methods described in the text (this table and table 3.2).*

Frequency (Hz)	Modulus ratio	Phase difference (rad)
2.90	0.0392 ± 0.0011	-0.225 ± 0.030
2.10	0.0434 ± 0.0016	-0.168 ± 0.037
3.00	0.0391 ± 0.0013	-0.202 ± 0.034
4.00	0.0367 ± 0.00054	-0.273 ± 0.015
5.00	0.03447 ± 0.00027	-0.3246 ± 0.0081
6.00	0.03336 ± 0.00025	-0.3876 ± 0.0076
8.90	0.0290 ± 0.00013	-0.5250 ± 0.0047
11.90	0.024539 ± 0.000060	-0.6298 ± 0.0036
16.00	0.019019 ± 0.000056	-0.6718 ± 0.0031
36.00	0.014448 ± 0.000046	-6.2555 ± 0.0033
66.00	0.02591 ± 0.00021	-0.0298 ± 0.0083
116.00	0.0394 ± 0.0032	-0.463 ± 0.084

Table 3.5: ***NE marionette to mirror actuation TF ratio.***

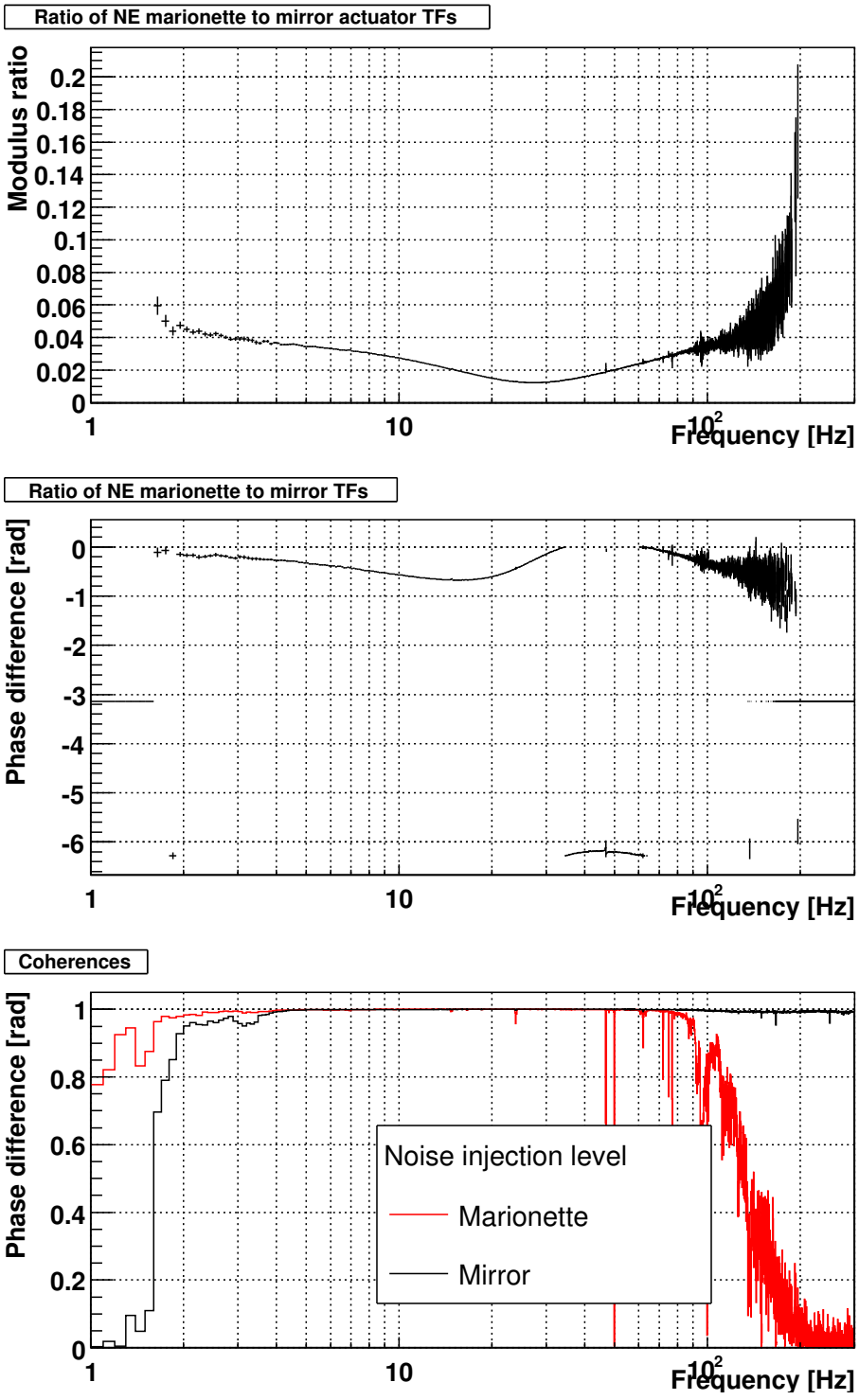

Figure 3.5: ***NE marionette to mirror TF ratio.*** *Modulus ratio and phase difference of the ratio of the TFs. The ratio has been corrected for the pendulum mechanical response models given in the text. All points with coherence higher than 70% were used. The errors are computed from the coherence value. The coherences of the dark fringe with the noise injected on* Sc_NE_LoopIn *are shown for both datasets.*

Frequency (Hz)	Gain ($\mu m/V$)	Phase (rad)
1.90	0.671 ± 0.032	2.981 ± 0.049
2.10	0.612 ± 0.022	2.964 ± 0.037
3.00	0.552 ± 0.018	2.925 ± 0.034
4.00	0.5170 ± 0.0075	2.849 ± 0.015
5.00	0.4862 ± 0.0038	2.7929 ± 0.0081
6.00	0.4704 ± 0.0035	2.7252 ± 0.0076
8.90	0.4086 ± 0.0018	2.5741 ± 0.0047
11.90	0.3455 ± 0.0012	2.4552 ± 0.0036
16.00	0.26735 ± 0.00079	2.3940 ± 0.0031
36.00	0.20029 ± 0.00064	-3.2798 ± 0.0033
66.00	0.3481 ± 0.0028	2.8253 ± 0.0083
116.00	0.503 ± 0.041	2.225 ± 0.084

Table 3.6: ***NE marionette actuation TF.*** *Modulus and phase of the marionette assuming a pendulum mechanical response equal to f^{-4} in modulus and no phase effect.*

$g = 0.5296 \pm 0.0004\,\mu\mathrm{m/V}$
$t_d = 2.382 \pm 0.003\,\mathrm{ms}$
$f_p = 15.94 \pm 0.14$ Hz
$f_p = 26.16 \pm 0.39$ Hz
$f_p = 150$ Hz
$f_0 = 57.55 \pm 0.47$ Hz
$f_0 = 26.933 \pm 0.014$ Hz, $Q = 1.18143 \pm 0.00079$

Table 3.7: ***Parameters of the NE marionette TF fit*** *with a three simple poles, a simple zero and a complex zero.*

The TF has been fit using two simple poles, a simple zero and a complex zero. In order not to have any divergency at high frequency, a pole has been arbitrarily set 150 Hz. The fit parameters are given in the table 3.7. The fit and its residuals are shown on the figure 3.7. The model matches the modulus within ±2% and the phase within ±0.03 rad (1.7°) between 5 and 70 Hz. This might increase up to ±5% and ±0.05 rad at 100 Hz.

3.2.3 NE marionette actuation TF from 1 to 10 Hz

The NE marionette actuation TF measured from 1 to 10 Hz using free Michelson data is shown on the figure 3.8 and in the table 3.8.

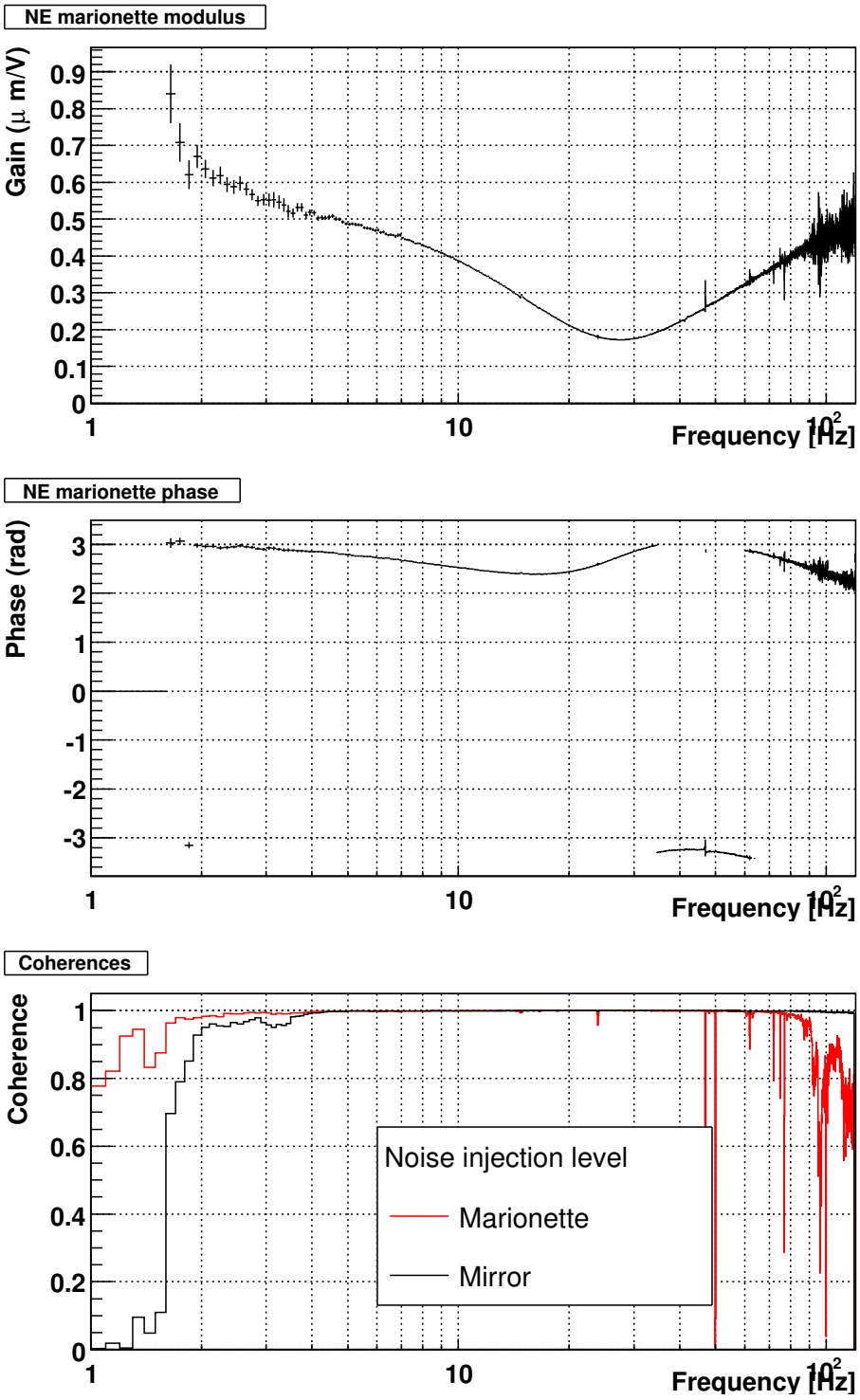

Figure 3.6: ***NE marionette actuation TF.*** *Modulus and phase of the marionette assuming a pendulum mechanical response equal to f^{-4} in modulus and no phase effect.*

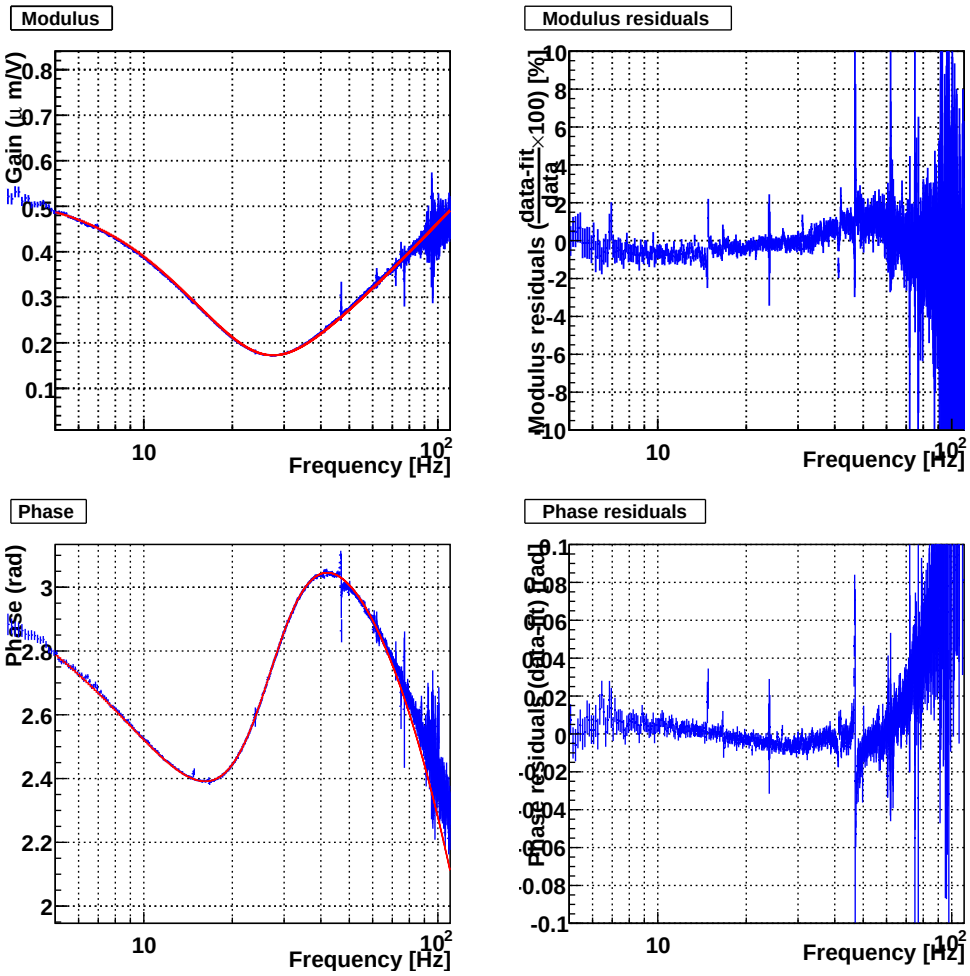

Figure 3.7: ***Fit of the NE marionette actuation TF.*** *The data (modulus and phase) and superposed fit function are given on the left column. The fit residuals are shown on the right column.*

Frequency (Hz)	Gain G_{FM} (μm/V)	Phase Φ_{FM} (rad)	$\frac{G_{FM}-G_R}{G_R}$ (%)	$\Phi_{FM} - \Phi_R$ (rad)
1.4	0.830 ± 0.002	3.0385 ± 0.0029	-	-
2.1	0.603 ± 0.001	2.9894 ± 0.0031	-1.5 ± 3.7	0.026 ± 0.041
3.0	0.544 ± 0.001	2.9265 ± 0.0029	-1.5 ± 3.4	0.002 ± 0.036
4.0	0.511 ± 0.002	2.8656 ± 0.0067	-1.2 ± 1.8	0.017 ± 0.022
5.0	0.499 ± 0.005	2.7780 ± 0.0146	2.6 ± 1.8	-0.015 ± 0.023
6.0	0.465 ± 0.007	2.7249 ± 0.0208	-1.2 ± 2.2	0.000 ± 0.028

Table 3.8: ***Time-average actuation TF of the NE marionette****. First two columns: TF of the NE marionette. The modulus is corrected for a f^4 factor for the 2-stage mechanical pendulum response. All data with coherence higher than 15% were used. Last two columns: comparison between the modulus and phase measured with the two methods discussed in the text (this table and table 3.6).*

Comparison of both methods

The two independent methods used to measure the NE marionette TF are compared in the range 1 to 10 Hz in the table 3.8. The relative modulus difference and the phase difference between both methods are given.

No systematic effects is visible above the statistical uncertainties. The systematic errors are thus determine to be less than 3% on the modulus and less than 0.03 rad (1.7°) on the phase.

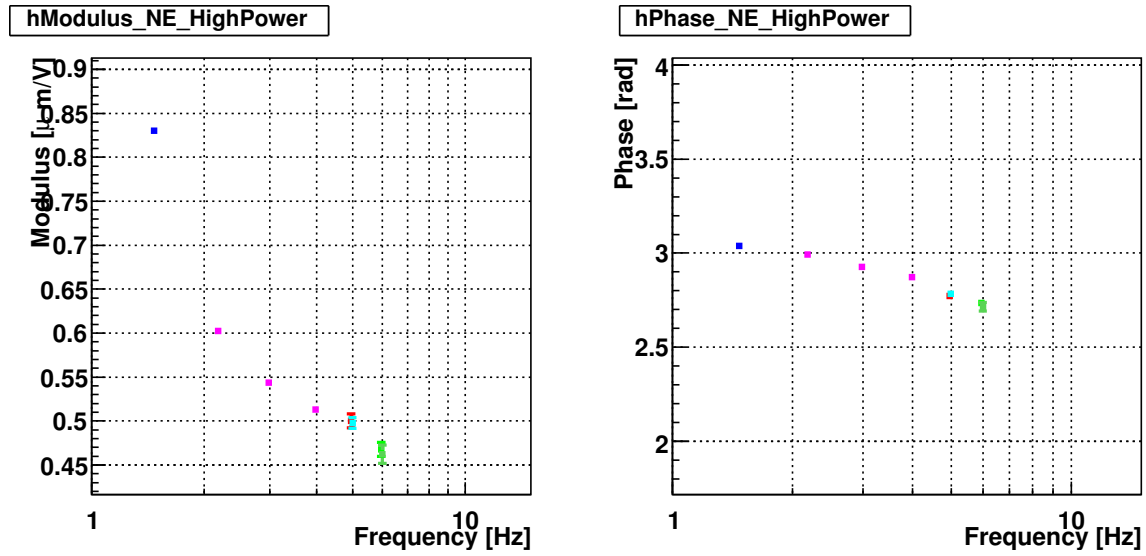

(a) NE marionette TF.

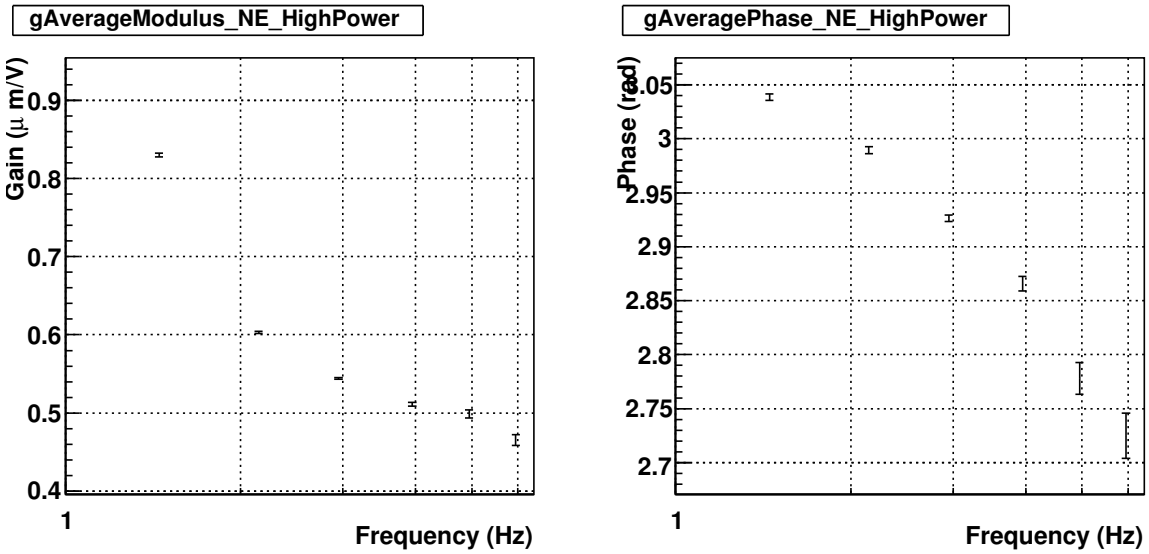

(b) NE time-averaged marionette TF.

Figure 3.8: ***NE marionette actuation TF.*** *(a) Measurements from the different datasets (colors) (October-December 2007). (b) Time-averaged modulus and phase as function of frequency. The modulus is corrected for a f^4 factor for the 2-stage mechanical pendulum response.*

3.3 Conclusions about the marionette actuation TFs

The NE and WE marionette actuation TFs have been measured between 1 and 100 Hz from white noise injections with the ITF locked. The statistical errors of the measurements are of the order of 0.5% on the modulus and 0.01 rad (0.6°) on the phase. The TFs have been parametrized using simple and complex poles and zeros. The parametrisations are given in the tables 3.3 and 3.7. They match the measurements **within 2% and 0.03 rad on the modulus and phase respectively below ~ 70 Hz.**

An independent method using free Michelson data has been used to measure the marionette TFs from 1 to 10 Hz. No systematic effect is seen from the comparison of both measurements in this low frequency range. **The systematic errors are estimated to be lower than 3% and 0.03 rad on the modulus and the phase respectively.**

Both methods use asymmetric free swinging Michelson data:

- the first measurements are derived from the mirror actuation measurements in HP mode,
- the second measurements are directly computed from free swinging Michelson data.

A systematic error coming from the analysis of such data would not be visible in the current comparison.

Bibliography

[1] L. Rolland, D. Huet, *Mirror actuation configuration during VSR1* (2008) VIR-051A-08

[2] L. Rolland, B. Mours, F. Marion, VIRGO note in preparation

[3] L. Rolland, B. Mours, A. Masserot, *Timing calibration during VSR1* (2008) VIR-028B-08

[4] O. Véziant, Thèse de l'Université de Savoie (2003)

[5] S. Vilalte (2004), http://wwwlapp.in2p3.fr/virgo/notes/Notes2004/Vilalte_CompressionFilter.pdf

[6] G. Vajente, E. Campagna, B. Swinkels *Locking characterisation* (2008) VIR-0051-08

[7] E. Majorana, P. Puppo, P. Rapagnani, F. Ricci *The BS payload* (2001) VIR-NOT-ROM-1390-179

[8] A. Bernardini et al. **Review of scientific instruments 70**, 8 (1999).